Generation and Optimisation of Picosecond Optical Pulses for use in Broadband Communication Systems.

A Thesis Submitted for the Degree of

Master of Engineering

By

Marc Rensing
BSc., H. Dip.

School of Electronic Engineering
Faculty of Engineering and Computing
Dublin City University

Research Supervisor

Dr. Liam Barry

August 2006

Declaration

I hereby certify that this material, which I now submit for assessment on the programme of study leading to the award of Master of Engineering is entirely my own work and has not been taken from the work of others save and to the extent that such work has been cited and acknowledged within the text of my work.

Signed: Marc Kensing

ID No: 54175364

Date: 25/8/06

Acknowledgements

I would like to first of all thank my supervisor Dr. Liam Barry for giving me the opportunity to carry out this work. His support, advice and easily approachable nature have made this project possible and enjoyable. Secondly I would like to extend my gratitude to Dr. Prince Anandarajah, without his expertise, guidance and patience this work would have been a lot more difficult. Prince's door has always been open and his help much needed and appreciated.

A special thanks goes to my family for all the support and encouragement they have given me through my years of study, without them I wouldn't be where I am today. And to my good friends who have helped me unwind during my studies and have always been there.

To my friends and colleagues in the lab who have lent a hand and made my time here extremely enjoyable, I would just like to say "thanks guys": Dr. Paul Maguire, Dr. Brendan Kennedy, Frank Smyth, Aisling Clarke, Robert Maher, Eoin Connolly, Dr. Aleksandra Kaszubowska, Dr. Celine Guignard, Krzysztof Bondarczuk, Sylwester Latkowski, past member Ling Hu, and honorary lab members Dr. Eoin Kennedy and Damien O'Rourke.

Table of Contents

List of Figures.

List of Tables.

List of Acronyms

AWG	Arrayed Waveguide Grating
APD	Avalanche Photodiode
CW	Continuous Wave
CWDM	Course Wavelength Division Multiplexing
DBR	Distributed Bragg Reflector
DCF	Dispersion Compensating Fiber
DFB	Distributed Feedback Laser
DSF	Dispersion Shifted Fiber
DWDM	Dense Wavelength Division Multiplexing
BER	Bit Error Rate
BL	Bit-Rate-Distance Product
EAM	Electro Absorption Modulator
EDFA	Erbium Doped Fiber Amplifier
EM	Electromagnetic
EO	Electro-Optic
ETDM	Electrical Time Division Multiplexing
FBG	Fibre Bragg Grating
FDM	Frequency Division Multiplexing
FWM	Four Wave Mixing
FP	Fabry-Perot
FROG	Frequency Resolved Optical Gating
FWHM	Full Width Half Maximum
GDR	Group Delay Ripple
GRIN	Graded Index
ISI	Intersymbol Interference
ITU-T	Telecommunications Standardisation Sector of ITU
LED	Light Emitting Diode
LOS	Line of Sight
MPN	Mode Partition Noise
MZM	Mach-Zehnder modulators
NC FBG	Non-Linearly Chirped Fiber Bragg Grating
NRZ	Non-Return-To-Zero
OADM	Optical Add Drop Multiplexers
OE	Opto-Electric
OFPTF	Optical Fabry Perot Tunable Filter

OSA	Optical Spectrum Analyser
OTDM	Optical Time Division Multiplexing
PC	Polarisation Controller
RZ	Return-to-Zero
SHG	Second Harmonic Generation
SMSR	Side Mode Suppression Ratio
SNR	Signal to Noise Ratio
SOA	Semiconductor Optical Amplifier
SPM	Self Phase Modulation
SRS	Stimulated Raman Scattering
SSGS	Self Seeded Gain Switched
SSMF	Standard Single Mode Fiber
STM	Synchronous Transfer Module
TBP	Time Bandwidth Product
TDM	Time Division Multiplexing
TOF	Tunable Optical Filter
TOJ	Turn On Jitter
TPSR	Temporal Pedestal Suppression Ratio
VOA	Variable Optical Attenuator
WDM	Wavelength Division Multiplexing
XPM	Cross Phase Modulation

Abstract

Generation and Optimisation of Picosecond Optical Pulses for use in Broadband Communication Systems.

Marc Rensing

The continued growth of the internet driven by the demand for media rich content and escalating IP traffic has been fuelling the massive growth in demand for bandwidth to handle very high data rates. In order to meet this demand for capacity, optical multiplexing techniques such as wavelength division multiplexing (WDM), optical time division multiplexing (OTDM) and hybrid WDM/OTDM systems need to be utilised.

The development of a source of wavelength tunable picosecond optical pulses with excellent temporal and spectral purity at high repetition rates is extremely important for use in such high-speed optical communication systems. The technique of gain switching a commercially available laser diode and self seeding it is shown to be one of the simplest and most cost effective methods of generating transform limited, wavelength tunable pulses with a high Side Mode Suppression Ratio (SMSR).

This thesis examines the use of optical gain-switching for the generation of optical pulses that may be used in high-speed OTDM and WDM/OTDM systems. This work specifically deals with the investigation and characterisation of the SMSR and non-linear chirp of optical pulses generated using the gain-switching technique, and outlines how these characteristics, that may degrade system performance, can be optimised such as that optimum performance is attained. In particular, the work demonstrates the development of an optical pulse source with duration < 4ps, SMSR > 30 dB, jitter < 800 fs, and extinction ratio > 30 dB, that would be suitable for use in OTDM systems operating at 80 Gbit/s.

Introduction

With the growing demand for bandwidth, driven by the massive increase in internet usage and other broadband services, showing no signs of abating, it will be necessary to develop optical technologies that can handle extremely high data rates. This increase in demand for bandwidth and the speed limitations of electronic components has led to the introduction of various optical multiplexing techniques such as wavelength division multiplexing (WDM) and optical time division multiplexing (OTDM). A key component to enable high-speed optical transmission systems is a source of ultra short optical pulses which are spectrally and temporally pure. This thesis focuses on the generation of such optical pulses and their usefulness in high-speed optical communication systems. The technique of gain switching is given prominence as it is one of the simplest, most reliable and cost effective methods available to generate ultra short optical pulses. Experimental results obtained demonstrate that through self seeding and external injection, an improvement in the impairments associated with this technique can be achieved.

One of the important parameters of self seeded gain switched (SSGS) pulses is the side mode suppression ratio (SMSR). This work examines the importance of achieving a high SMSR when generating pulses using the SSGS technique especially when optical filtration is used. Experiments carried out on pulses that exhibit a poor SMSR which are then filtered, reveal that they posses a large amplitude jitter. This noise will degrade the signal-to-noise ratio (SNR) regardless of the output SMSR being maintained at a high level, and may render such pulses unsuitable for data transmission in high-speed optical networks.

In addition to the SMSR characterisation, this work also examines a novel compensation technique used to counteract the linear and non-linear chirp presented by gain switched pulses. This large frequency chirp is induced on a gain switched pulse due to the direct modulation of the laser diode and can degrade the performance of optical communication systems employing these pulses. Various compression techniques used to compress the gain switched pulse, typically result in the creation of temporal pedestals on either side of the pulse which ultimately renders such pulses unsuitable for use in practical high-speed optical communication systems. We demonstrate the generation of transform limited short optical pulses which display excellent spectral and temporal purity by employing a novel technique that combines an externally injected gain switched laser with a non-linearly chirped fiber Bragg grating (NC FBG). We also fabricated a linearly chirped fiber Bragg grating (LC

FBG) and compared pulses compressed with the linear grating to those compressed with the non-linear grating.

This thesis is divided into 5 chapters with the following layout:

Chapter 1: A brief introduction into the origin of optical communications is given along with the advantages of utilising optical fibers. A basic fiber optic communication system is described as well as the methods used for measuring the system performance.

Chapter 2: This chapter describes the basic operation of two of the most common optical multiplexing techniques, namely wavelength division multiplexing (WDM) and optical time division multiplexing (OTDM). Major enabling technologies and limiting factors are discussed regarding both types of networks. Hybrid WDM/OTDM networks that combine the merits of both technologies are also considered.

Chapter 3: Here we describe the various methods of generating short optical pulses for use in high-speed optical networks. Particular attention is given to the technique of gain switching and experimental results are presented for pulses generated using this method. Pulses generated via gain switching exhibit a large frequency chip, degraded side mode suppression ratio (SMSR), and large timing jitter. It is shown that by utilising self seeding and external injection, these impairments may be partially overcome.

Chapter 4: In this chapter we present a detailed investigation into the effects of SMSR on the performance of SSGS pulses in optical communication systems. Pulses portraying various SMSRs are optically filtered and the interaction of mode partition noise (MPN) is investigated. We also demonstrate the compression of a gain switched pulse and the compensation of the linear and non-linear chirp across the centre and wings of the pulse respectively, resulting in the generation of ultra short optical pulses that are suitable for use in a high-speed 80 Gb/s OTDM communication system.

Chapter 5: Finally we present the conclusions of this work.

1. Basic Optical Networks

1.1 Historical Development

Since ancient times there has always been an interest in developing communications systems to send messages from one point to another. Many forms of communications systems have been developed over the years with each system trying to improve on the previous one in terms of enhancing the transmission reliability, increasing the data rate or increasing the transmission distance between relay stations. Up until the nineteenth century all communication systems had a very low data rate and employed optical or acoustical methods such as signal lamps or horns. One of the earliest known optical systems was the use of signal fires used by the Greeks in the eighth century BC to communicate specific messages such as alarm calls or declare specific events. However, the meaning of the signal had to be prearranged between the sender and the receiver and it was not until about six hundred years later that the signals were encoded in relation to the alphabet allowing any message to be sent. This technology was limited to line of sight (LOS) transmission and detrimental changes in the weather made the transmission path unreliable. The invention of the telegraph by Samuel Morse in 1838 lead the way for a new period in communications using electrical technology. The first commercial telegraph service using wire cables was implemented in 1844 and the use of wire cables for information transmission expanded when the first telephone exchange was setup in New Haven, Connecticut in 1878. Wire cable was the only medium for electrical communication until Heinrich Hertz discovered long wavelength electromagnetic radiation in 1887 and the first implementation of this was the radio demonstration by Guglielmo Marconi in 1895 [1].

1.2. Information Carrying Capacity

In the years that followed, more and more portions of the electromagnetic (EM) spectrum were used to convey information from one point to another. The reason for this is that in electrical systems, data is usually transferred over the communication channel by superimposing the information signal onto a sinusoidally varying EM wave known as a carrier wave. As the frequency range over which the carrier wave operates determines the amount of information that can be transmitted, increasing the carrier frequency increases the available transmission bandwidth and as a result provides a larger information capacity. This is known as the Shannon-Hartley theorem, from information theory. As a result of this theorem, the trend was to employ progressively higher frequencies (shorter wavelength)

which offered corresponding increases in bandwidth and therefore increased information capacity. As a rule of thumb, bandwidth is approximately 10% of the carrier frequency so if a microwave channel uses a 10 GHz carrier signal, then its bandwidth is about 100 MHz. A copper wire can carry a signal up to 1 MHz over a short distance, a coaxial cable can propagate a signal up to 100 MHz while radio frequencies are in the range of 500 KHz to 100 MHz. Microwaves, which include satellite channels, operate up to 100 GHz. Fiber optic communication systems use light as the signal carrier which has frequencies between 100 and 1000 THz, so even at a carrier frequency of 500 THz, we can estimate the available bandwidth to be about 50 THz [2]. To demonstrate this point further, consider the following transmission media shown in Table 1.1 in terms of their capacity to carry, simultaneously, a specific number of one-way voice channels. Bear in mind that the numbers mentioned here only represent orders of magnitude and not actual values.

Medium	No. Of One-Way Channels
Single Coaxial Cable	13,000
Microwave	20,000
Satellite Link	100,000
Single Fiber Optic Link	300,000 Two way Chns.

Table 1.1 Carrying capacity of various transmission media

As we can see from the table above, one fiber optic communication link, can carry 300,000 two way voice channels simultaneously. This explains why fiber optic communication systems form the backbone of modern telecommunications and will more than likely continue to shape the future [2].

1.2.1 Advantages of Optical Fibers.

Apart from the superior capacity optical fiber offers over other forms of communication systems, other advantages include:

Low Loss: Optical fibers have lower transmission losses and wider bandwidths compared with copper wires. An attenuation of a few tenths of a dB/km is typical of commercial glass fibers operating at 1.3 μm and 1.55 μm, resulting in more data being sent over longer distances and reduces the number of repeaters needed, which in turn decreases the system cost and complexity.

Small size and weight:

The low weight and small size of fibers have a distinct advantage over bulky wire cables in terms of handling in crowded environments such as underground ducts or ceiling mounted cable trays.

Security and reliability:

Due to their dielectric nature, optical fibers are immune to electromagnetic interference from signal carrying wires and lightning. Fiber also provides a high degree of data security as the optical signal is confined within the waveguide.

Abundant Raw Material:

As silica is the principle material of which optical fibers are made and is found in sand, the raw material is abundant and inexpensive. The real expense is in the purification process.

1.3 Basic Optical Communication System

A basic communication system consists of a transmitter, a receiver and an information channel as shown in Figure 1.1. At the transmitter, the data is generated and put into a format that is suitable for transmission over the optical fibers. The information travels from the transmitter to the receiver, via the information channel, where the data is extracted and put into its final form.

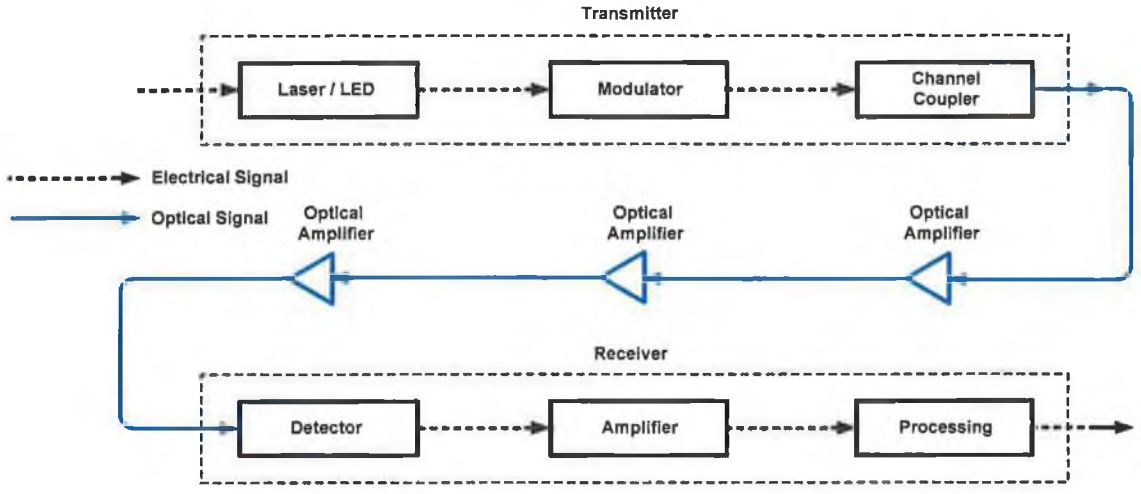

Fig. 1.1 General Fiber Optic Communication System

1.3.1 Transmitter

At the heart of the transmitter is a light source, the major function of which is to convert an electrical data signal into an optical signal. Fiber optic communication systems use either light emitting diodes (LED) or laser diodes as transmitters.

When choosing an optical source to be used with the optical waveguide various characteristics of the fibre must be taken into account such as geometry, attenuation as a function of wavelength, its group delay distortion and its modal characteristics. Then the characteristics of the optical source such as the emitted power, spectral width, radiation pattern, and modulation bandwidth must be compatible with the type of fiber chosen.

1.3.1.1 Light Emitting Diodes.

For optical communication systems requiring bit rates of about 100-200 Mb/s over a few kilometres and optical power in tens of microwatts, LEDs are usually the best choice. Generally LEDs are used with multimode fibres as usually the incoherent optical power can only be coupled into these types of fibres in sufficient quantities to be useful [3]. However, some applications have used specially fabricated LEDs with single mode fibres for data transmission at bit rates up to 1.2 Gb/s over several kilometers [4,5]. Figure 1.2, shows a multimode optical fiber inserted directly in the semiconductor material to place the fiber as close to the active area as possible. LED sources do not need as much complex circuitry as laser diodes because no thermal stabilisation circuits are required, they also have longer lifetimes and may be fabricated with less expense [1]. However, a major disadvantage, apart from a much bigger linewidth, is that they are very inefficient at coupling optical power into single mode fibres. This is due to a larger emitting area, greater beam divergence and incoherent light output [6].

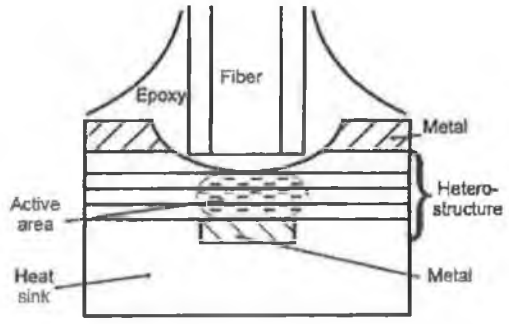

Fig 1.2 Schematic of LED structure [7]

1.3.1.2 Lasers

Semiconductor lasers are not unlike LED's in principle. However, unlike LEDs where the light output is generated by spontaneous emission, in a semiconductor laser most of the light is created by stimulated emission. As can be seen from Figure 1.3, a p-n junction provides the active medium which also acts as an optical waveguide and can be as simple as a high refractive index bulk semiconductor material or can contain a multiple quantum well stack set within a waveguide. To obtain laser action the requirements of population inversion and optical feedback must be met. A population inversion is accomplished by injecting a drive current along the length of the laser through contacts on the p- and n- doped sides of the laser diode. Usually, layers of semiconductor material are fabricated next to the active region to confine the current to a thin strip, carriers are then injected into the active region via the thin strip. Lasers may be classed as either multimode or single mode devices.

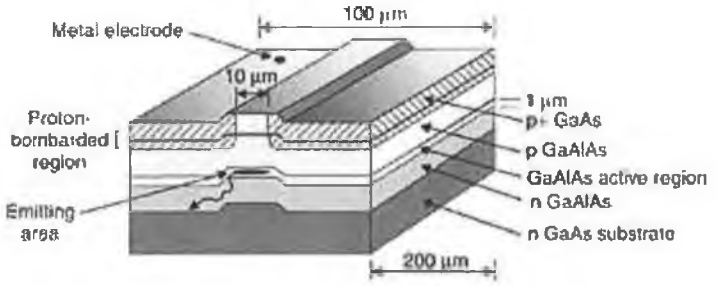

Fig 1.3 Schematic of diode laser [8]

(a) Multimode Lasers.

Fabry-Perot (FP) Lasers.

Optical feedback is provided by cleaving the ends of the semiconductor crystal to create mirrors at either end of the active medium forming a Fabry-Perot cavity. Standing waves, each of different frequency, are setup within the cavity and are referred to as longitudinal modes. The modes occur at wavelengths or frequencies where the electric field has an integral multiple of half wavelengths with zero magnitude at the mirror surfaces. The number of modes in the cavity is given by

$$f = \frac{mc}{2nL} \tag{1.1}$$

where m is an integer, c is the speed of light, n is the refractive index of the cavity and L the optical path length between the mirrors [1]. The frequency separation between each mode is given by

$$\Delta f = \frac{c}{2nL} \tag{1.2}$$

The output spectrum of the laser will contain only the modes which fall under the gain curve as shown in Figure 1.4 and such lasers are called multimode lasers.

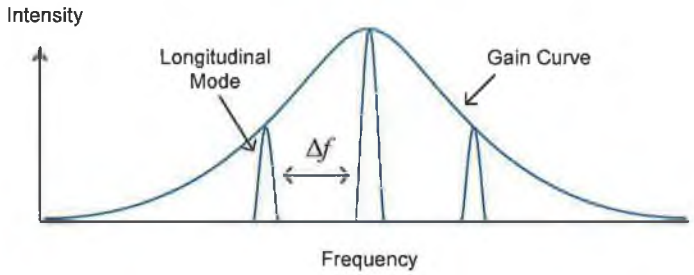

Fig 1.4 Gain Curve of FP Cavity

One of the major disadvantages of FP lasers is the multimoded output spectrum, shown in Figure 1.5. Each of these modes propagates with a different velocity in the fibre due to the refractive index of the fibre varying with wavelength. This can have a detrimental effect on the transmitted signal resulting in pulse broadening thereby limiting the bit-rate-distance product (BL).

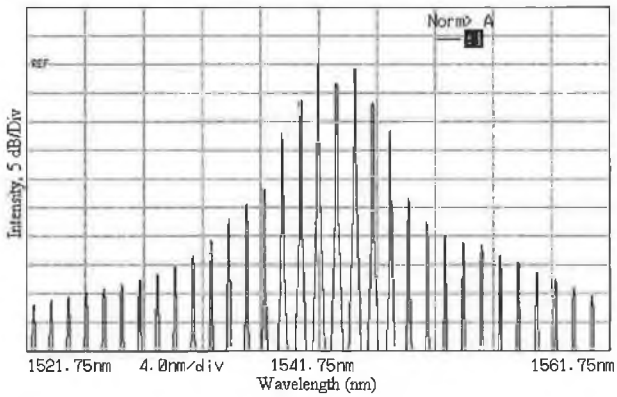

Fig 1.5 Continuous Wave Spectrum of a Fabry Perot multimode laser

(b) Single Mode Lasers.

A single mode output may be achieved through the use of distributed feedback (DFB) lasers or distributed Bragg reflector (DBR) lasers.

DFB Lasers

The feedback mechanism needed for laser action in a DFB is distributed throughout the cavity length and can be seen in Figure 1.6. This is achieved through the use of a grating etched on to one of the layers so that its thickness varies periodically along the cavity length. The resulting periodic variation of the refractive index provides feedback by means of the backward Bragg scattering which couples the forward and backward propagating waves.

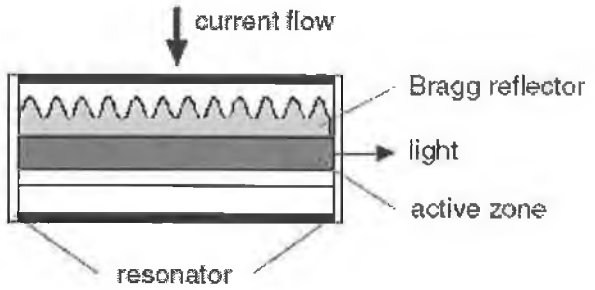

Fig 1.6 Schematic structure of a DFB laser [9]

Reflection at this periodic structure is wavelength sensitive, components reflected at each step are in phase if the periodic spacing Λ satisfies the Bragg condition

$$\Lambda = \frac{m\lambda}{2} \qquad (1.3)$$

where λ is the wavelength inside the laser medium and m is the order of Bragg diffraction induced by the grating [10]. Selecting an appropriate periodic spacing allows a single mode of oscillation for the laser as can be seen in Figure 1.7.

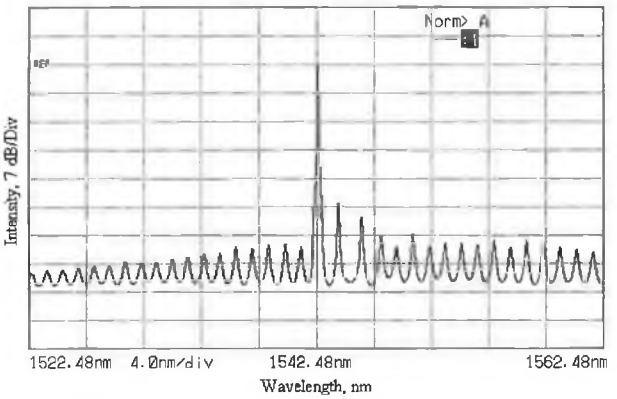

Fig 1.7 Continuous Wave Spectrum of a DFB laser

DBR Lasers

In DBR lasers the grating is etched near the cavity ends and the distributed feedback does not take place in the central active region, as can be seen in Figure 1.8. The unpumped corrugated ends act as wavelength selective mirrors while optical gain and wavelength tuning are provided by the active section and the Bragg section respectively.

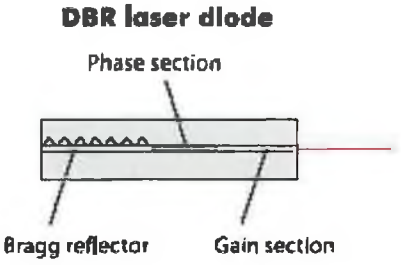

Fig 1.8 Schematic of a DBR laser [8]

1.3.1.3 Modulation

External Modulation

Also incorporated into the transmitter is a modulator which is used to vary the continuous light wave output from a laser diode. The modulator is placed in the optical path of the laser and an electrical signal representing the data stream acts upon the modulator which affects the CW light passing through the modulator and results in the output of an optical data signal. External modulation is most often performed using either electro-optic Mach-Zehnder modulators (MZMs) or electroabsorption modulators (EAMs) [11].

Mach-Zehnder Modulators.

The Mach-Zehnder modulator, depicted in Figure 1.19, operates by splitting light into two equal paths via a Y-splitter and then applying an electric field (voltage) to one of the arms inducing a refractive index change and thereby a relative phase shift between the two paths. The optical signals are then recombined and interfere with each other either constructively or destructively depending on the degree of phase shift. Constructive interference results when the waves are in phase and add together to give a higher output intensity. Destructive interference occurs when the waves are out of phase by 180^0 and cancel each other out resulting in no light.

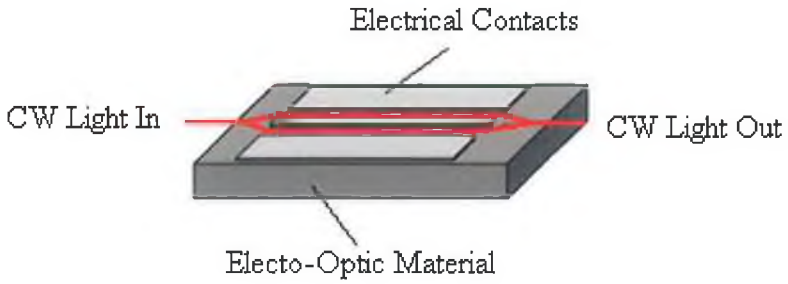

Fig 1.9 Mach-Zehnder modulator [8]

Electroabsorption Modulators.

The main materials used to fabricate EAMs as well as lasers, SOAs and photodetectors are III-V semiconductors which allow easy integration of EAMs with these components. Figure 1.10 shows the structure of an EA device. EA modulators operate via the electroabsorption effect; either the Franz-Keldysh effect in the bulk active layer or the quantum-confined Stark effect in multiple-quantum-wells [12]. Applying an electric field to a semiconductor material alters the band structure causing the amount of light absorbed to vary. By applying a reverse bias the light absorbed is increased and no light is transmitted, while applying no voltage to the EA modulator allows light to be transmitted.

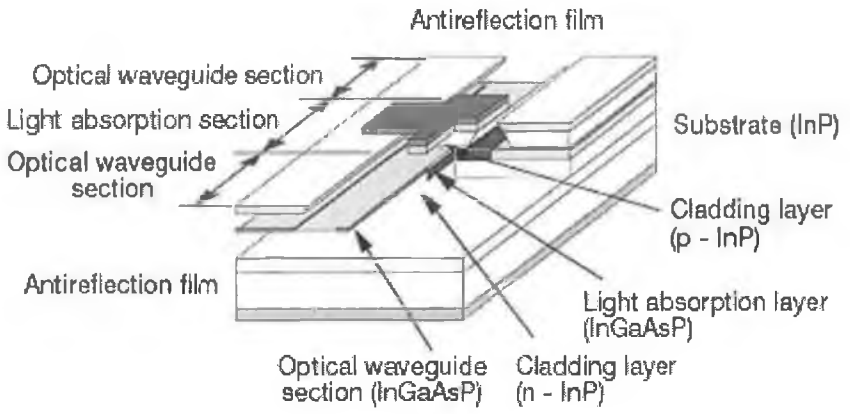

Fig 1.10 Structure of an EAM [13]

Direct Modulation

Direct modulation of the optical signal may be achieved by varying the voltage applied to the laser (i.e. bias and data) resulting in intensity modulation, as shown in Figure 1.11. The advantage of this method is the simplicity, lower cost and lower driving voltages. There are however two main drawbacks with direct modulation; the bandwidth is restricted by the laser diodes relaxation oscillation frequency and the creation of chirp produces a broadening of the spectrum. Chirp results from variations of the carrier density within the cavity which creates changes in the refractive index, which in turn varies the emitted wavelength.

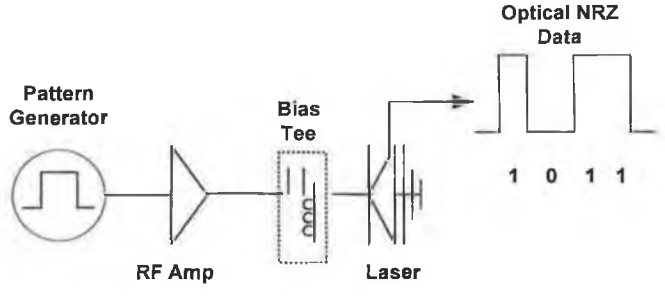

Fig 1.11 Direct Modulation

In contrast to direct modulation techniques, external modulators have negligible chirp because the modulating voltage is applied directly to the modulator, while the laser source remains at a constant voltage. However the disadvantage with external modulation is the extra cost of an additional component and the high insertion loss introduced to the system.

1.3.2 Fibre Medium

It has been recognised for a long time that light, with a carrier frequency of 10^{14} Hz, has the potential to be modulated at much higher frequencies than radio or microwaves and as a result allows for the possibility of a single communication channel with extremely high information content. However, one of the main problems in implementing this was that without some sort of guiding medium, any transmission would be limited to line of sight and subjected to the unexpected and uncontrollable changes of the weather. In 1870 John Tyndall demonstrated that light could be guided within a water jet due to total internal reflection but it was not until the mid 1960's that the idea of confining light within a circular cladded dielectric waveguide for use in communication systems was seriously considered [1]. The basic structure of such a guide, known as an optical fiber, consists of a core region surrounded by a cladding where the cores material has a higher refractive index than the cladding.

Optical fibres are available in two basic types; step index and graded index (GRIN), with both being divided into multimode and single-mode classes. Multimode fibre has a much larger core diameter compared to single mode fibre allowing many modes to travel through the waveguide.

1.3.2.1 Step Index Fibres

In step index fibres the refractive index remains constant across the diameter of the core and there is a sudden change in the refractive index at the core/cladding boundary. A step index single mode fiber is shown in Figure 1.12 which typicaly has a core radius of 5-10 μm and a cladding radius of 120 μm. Because of this, when light enters the optical fiber it propagates in just a single mode and experiences very little chromatic dispersion.

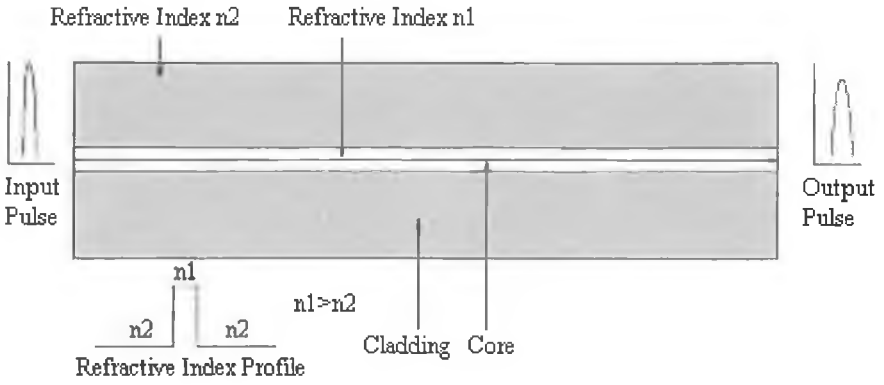

Fig 1.12 Single Mode Step Index Fibre [14]

In a multimoded step index fiber, shown in Figure 1.13, the core is relatively large compared to the cladding and there is a sharp change in the refractive index between the cladding and the core. The multiple modes result from this larger core diameter and from the fact that light will only propagate in the fiber core at discrete angles within the cone of acceptance. Light entering the core below the critical angle is guided along the fiber via total internal reflection. A disadvantage of multimode step index fibres is that they suffer from intermodal distortion which may be described as follows. When an optical pulse is launched into an optical fibre the optical power in the pulse is distributed over all of the modes of the fibre. Higher order modes, rays which entered the fiber at a higher angle, must travel further than lower order modes and so different modes arrive at the end of the fiber at different times resulting in distortion. This intermodal distortion maybe reduced by using a graded index profile in the fibre core.

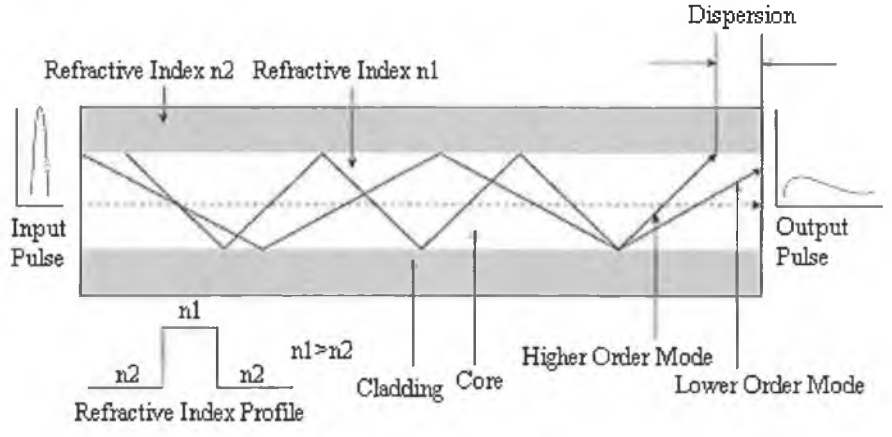

Fig 1.13 Multimode Step Index Fibres [14]

1.3.2.2 Graded Index Fibres

It can be seen in Figure 1.14 that for GRIN fibres the refractive index decreases from the core out towards the cladding. As a result the lower order modes experience a higher refractive index, so they travel slower than the higher order modes, which travel farther but move faster in the lower refractive index of the outer core region. The light rays no longer follow straight lines, but instead follow a serpentine path being gradually refracted back toward the centre by the continuously declining refractive index. This reduces the arrival time difference between the different modes and so they all arrive at the end of the fiber at about the same time.

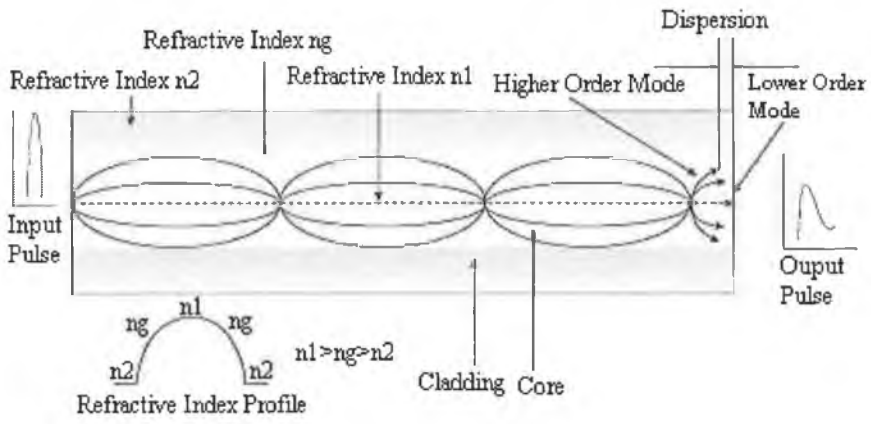

Fig 1.14 Multimode GRIN Fibres [14]

Although intermodal distortion is reduced in graded index fibres, it confines the use of multimode fibres to short or narrow band communication links. Long distance communications must use single mode fibres thereby avoiding the problems associated with intermodal distortion. However, these fibers still suffer from "intramodal dispersion", so called as it occurs within one mode. Intramodal dispersion is caused by material dispersion (chromatic dispersion), and waveguide dispersion.

1.3.2.3 Characteristic of Optical Fibres.

Material Dispersion

Material dispersion causes pulse spreading due to the dispersive properties of the material and arises because the refractive index of the fiber material is dependent on the wavelength. Pulse spreading occurs because every light source includes several wavelengths radiated by

the source, the components of the pulse will travel within the fibre at different velocities and arrive at the fibre end at different times, thus causing the pulse to spread.

Chromatic dispersion is the rate of change of the group delay with wavelength. In terms of the propagation constant, β_o, if it is expanded in a Taylor series [15], then

$$\beta(\omega) = \beta_0 + \beta_1(\omega - \omega_o) + 0.5\beta_2(\omega - \omega_o)^2 + \ldots \tag{1.4}$$

In this series, the term β_1 is the inverse of the group velocity,

$$\beta_1 = \frac{1}{v_g} \qquad \text{where} \quad v_g = \frac{d\omega}{dk} \tag{1.5}$$

and β_2 is the group velocity dispersion which causes the pulse broadening.

$$\beta_2 = \frac{\omega}{c}\frac{d^2 n}{d\omega^2} \tag{1.6}$$

The wavelength at which $\beta_2 = 0$ is called the zero dispersion wavelength.
The group velocity dispersion is related to the commonly used dispersion parameter D by the equation

$$D = -\frac{2\pi c}{\lambda^2}\beta_2 \tag{1.7}$$

To obtain the total dispersion, the material contribution must be added to the waveguide contribution. Generally the waveguide contribution to β_2 is negligible except near the zero dispersion wavelength at which point the two become comparable.

Waveguide Dispersion.

Waveguide dispersion is caused by the fact that light is being guided by a structure. After entering a single mode fibre the light pulse is distributed between the core and cladding. The major portion travels within the core while the rest travels in the cladding. Both portions travel at different velocities because the core and the cladding have different refractive

indices resulting in the pulse spreading. Waveguide dispersion in a standard single mode fiber (SSMF) is relatively small compared to material dispersion. An interesting feature of waveguide dispersion is that its contribution to D or (β_2) depends on the fibre design parameters such as the core radius and the core cladding index difference. This feature may be used to shift the zero-dispersion wavelength to 1.55 μm where the fibre loss is a minimum, as in dispersion shifted fibres (DSF).

Polarization Mode Dispersion.

All fibres have a certain degree of birefringence and have a core that is not perfectly circular over their entire length which leads to birefringence because of different mode indices associated with the orthogonally polarised components of the fundamental fiber mode. If the input pulse excites both polarisation components, it becomes broader at the fiber output since the two components disperse along the fiber because of the different group velocities. This phenomenon is particularly noticeable in single mode fibre transmission at ultra high bit rates.

Attenuation

It is important to consider the attenuation of a light signal as it propagates along a fiber as this is a major factor in determining the maximum transmission distance. The signal attenuation coefficient, α , expressed in decibels per kilometre, is defined as

$$\alpha = \frac{10}{L}\log\left(\frac{P_{in}}{P_{out}}\right) \tag{1.8}$$

where P_{out} is the optical output power from a fiber of length L and P_{in} is the optical input power [6]. This attenuation coefficient varies as a function of wavelength as can be seen in Figure 1.15.

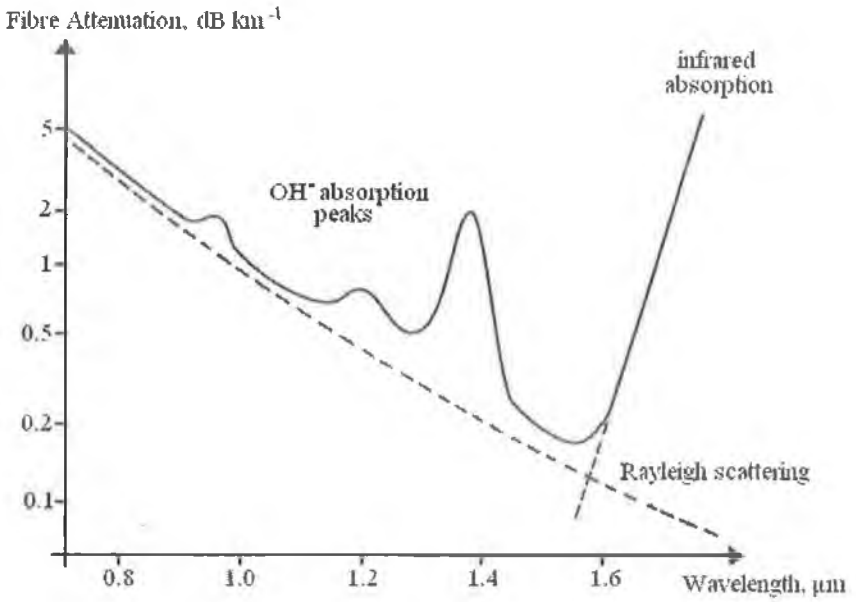

Fig 1.15 Attenuation versus wavelength for a glass optical fiber [15]

Attenuation of light in optical fibers is due to two physical processes; absorption and scattering. The dashed line in Figure 1.15 represents attenuation due to Rayleigh scattering caused by incomplete molecular bonds or variations in molecular spacing that result in photons being scattered out of the fiber by small refractive index variations in the glass. The peaks in the plot are due to absorption of light by molecules in the fiber, mainly due to OH ions created during the manufacturing process [15]. Conventional single mode fibers have two low attenuation ranges, one at about 1.3 µm and another about 1.55 µm. ITU-T G.652 recommends losses below 0.5 dB/km in the region of 1310 nm, and below 0.4 dB/km in the 1500 nm region with most SSMF typically having a loss of 0.2 dB/km [15].

1.3.3 Receiver

At the output end of an optical transmission line there must be a receiving device to interpret the information contained in the optical signal. The first element of this receiver is a photodetector. The photodetector detects the radiated power falling on it and converts the varying optical power into a correspondingly varying electric current. As the optical signal at the end of the optical fibre is usually weakened and distorted, the photodetector must meet very high performance requirements. These requirements include a high response or sensitivity to the wavelength range of the optical source, a minimum addition of noise to the system, and a fast response speed or sufficient bandwidth to handle desired data rate. The detector should also be insensitive to variations in temperature, have a reasonable cost in relation to the other components of the system and have a long life span. Semiconductor photodiodes are used almost exclusively in fiber optic systems due to their small size,

suitable material, high sensitivity and fast response time. The two types of photodiodes used are the pin photodetector and the avalanche photodiode (APD)

1.3.3.1 The pin Photodiode

Fig 1.16 pin Photodiode [16]

The pin Photodiode includes an extra intrinsic semiconductor layer between the p-type and n-type layers thereby improving on the standard pn junction. This synthetic increase in the depletion region increases the chances of intercepting a photon. Applying a small reverse biasing voltage can extend the depletion region which has a number of beneficial effects. In the standard construction of a photodiode light enters through the p-type layer, if this is now part of the depletion region, the chances of creating an electron hole pair in this critical region is improved as well as the efficiency of the device. The performance of pin photodiodes maybe improved by using a double-heterostructure design similar to that shown in Figures 1.16 and 1.17. The middle i-type layer is sandwiched between the p-type and n-type layers of a different semiconductor whose bandgap allows light in the wavelength region of 1.3-1.6 μm to be absorbed only in the middle layer. InGaAs is commonly used for the middle layer and InP for the surrounding p-type and n-type layers.

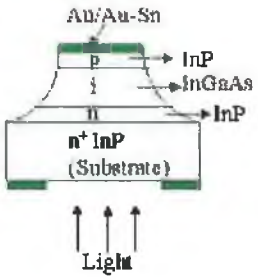

Fig 1.17 Design of an InGaAs pin Photodiode [16].

1.3.3.2 The APD

The avalanche photodiode provides considerably increased photocurrents by internally amplifying the number of charge carriers produced from a single photon interaction. This internal amplification is achieved by operating the diode with a reverse bias voltage of

approximately 100-200V, very near the breakdown voltage of the diode. Electron hole pairs are created when light enters the p layer and as electrons drift down towards the positive potential they are accelerated in a zone of high electric field created between the p and n layers. This gives each electron enough energy to excite another electron, through impact ionisation, into the conduction band, which in turn excite further electrons and so an avalanche of electrons is created. Each electron leaves a corresponding hole which moves upwards towards the negative potential, resulting in a large number of charge carriers created from a single photon interaction. Figures 1.18 shows a commonly used structure called a reach through avalanche photodiode that creates little excess noise during the carrier multiplication process.

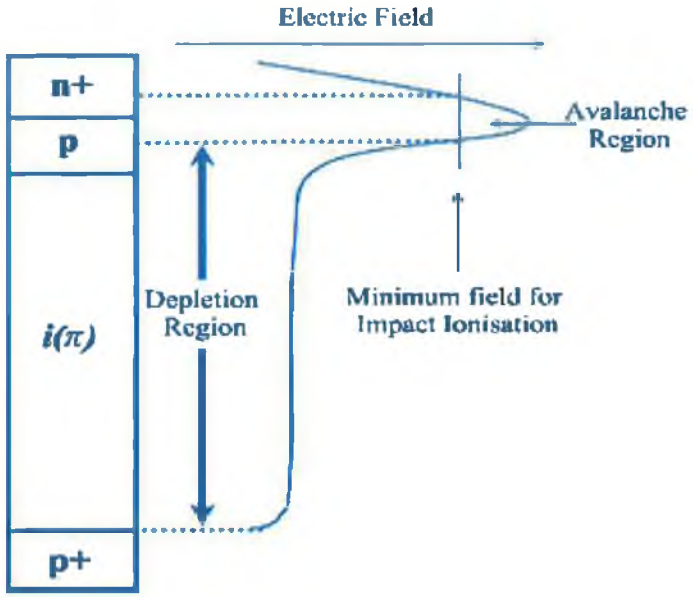

Fig 1.18 Reach-through avalanche photodiode structure

In general APD photodetectors have a much higher gain than pin photodetectors and are useful high sensitivity detectors, but pins have a much faster switching speed, and as a result have been largely deployed in high bit rate detection [15].

Now that we have looked at the components needed for a basic optical communications system we will take a look at two major methods of measuring system performance.

1.4 System Performance.

Bit Error Rate (BER)

The performance of a digital lightwave system is characterised through the bit-error rate (BER). The BER is usually defined as the average probability of incorrect bit identification, for example a BER of 10^{-6} corresponds to an average of one error per million bits. Most lightwave systems specify a BER of 10^{-9} as the operating requirement. The BER depends on interchannel interference, optical power at the receiver with respect to the sensitivity of the receiver, modulation technique and noise sources. An important parameter that is indicative of receiver performance is the receiver sensitivity and is defined as the minimum average received optical power for which the BER is 10^{-9}. Receiver sensitivity depends on the signal to noise ratio (SNR), which in turn depends on various noise sources that corrupt the signal received.

Eye Diagrams

Eye diagrams are a very successful way of quickly and intuitively assessing the quality of a digital signal. A properly constructed eye should contain every possible bit sequence from simple 101's and 010's, as shown in Figure 1.19. The size of the interior region of the eye pattern, known as the eye opening, can reveal information such as the rise time, over shoot, dispersion, and jitter. While the width of the eye opening shows the amount of inter-symbol interference that may be tolerated and the height relates the noise margin of the system.

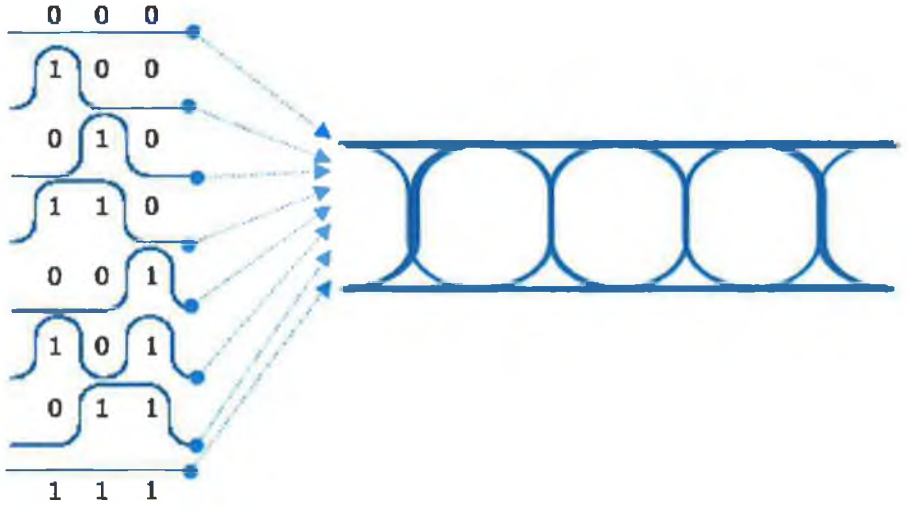

Fig 1.19 Overlapping of bit sequence to form an eye diagram [17]

Although the channel capacity of a basic optical communication system is larger by a factor of nearly 10,000 than that of microwave systems, they still operate well below this capacity, mainly due to the speed of currently available electronics. To overcome this limitation it is necessary to use optical multiplexing techniques to increase the number of optical data channels per fiber and thereby increase the aggregate data rate [18].

Line Codes

The type of modulation format employed is also an important consideration as it can enhance the system performance. Non-return-to-zero (NRZ) and return-to-zero (RZ) are the most common types. With the RZ format each optical pulse representing a 1 is shorter than the bit slot and its amplitude returns to zero before the bit duration is over. In the NRZ format the optical pulse remains on throughout the bit slot and its amplitude does not drop to zero between two or more successive logic 1's. The RZ code is more stable than NRZ for long haul high-speed transmission as it is more resilient to dispersion and non-linearities while also offering higher receiver sensitivities [19].

Summary.

A brief introduction to the historical origin of optical communications has been given followed by a discussion on the capacity of various communication methods and the advantages of using optical fibers. A basic optical communication system comprising of a transmitter, transmission medium and receiver has also been described. The chapter concluded with descriptions of bit error rates and eye diagrams to qualitatively and quantitatively measure the system performance. Modulation formats were also discussed. The following chapter will discuss the need for high-speed networks and describe various multiplexing techniques used to achieve higher data rates.

References

[1] G. Keiser, "*Optical Fibre Communications*", McGraw Hill, 3rd Ed., 2000.

[2] D. K. Mynbaev, L. L Scheiner, *"Fiber-Optic Communications Technology"*, Prentice Hall, 2001.

[3] L. A. Reith and P. A. Shumate, *"Coupling Sensitivity of an Edge Emitting LED to a single mode fiber"* J. Lightwave Technol., pp. 29-34, Jan. 1987.

[4] D. N. Christodoulides, L. A. Reith, and M. A. Saifi, *"Theory of LED coupling to single mode fibers"* J. Lightwave Technol., pp. 1623-1629, Nov. 1987.

[5] T. Ohtuska, N. Fujimoto, K. Yamguchi, A. Taniguchi, H. Naitou, and Y. Nabeshima, "*Gigabit Single-Mode Fiber Transmission Using 1.3-pm Edge-Emitting LEDs for Broad-Band Subscriber Loop"* IEEE J. Lightwave Technol., pp. 1534-1541, Oct 1987.

[6] J. Wilson, J. Hawkes, "*Optoelectronics an introduction*", Prentice Hall, 3rd Ed., 1998.

[7] http://zone.ni.com/devzone/conceptd.nsf/webmain.

[8] http://www.educatorscorner.com/media/LW_Back2Basics_Optical_Comm.pdf

[9] http://privatewww.essex.ac.uk/~mpthak/Basics%20of%20Laser%20Diodes.pdf

[10] J. C. Palais, *"Fibre Optic Communications"*, Prentice Hall, 5th Ed., 2005

[11] J. T. Gallo, R. Whiteman, *"Optical Modulators for Fiber Systems"*, IEEE GaAs Digest, 2003.

[12] G. L. Li, P. K. L. Yu, *"Optical Intensity Modulators for Digital and Analog Applications"*, IEEE J. Lightwave Technol., vol. 21, pp. 2010-2030, Sept. 2003.

[13] K. Nagai, H. Wada, *"40 Gb/s EA Modulators"*, OKI Technical Review, vol. 69, no.2. April 2002.

[14] http://www.ciscopress.com/articles/article.asp

[15] S.V. Kartalopoulos, "*DWDM Networks, Devices and Technology*", Wiley Interscience, 2003.

[16] G. P. Agrawal, "*Fiber-Optic Communication Systems*", Wiley Interscience, 2 Ed, 1997.

[17] http://www.bertscope.com/Literature/Primers/Eye_Anatomy.pdf

[18] L. Barry, P. Guignard, J. Debeau, R. Boittin, M. Bernard, *"A High-Speed Optical Star Network Using TDMA and All-Optical Demultiplexing Techniques"*, IEEE J. Select. Areas Commun., vol. 14, no. 5, pp. 1030-1038, 1996.

[19] J.X Cai, M. Nissov, C. R. Davidson, A. N. Pilipetskii, G. Mohs, H. Li, Yi Cai, E. A. Golovchenko, A. J. Lucero, D. G. Foursa, and N. S. Bergano, *"Long-Haul 40 Gb/s DWDM Transmission With Aggregate Capacities Exceeding 1 Tb/s"*, IEEE J. Lightwave Technol., vol. 20, no. 12, pp. 2247-2258, Dec 2002.

2. High-Speed Optical Networks

Introduction

This chapter introduces the origins of optical multiplexing and describes the basic operation of two of the most common optical multiplexing techniques, namely wavelength division multiplexing (WDM) and optical time division multiplexing (OTDM). A brief outline of the main components of each technology is given along with a description of the fiber parameters which can have a detrimental affect on the performance of both systems. Emphasis is placed on some important features of a pulse source to be used in an OTDM system before describing a hybrid system which combines the merits of both WDM and OTDM.

2.1 Need for High-Speed Networks

The demand for bandwidth continues to grow, mainly driven by the massive increase in internet usage and other high capacity features such as high definition TV, high resolution video conferencing and high performance computing. As a result, it will be necessary to have communication networks that can handle these very high data rates. Current technologies such as copper wire, radio or satellite communication systems lack the bandwidth needed to cope with these higher data rates and as a result optical networks are seen as the only possibility to provide the necessary bandwidth. However, this increasing demand for higher bandwidth will require much higher transfer capacities per optical fiber than currently available. There are a number of ways to increase the transmission capacity of a fiber. One way is to increase the bit rate of a single channel, which requires higher speed electronics. A second method is to increase the number of data channels per fiber by multiplexing the base data rate to increase the overall transmission capacity. Multiplexing may be carried out via frequency division multiplexing (FDM) or time division multiplexing (TDM), both of which can be realized in the electrical or optical domain. In the optical domain FDM is known as wavelength division multiplexing (WDM) and TDM is known as optical time division multiplexing (OTDM). For a long time electrical time division multiplexing (ETDM) had been the method used to combine information channels.

2.2 ETDM in Optical Networks

In an ETDM communication system, depicted in Figure 2.1, messages are multiplexed in the electrical domain. The multiplexed electrical signal then modulates an optical source, such as a laser, in the electro-optic (EO) converter which converts it to an optical signal. The optical signal travels down the fiber until it reaches the receiver where it is detected in the opto-electric (OE) converter and converted back to an electrical signal. This received signal is then demultiplexed and each electrical message is sent to its intended destination. The multiplexed bit rate may be defined as nB, where n is the number of channels and B is the bit rate of each channel. The capacity of ETDM is mainly limited by the speed of the electronics which results in the formation of bottlenecks that occur in the multiplexer, EO and OE converters and the demultiplexer, where the electronics have to operate at the full multiplexed bit rate. These bottlenecks arise due to a number of reasons, including; the speed limitations of digital integrated circuits and of high power/low noise linear amplifiers used to drive the laser or modulator in the EO and OE converters and also because of the limited bandwidth of lasers and modulators [1]. Experimental demonstrations have shown that the technique of ETDM could be used to achieve bit rates of 40 Gb/s [2, 3, 4, 5]. More recently, experiments have shown rates of 85.4 and 107 Gb/s are attainable [6, 7], however it is important to note that the current commercial operating limit of ETDM is around 10 Gb/s [8].

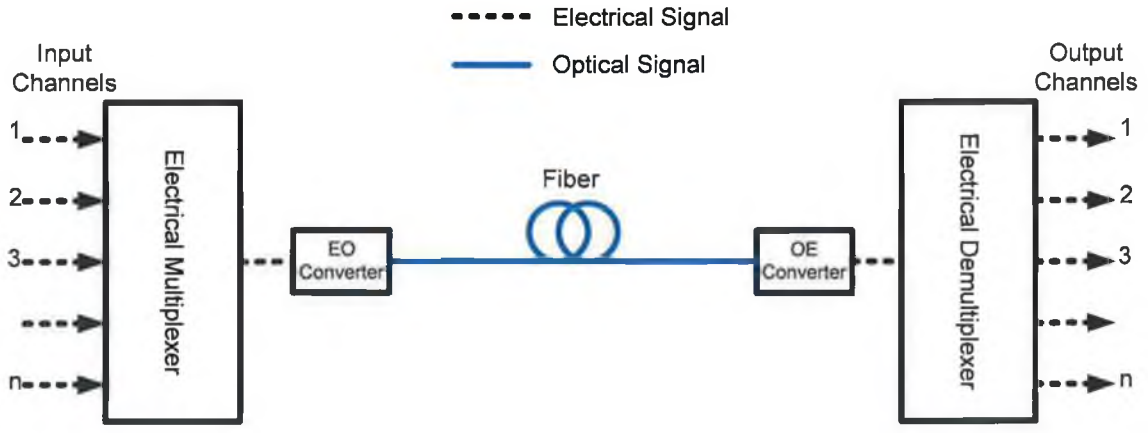

Fig 2.1 Schematic of a basic ETDM communication system

As the ETDM bit rate of commercial systems is restricted by the speed of electronics, alternative technologies for the development of high-speed networks have to be considered. If the multiplexing and demultiplexing stages are carried out in the optical rather than the electrical domain, then the previously mentioned bottlenecks could be avoided. WDM eases

this problem by taking the 10 Gb/s electrical bit rate and optically multiplexing many channels, for example 16, to increase the bit rate to 16 x 10 Gb/s or 160 Gb/s. Consequently ETDM and WDM technologies typically make up today's fiber optic networks.

2.3 WDM

The basic principle of WDM is to use the wavelength of light as a degree of freedom to simultaneously transmit a number of different wavelength signals through a fiber. WDM technology was aimed at upgrading the capacity of installed point to point transmission systems. Initial development involved adding two, three or four additional wavelengths separated by several ten or even hundreds of nanometers in wavelength [9]. The operating principle of a WDM system is shown in Figure 2.2. The electrical data is modulated onto optical carriers each emitting at different discrete wavelengths. The modulation process may be carried out by either direct or external modulation. The first transmitter, TX 1, generates a data stream at wavelength λ_1, TX 2 uses λ_2 and so on. All these signals are combined by a multiplexer (coupler) and then transmitted over a single optical fiber. A demultiplexer, at the receiver end, can extract a single channel from the aggregate signal via a tunable optical filter (TOF) or can separate the aggregate signal into individual channels using an arrayed waveguide grating (AWG). The chosen channel/s can then be directed to the appropriate receiver/s.

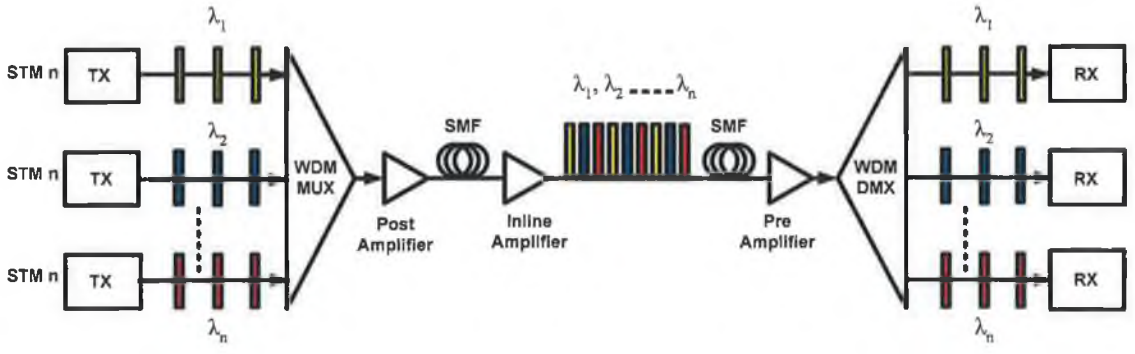

Fig 2.2 Basic WDM transmission system with N different wavelength channels.

Wavelength division multiplexing allows parts of the optical spectrum, depending on the optical amplifier used, to be divided up into discrete wavelengths (channels) with each wavelength allocated to an individual channel. This process is similar to frequency division multiplexing in radio technology. Generally in WDM systems, transmission is usually kept to the Conventional (C) band (1535 – 1560 nm) in order to utilize current amplification technology, and also because of the low loss transmission window at 1.5μm for standard

singe mode fiber. The spacing between the channels within this band has been laid out by the International Telecommunications Union (ITU). The standard channel spacing involves increments of 25, 50, 100, 200 and 400 GHz, corresponding to wavelength spacing of 0.2, 0.4, 0.8, 1.6 and 3.2 nm at 1550 nm. When the wavelength spacing is on the order of a nanometer, it is common to refer to such systems as dense wavelength division multiplexed (DWDM) systems, although no formal definition has been established [9]. Some major advantages of WDM systems are that they are transparent to bit rates, protocol and modulation formats.

Some challenging issues of WDM networks that wish to exploit the fiber bandwidth include developing broadband, rapidly tunable laser sources to achieve a large number of closely spaced channels, fiber non-linearities and the spectral dependence of the amplifier gain. All these conditions determine the maximum number of wavelength channels and the transmission distance [10].

2.3.1 Enabling Technologies

Two of the main technologies used in WDM systems include, optical filtering, for wavelength-division multiplexing and demultiplexing and broadband optical amplification [11], both of which are described below.

Optical Amplifiers

The first practical optical amplifier was the erbium doped fiber amplifier (EDFA), and it is still the dominant amplifier technology. By 1991 it was apparent that they would be widely used in long-haul optical fiber communications systems. Systems based on EDFAs were much cheaper than systems based on electronic repeaters, as each channel required a repeater, and they avoided the necessary opto-electric conversion. Also, they took advantage of the broad gain bandwidth of erbium to transmit many wavelengths at once. Due to their large gain and high output powers, the spacing of amplifiers could be increased to two or three times that of electronic repeaters which helped to significantly reduce the cost of transmissions systems [12]. EDFA's show a relatively flat gain spectrum from 1540-1560 nm and belong to a category of amplifiers called rare earth doped fiber optical amplifiers which also include the following amplifiers; Thulium-Doped fiber amplifiers that operate between 1440-1520 nm, Neodymium-doped fiber amplifiers which amplifies light at about 1400 nm and Tellurium based Erbium doped fiber amplifiers that provide amplification in the C and L bands 1532-1608 nm [13]. Other types of amplifiers include Raman amplifiers which can also be used in conjunction with EDFAs to enhance amplification and extended

the distance before regeneration is needed. In its most basic form, shown in Figure. 2.3, an EDFA contains a section of erbium doped fiber (EDF), a pump laser and a coupler for combing the signal and the pump power. The core section of the EDF contains approximately 10^{18} erbium ions/cm^3, which is then pumped using a 980 nm or 1480 nm laser. An optical isolator is also incorporated to prevent back reflections.

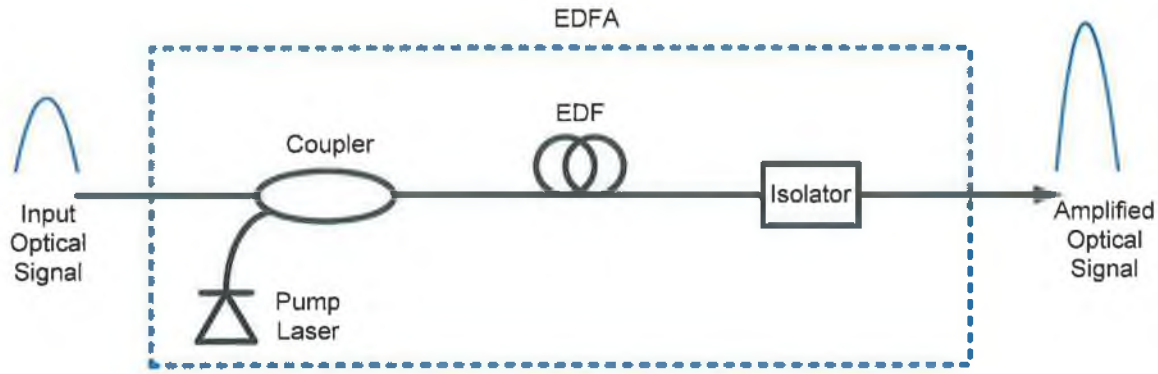

Fig 2.3 Schematic of EDFA

In terms of their use in WDM systems, slightly different characteristics of EDFAs are required at various points along the link. A post amplifier, or booster amplifier, placed immediately after the transmitter, is designed to provide maximum output power, not maximum gain, and raises the power of an optical signal to the highest level, maximizing the transmission distance. This relieves pressure on the transmitter to produce maximum optical power, which can degrade the quality of the signal. An inline amplifier has moderate gain, noise and saturation output characteristics. Gain flatness is a major requirement for in-line amplifiers because there are usually many of them cascaded along the long distance link. If the gain varies significantly at different wavelengths then there will be a difference in power of multiplexed channels. The preamplifier is placed directly in front of the receiver and is used to amplify a weak optical signal after a long transmission. Its major features should be low noise, high gain and high sensitivity.

Filters

Optical filters are used in WDM systems to perform simple filtering in multiplexers and demultiplexers along with advanced functions such as gain equalization, channel monitoring and dynamic provisioning in optical add drop multiplexers (OADMs) [14]. Optical filtering is based on interference or absorption and they are distinguished as fixed optical filters and tunable optical filters (TOF). Fixed optical filters are made for a specific application and a specific narrow slice of the spectrum, they are simpler and less expensive compared to

tunable optical filters. The most common parameters specific to filters are; passband, finesse (FP filter), cutoff wavelength and extinction ratio. TOFs are constructed with passive or active optical components and provide the flexibility to select a range of wavelengths. The following requirements must be met for TOFs to be useful in optical communication systems; wide tuning range, narrow bandwidth, fast tuning, low cross talk and insensitivity to temperature. Some common filters used in optical networks include Fabry-Perot (FP) interferometers, fiber Bragg gratings (FBG) and arrayed waveguide gratings (AWG) which are described below.

The Fabry Perot interferometer consists of two parallel reflectors separated by a small distance from each other forming an FP etalon. Multi-wavelength signals travel back and forth within the cavity with some wavelengths, known as the resonant wavelengths of the cavity, adding in phase and being transmitted. The number of wavelengths that can pass through the FP resonator without severely interfering with each other determines the finesse of the filter. The higher the finesse, the narrower the resonant linewidth. Tunable FP filters can be attained by varying the cavity length.

Fiber Bragg gratings, shown in Figure 2.4, are similar to FP interferometers and have many uses such as narrow bandpass filters, band rejection filters and add-drop filters. They consist of a segment which has a periodically varying refractive index along its core, which is formed by exposing the core to an intense ultraviolet optical interference pattern. It works as a highly reflective narrowband mirror, reflecting one wavelength and transmitting all others. The wavelength being reflected is called the Bragg wavelength (λ_B) and is determined by the Bragg condition:

$$2\Lambda n_{eff} = \lambda_B \tag{2.1}$$

Where Λ is the grating period and n_{eff} is the effective core refractive index [15].

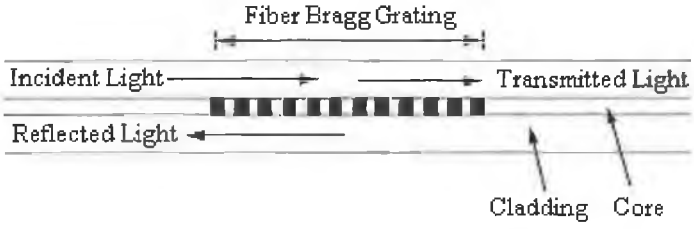

Fig 2.4 Schematic structure of fiber Bragg grating [15].

Tuning of the Bragg grating (varying the Bragg spacing), can be achieved by either mechanical or thermal means.

Another useful filter is the arrayed waveguide grating (AWG) which uses an array of waveguides whose lengths differ by a set amount [16]. The difference in length varies the phase of the light travelling in each waveguide with respect to each other. This results in a wavelength dependent diffraction pattern and each wavelength is then directed to different output fibers thereby acting as a wavelength multiplexer or demultiplexer.

As already mentioned, much higher transfer capacities per fiber than is currently available will be needed to satisfy the increasing demand for bandwidth. Whether this will be achieved by a higher number of wavelengths per fiber or by higher bit rates per wavelength is still an open issue. It is also possible that by combing both technologies the demand for bandwidth may be satisfied. Generally for data rates of 80 Gb/s or more per wavelength, OTDM has to be applied as electronic processing is not yet possible at these high-speeds [17]. Compared to WDM, OTDM is not as mature and has been limited to high-speed experiments. In the short term, potential applications are limited to systems requiring extremely high transmission speeds, such as high resolution medical imaging systems or arrays of radio telescopes [18]. In the long run, OTDM is seen as a viable alternative for transmitting large volumes of data that are currently divided into many optical channels using WDM.

2.4 OTDM

OTDM was first proposed around 1988 to overcome the speed limitations of electronic devices in ETDM systems by multiplexing optical data channels in the temporal domain [1]. OTDM systems mainly operate in the 1.55 μm transmission window because of the availability of Erbium Doped Fiber Amplifiers (EDFA's). A vital component for OTDM transmission is a source of RZ pulses because a number of pulses must be time interleaved within the bit period to generate a much higher aggregate signal [19].
This thesis focuses on the generation of optical pulses for use in high-speed optical networks, and, careful consideration is given to some of the important parameters of these pulses. Various pulse generation techniques are discussed in detail in Chapter 3.

2.4.1 General System

The basic configuration for an OTDM system is shown in Figure 2.5. A vital component of this system is a source of ultra short optical pulses, generated at a repetition rate R. The pulse train is split using a passive optical fiber coupler into N different channels before each channel is passed through a modulator to be modulated with electrical data, operating at a bit rate B, where R = B. The output from each modulator is essentially an optical RZ data

channel with the data being represented by ultra short optical pulses. Each channel is passed through a fixed fiber delay line which delays it by $\frac{1}{RN}$ relative to the adjacent channel, in a process known as bit interleaving. The N modulated and delayed optical data channels are then recombined using another passive fiber coupler, forming the OTDM data signal. The multiplexed signal is then transmitted over the fiber before arriving at the receiver where it is then demultiplexed.

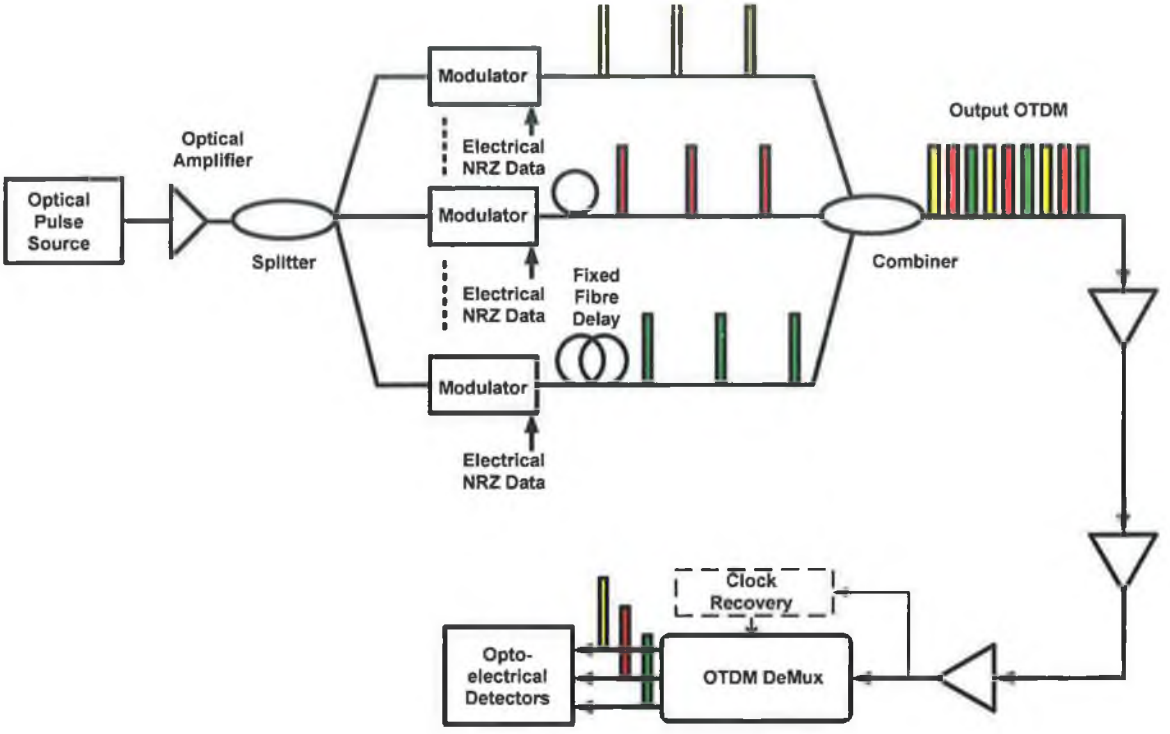

Figure 2.5 Schematic of generalised OTDM system.

In order to achieve very high-speed OTDM transmission systems, it is necessary for optical pulse sources to generate picosecond transform limited (chirp free) pulses at high repetition rates. There are a number of ways to generate ultra short pulses for use in OTDM systems including; mode locking of a semiconductor laser, Q-switching, gain switching and pulse shaping using an external modulator, all of which are described in more detail in the next chapter. As already mentioned, the optical pulse source is one of the most important components in a high-speed OTDM network and for optimum performance, the pulse sources need to satisfy certain requirements, the most important of which are outlined below.

Pulse Parameters

Pulse Width: The pulse width of the optical signal determines the upper limit of the aggregate bit rate [20] and must be significantly less than the allowed timeslot to avoid crosstalk. As a rule of thumb, for long distance high capacity transmission, a duty cycle of about a third is required [21]. As shorter pulses have a wider optical spectrum, decreasing the pulse width may increase dispersion resulting in a compromise between system crosstalk and pulse spreading caused by dispersion [1].

Spectral Width: The transmission length is one of the factors influenced by the pulse spectral width. As a result pulses have to be as spectrally pure as possible to minimize pulse broadening due to the interaction of source chirp with fiber chromatic dispersion. The figure of merit used is the time-bandwidth product, $\partial v \partial t$, where ∂v is the spectral width and ∂t is the temporal width. Optimum systems performance can be better achieved if the pulses are transform limited, i.e. the spectral width of the pulse is as small as possible for a given pulse width [22]. The transform limited value of the time bandwidth product for a Gaussian pulse is 0.44 and 0.31 for a secant pulse.

Side Mode Suppression Ratio (SMSR): The SMSR of an optical pulse is a measure of the intensity difference between the main longitudinal mode and the largest side mode and usually expressed in decibels. Generally an SMSR of >30 dB is preferred for optical communication systems (in particular, multi-channel systems employing optical pulses). Any less than this can result in the build up of noise on the optical pulses due to mode partition noise [22].

Temporal Pedestal Suppression Ratio (TPSR): For high-speed OTDM transmission at 40 Gb/s and above, a poor TPSR can severely limit the performance of the system by creating interference noise between individual channels (inter-symbol interference). For better system performance a TPSR of over 30 dB is required [23].

Timing Jitter: Another factor affecting the performance of high-speed OTDM systems is timing jitter. This can limit the overall data rate by limiting the number of channels in an OTDM system and can also affect the BER by adding errors caused by the uncertainty of a pulses position within the bit period [24]. Timing jitter can be classed as either correlated or uncorrelated. Correlated jitter is negligible but uncorrelated timing jitter, which is related to spontaneous noise and pulse turn-on dynamics, has much larger amplitude and is the dominant contribution to the total timing jitter [25].

Multiplexer

High-speed multiplexing / demultiplexing is the process where channels of the lower digital hierarchy signals are multiplexed to those of the higher hierarchy signals (MUX) and visa versa (DEMUX) and is one of the key functions to achieve ultra high-speed optical transmission [26]. The operation of multiplexing may be described as three sub functions; sampling, timing and combining. Sampling identifies the base band data stream, determining the value of each incoming bit. Timing ensures the samples are available at the right time slots on the multiplexed channel and the combining function assembles all the base band data streams to create the higher bit rate multiplexed data stream [1]. Sampling can be carried out using on optical modulator to sample incoming electrical data (STM-n) with ultra short pulses, creating N optical RZ data channels. The value of the electrical data stream is represented by an optical pulse in a bit slot to correspond to a one or no optical pulse to correspond to a zero. Timing is achieved by delaying the modulated pulse stream by 1/NR relative to adjacent channels. Combining these channels together to form the higher aggregate data rate is done using a coupler. The interleaved signal then has a data rate of N x STM-n. This interleaving may be carried out either by bit interleaving or packet interleaving.

Demultiplexer

The demultiplexer is the most critical element of an OTDM system and may be achieved either electrically or optically depending on the aggregate bit rate. Electro-optic demultiplexing commonly uses electro-absorption (EA) and Mach Zehnder (MZ) modulators which have suitable characteristics to allow channels from the data stream to be removed or added [18]. The modulators can pick out a base channel data rate up to 40 Gb/s but to fully demultiplex the aggregate data stream a modulator is required for each channel. Above 40 Gb/s it is necessary to use all-optical switching techniques which are based on optical non-linearities in an optical fiber or a semiconductor device [27, 28]. In this case, the OTDM signal and a high power ultra short optical control signal are inserted into the non-linear device. The control signal operates at a rate equal to the base rate of the OTDM signal and is synchronised to one of the OTDM channels to demultiplex it from the other high-speed channels.

2.5 Performance Limitations of WDM and OTDM Systems

There are a number of limitations imposed on optical transmission by the fiber medium which degrade the optical signal and limit the system performance. These limitations maybe broadly classified as linear and non-linear effects. Attenuation and dispersion are classed as linear while the remaining non-linear effects include; Self Phase Modulation (SPM), Cross Phase Modulation (XPM) and Four Wave Mixing (FWM), each of which is described further below.

Attenuation

Fiber attenuation varies significantly with wavelength, losses in the 1310 nm region are about 0.35 dB/Km and about 0.2 dB/Km in the 1550 nm window. This can cause unequal channel powers when the channel spacing is very large for example in coarse wavelength division multiplexing (CWDM). Optical amplifiers are used to overcome attenuation by amplifying all signals within their specific operating range. To accommodate more channels, the channel separation maybe decreased, but this increases the chances of non-linear effects degrading the system performance. Also as the gain of an amplifier is not entirely flat over the C band, this causes different signal-to-noise ratios (SNR) for different channels, degrading the overall system performance.

Dispersion

Material (chromatic) dispersion is the most detrimental type of dispersion faced by WDM systems as it results in broadening of the optical signal in time which in turn leads to intersymbol interference (ISI) and ultimately limits the transmission distance. It arises because the refractive index of the fiber is dependant on the wavelength which causes different wavelengths to travel at different speeds down a fiber. A few ways to compensate for this dispersion would be to incorporate dispersion compensating fiber (DCF) or chirped fiber Bragg gratings (FBG). Using these mentioned techniques exact compensation is achieved for only one wavelength. Consequently, other wavelengths experience different compensation resulting in residual dispersion that accumulates over distance. To compound the problem, each of the different channels in a WDM system will experience a different dispersion factor making it necessary to consider the rate of change of dispersion with wavelength (dispersion slope). Small pulse widths in high bit rate OTDM transmission systems are more susceptible to dispersion due to the wider spectrum which can lead to cross talk between adjacent channels and in turn a loss of signal integrity due to ISI.

Non-linear Effects

There are two categories of non-linear effects. The first arises due to the interaction of light waves with phonons in the silica medium, also called non-linear inelastic scattering. The two main effects in this category are stimulated Brillouin scattering (SBS) and stimulated Raman scattering (SRS). The second and main category of interest arises due to the dependence of the refractive index on the intensity of the applied electric field. This produces effects such as self phase modulation (SPM), cross phase modulation (XPM) and four wave mixing (FWM). These are the most important effects for WDM and OTDM systems.

SPM, which is present in both single and multi-wavelength systems, arises because the refractive index of the fiber has a weak dependence on the intensity of the optical signal and is given by

$$n = n_0 + n_2 I = n_0 + n_2 \frac{P}{A_{eff}} \qquad (2.2)$$

Where n_0 is the ordinary refractive index of the material, n_2 is the non-linear coefficient, P is the power and A_{eff} is the effective area [15]. This non-linear refractive index causes a phase shift proportional to the intensity of the pulse, and so consequently, different parts of the pulse experience different phase shifts that result in chirping of the pulse. As a result, the rising edge of an unchirped pulse experiences a red shift in frequency (toward lower frequencies), seen in Figure 2.6, and the trailing edge experiences a blue shift (toward higher frequencies). This chirping is proportional to the signal power meaning that SPM is more pronounced in systems using high transmitted powers. Also, the SPM induced chirp affects the pulse broadening effects of chromatic dispersion and so it is important to consider this for high-bit-rate systems that already have significant chromatic dispersion limitations [9].

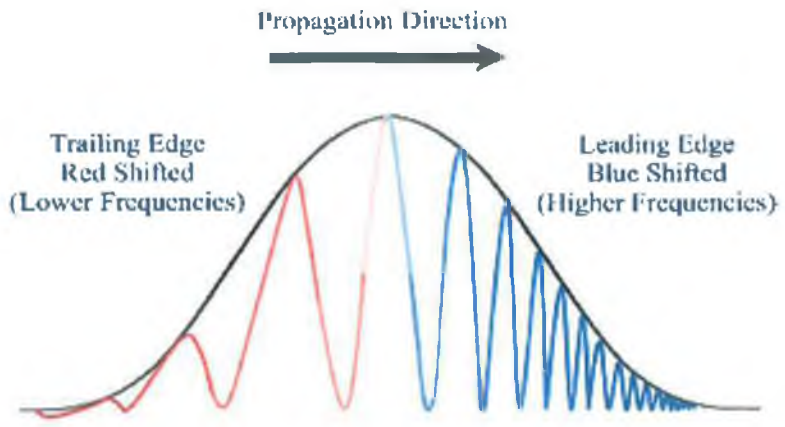

Fig 2.6 SPM induced frequency chirp

XPM also arises from the refractive index non-linearity in multi-channel (WDM) systems, which converts power fluctuations in a certain wavelength channel to phase fluctuations in other channels. When several channels propagate in a fiber, the non-linear phase shift of a specific channel depends on the power of that channel as well as the power of the other channels. XPM hinders systems performance via the same mechanisms as SPM; frequency chirping and chromatic dispersion, and for pulses of equal intensity, it introduces twice the amount of distortion as SPM [29]. The influence of XPM becomes greater with the increase of more wavelength channels.

FWM is an effect where two signals on different wavelengths interact through the non-linear refractive index of the fiber, to generate additional sum and difference frequencies. Consequently, FWM does not occur in single wavelength OTDM networks. The magnitude of these new components depends on the channel separation (increasing with decreasing separation), the fiber dispersion (increasing as dispersion decreases) and the power per channel. Performance degradation is caused in two ways: first, the generation of new components at different frequencies represents a loss of signal energy and hence an increase in the bit error rate; second in systems with a large number of equally spaced channels the new components may fall directly on frequencies allocated to other channels; this can cause severe crosstalk. A number of techniques are available to overcome this limitation, one of which involves combing standard fiber sections with dispersion compensating fiber sections to significantly reduce the generation and accumulation of FWM components [30].

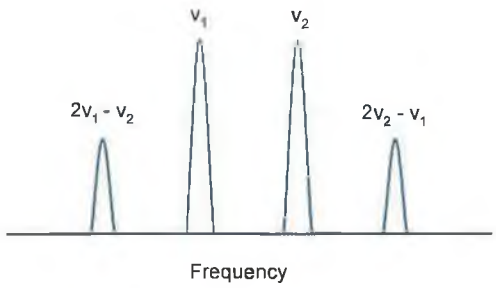

Fig. 2.7 Two optical frequencies mix generating two third order side bands.

2.6 Hybrid WDM/OTDM Networks

As we have seen, OTDM can be used to increase the bandwidth of a single wavelength channel. However, it can also be combined with WDM to increase the network capacity further [10]. To increase the speed of optical communication networks and push them into the Tb/s realm, problems with both WDM and OTDM must be addressed. For high capacity WDM networks, broadband amplifiers are needed to support the large frequency span, creating design and cost problems because the attenuation coefficient of the fiber and the gain of the optical amplifiers are both wavelength dependant. The increase in wavelengths can cause problems when attempting to compensate for dispersion as each wavelength is not compensated to the same degree which results in residual dispersion that accumulates over distance. Also the separation between channels will have to be reduced to allow for further expansion, increasing the chances of non-linear effects degrading system performance. For OTDM systems operating at 1 Tb/s, the bit slot is set at 1 ps and so sub-picosecond pulses are required. Assuming transform limited pulses, the spectral width would be about 12 nm (THz range) making dispersion management very difficult. The small bit slot also brings about the need for greater timing accuracy and requires timing jitter to be dealt with precisely. The major advantage of combining both WDM and OTDM schemes, first proposed by Ali and Fussgaenger in 1986 [31], is that neither one is pushed to their limits. Other advantages include a smaller number of pulse sources and better spectral efficiency (the ratio of bit rate to available bandwidth). Spectral efficiencies of 0.4 bps/Hz are acceptable for standard RZ coding schemes [32] with better efficiencies achievable using more complex modulation formats such as Carrier Suppressed Return to Zero (CSRZ), Single Side Band Return to Zero (SSB-RZ), and duo-binary modulation formats.

Figure 2.8 below shows a possible layout for a hybrid WDM/OTDM system. It consists of 4 bit-interleaved OTDM systems each operating at a different wavelength. Each OTDM system consists of three different channels, each operating at a base rate of 40 Gb/s resulting

in a 120 Gb/s aggregate signal from each bit-interleaved system. When WDM is included, an overall aggregate hybrid transmission rate of 480 Gb/s can be achieved.

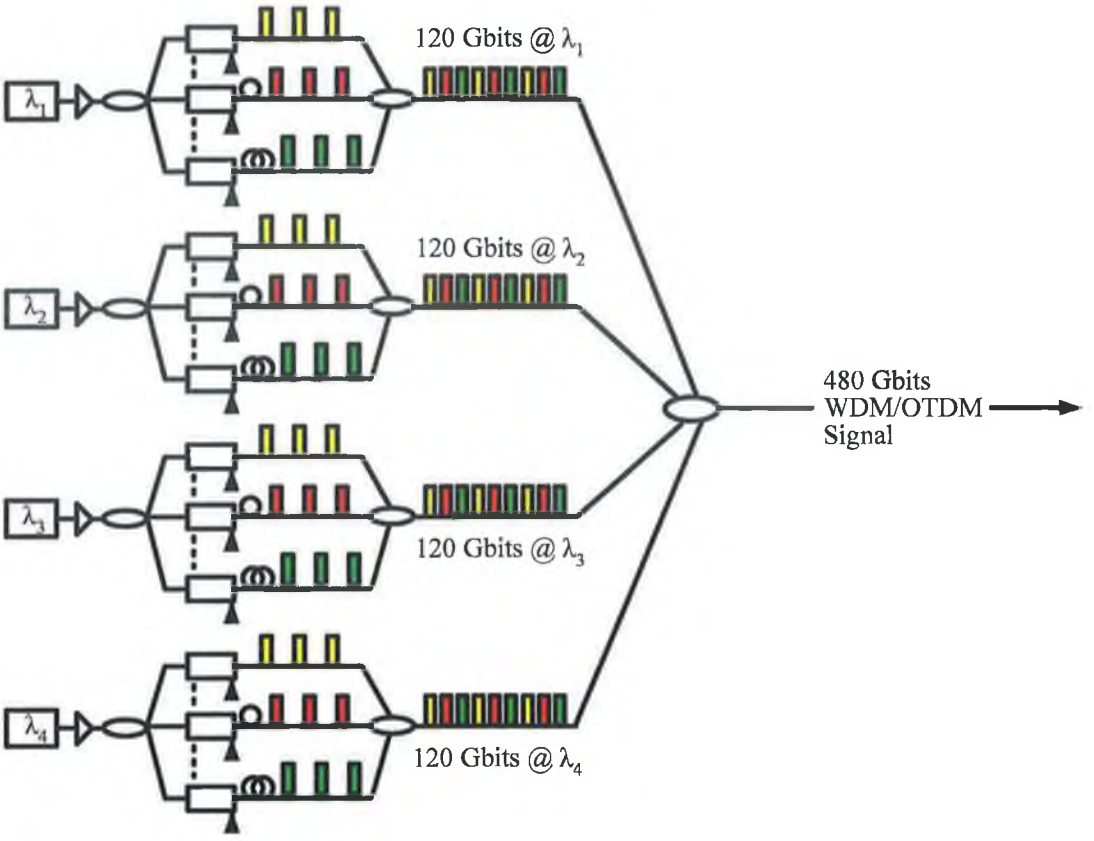

Fig. 2.8 Schematic for possible layout of hybrid WDM/OTDM network.

In 1996 the first OTDM/WDM transmission experiment with a total capacity of 400 Gb/s was demonstrated using 100 Gb/s x 4 WDM channels exhibiting pulse widths of less than 3 ps [33]. Recent experiments have demonstrated 1.28 Tb/s transmission over 420 km of SSMF using 8 channels, each operating at 170 Gb/s [34]. Even higher rates of 3 Tb/s have been achieved using 19 WDM channels of 160 Gb/s OTDM signals [35].

Summary

This chapter began by describing the need for high-speed optical networks, before talking about electrical multiplexing and progressing onto the optical multiplexing techniques of WDM and OTDM to take advantage of the vast bandwidth available in an optical fiber. Major enabling technologies as well as the limiting factors for both types of networks are discussed. Particular attention is given to the parameters of the pulse source, a vital component for an OTDM network. Finally, the operation of a hybrid network that combines

both technologies to achieve data rates in excess of 1 Tb/s is considered along with some of the problems which must be tackled.

References

[1] R. S. Tucker, G. Eisenstein and S. K. Korotky, "*Optical Time Division Multiplexing For Very High Bit-Rate Transmission*", J. Lightwave Technol., vol. 6. no. 11, pp 1737-1749, 1988.

[2] W. Bogner, E. Gottwald, A. Schopflin, and C. J. Weiske, *"40Gbits/s unrepeatered optical transmission over 148km by electrical time division multiplexing and demultiplexing"*, Electron. Lett., vol. 33, pp 2136-2137, 1997.

[3] K. Takahata, Y. Miyamoto, Y. Muramoto, H. Fukano, and Y. Matsuoka, *"50Gbits/s operation of a monolithic wave guide pin photodiode / HEMT (high mobility electron transistors) receiver opto-electronic IC module"*, in Proc. 24th Euro. Conf. Optical Comm. (ECOC 98), Madrid, September, vol. 3, pp. 67-69, 1998.

[4] V. Hurm, *"40Gbits/s 1.55μm monolithic integrated GaAs based PIN-HEMT photo-receiver"*, in Proc. 24th Euro. Conf. Optical Comm. (ECOC 98), Madrid, September, vol. 3, pp. 119-121, 1998.

[5] K. Yonenaga, A. Matsuura, S. Kuwahara, M. Yoneyama, Y. Miyamoto, K. Hagimoto and K. Noguchi, *"Dispersion compensation free 40Gbits/s x 4 channel WDM transmission experiment using zero-dispersion flattened transmission line"*, in Proc. Optical Fiber Conf., (OFC 98), Dallas, Paper PD20, 1998.

[6] K. Schuh, B. Junginger, H. Rempp, P. Klose, D. Rosener, E. Lach., *"85.4 Gbit/s ETDM Transmission over 401km SSMF Applying UFEC"*, in Proc.31st Euro. Conf. Optical Comm. (ECOC 2005), Glasgow, vol. 6, Paper PD Th4.1.4, 2005.

[7] P.J. Winzer, G. Raybon, M. Duelk, *"107 Gb/s Optical ETDM Transmitter for 100G Ethernet Transport"*, in Proc.31st Euro. Conf. Optical Comm. (ECOC 2005), Glasgow, vol. 6, Paper PD Th4.1.1, 2005.

[8] R. Ramaswami, K. N. Sivarajan, *"Optical Networks A Practical Perspective"*, 2nd Ed., Morgan Kaufmann, 2002.

[9] C. A. Brackett, *"DWDM Networks: Principles and Applications"*, IEEE, J. Select. Areas Commun., vol. 8, no. 6, pp. 948-964, 1990.

[10] S. Seo, K. Bergman, and P. R. Prucnal, *"Transport Optical Networks with Time-Division Multiplexing"*, IEEE J. on Select. Areas Commun., vol. 14, no. 5, pp 1039-1051, 1996.

[11] S. Kawanishi, *"High Bit Rate Transmission over 1 Tbit/s"*, IEICE, Transactions on Communications, pp 1135-1141, May 2001.

[12] M. J. Yadlowsky, E. M. Delsio and V. L. Da Silva, *"Optical Fibers and Amplifiers for WDM Systems"*, Proceedings of the IEEE vol. 85, no. 11, pp 1765-1777, 1997.

[13] S.V. Kartalopoulos, "*DWDM Networks, Devices and Technology*", Wiley Interscience, 2003.

[14] B. Glance, *"Wavelength Tunable Add/Drop Optical Filter"*, IEEE Photon. Technol. Lett., vol. 8, pp 245-247, 1996.

[15] G. Keiser, "*Optical Fibre Communications*", McGraw Hill, 3rd Ed., 2000.

[16] K. A. McGreer, *"Arrayed Waveguide Gratings for Wavelength Routing"*, *IEEE* Communications Magazine, vol. 36, pp 62-68, 1998.

[17] J.P. Turkieicz, E. Tangdiongga, G. Lehmann, H. Rohde, W. Schairer, Y. R. Zhou, E. S. R. Sikora, A. Lord, D. B. Payne, G. D. Khoe and H. de Waardt, *"160Gb/s OTDM Networking Using Deployed Fiber"*, J. of Lightwave Technol., vol. 23, no. 1, pp 225-235, 2005.

[18] J. Hecht, *"OTDM promises higher communications speeds using optical proccessors"*, Laser Focus World, pp 121-124, Nov. 2003.

[19] P. Bayvel, *"Future High Capacity Optical telecommunications networks"*, The Royal Society, 2000.

[20] S. Kawanishi, *"Ultrahigh-Speed Optical Time-Division-Multiplexed Transmission Technology Based on Optical Signal Processing"*, IEEE J. Quantum Electron., vol. 34, vo. 11, pp 2064-2079, 1998.

[21] D.M Spirit, A. D. Ellis, and P. E. Barnsley, *"Optical Time Division Multiplexing: Systems and Networks."* IEEE, Communications Magazine, pp 56-62, December 1994.

[22] L. P. Barry, P. Anandarajah, *"Effect of Side-Mode Suppression Ratio on the Performance of Self-Seeded Gain-Switched Optical Pulses n Lightwave Communications Systems"*, IEEE Photon. Tech. Letters, vol. 11, no. 11 pp 1360-1362, 1999.

[23] P. L. Mason, A. Wonfor, D. D. Marcenac, D. G. Moodie, M. C. Brierley, R. V. Penty, I. H. White and S. Bouchoule, *"The effects of pedestal suppression on gain-switched laser sources for 40Gbits/s OTDM transmission"*, 10th Annual Meeting of IEEE LEOS, vol. 1, pp 289-290, 1997.

[24] P. Vasil'ev, *"Ultrafast Diode Lasers - Fundamentals and Applications"*, Artech House, 1995.

[25] A. Shen, S. Bouchoule, P. Crozat, D. Mathoorasing, J.-M. Lourtioz and C. Kazmierski, *"Low timing jitter of gain- and Q-switched laser diodes for high bit rate OTDM applications"*, Electron. Lett., vol. 33, pp 1875-1877, 1997.

[26] M. Saruwatari, *"All-Optical Signal Processing for Terabit/Second Optical Transmission"*, IEEE J. Select. Topics of Quantum Electron., vol. 6, no. 6, pp 1363-1374, 2000.

[27] P. J. F. Maguire, M. Ruffin and L. P. Barry, *"All Optical Switching Techniques to Enable High-Speed Next Generation Photonic Transport Systems"*, First Joint IEI/IEE symposium on Telecomm. Systems Research, Nov. 2001.

[28] B. Guenther and D. Steel, *"Encyclopedia of Modern Optics"*, Elsevier, 1st Ed., 2005

[29] G. P. Agrawal, "*Fiber-Optic Communication Systems*", Wiley Interscience, 2 Ed, 1997.

[30] M.J. O'Mahony, *"Optical Multiplexing in Fiber Networks: Progress in WDM and OTDM"*, IEEE Communications Magazine, vol. 33, pp 82-88, 1995.

[31] A.M. Ali and K.W.Fussgaenger, *"Services Integration and Multiplexing for Broad-Band Communication Systems,"* IEEE J. Select. Areas Commun, SAC-4, no. 4, pp. 551–564, 1986.

[32] A. Hodzic, B. Konrad and K. Petermann, *"Alternative Modulation Formats in N x 40 Gb/s WDM Standard Fiber RZ-Transmission Systems"*, IEEE J. Lightwave Technol., vol. 20, pp 598-607, 2002.

[33] T. Morioka, S. Kawanishi, H. Takara, O. Kamatani, M. Yamada, T. Kanamori, K. Uchiyama and M. Saruwatari, *"100 Gbit/s x 4ch, 100 km repeaterless TDM-WDM transmission using a single supercontinuum source"*, Electron. Lett., vol. 32, pp 468-470, 1996.

[34] S. Vorbeck, M. Schmidt, R. Leppla, W. Weiershausen, M. Schneiders, E. Lach, *"Long Haul Field Transmission Experiment of 8x170 Gbit/s over 421 km Installed Legacy SSMF Fiber Infrastructure"*, ECOC Proceedings, Vol. 3, Paper We3.2.1, 2005.

[35] S. Kawanishi, H. Takara, K. Uchiyama, I. Shake and K. Mori, *"3 Tbit/s (160 Gbit/s x 19 ch) OTDM/WDM Transmission Experiment"*, Optical Fiber Communication Conference and the International Conference of Intergrated Optics and Optical Fiber Communications (OFC/IOOC '99), 1999.

3. Ultra Short Pulse Generation

Introduction

As the demand for bandwidth continues to grow, so too does the necessity to develop high-speed optical technologies to construct large capacity networks such as high-speed OTDM and hybrid WDM/OTDM networks. A key component of such high-speed systems is a source of ultra short optical pulses with high repetition rates. Various applications such as demultiplexing, clock recovery, signal processing and sampling are also dependant on the generation of such pulses. There are a number of important parameters which the pulse source must meet to be useful in such high capacity networks. These include pulse duration, spectral width, timing jitter and side mode suppression ratio (SMSR). Various pulse generation schemes are available and some of the more popular schemes are discussed here, these include mode locking, Q-switching, pulse shaping using an electro-absorption modulator and gain switching. However, particular attention is paid to the technique of gain switching due to its simplicity and cost effectiveness. It will be shown how this method of generating short optical pulses has a number of short comings associated with it and how we can overcome these problems by using the techniques of self seeding and external injection.

3.1 Pulse Generation Techniques

3.1.1 Mode Locking

Mode locking is one of the most popular ways to produce high repetition rate ultra short optical pulses and is commonly carried out on semiconductor laser diodes and fiber ring lasers [1-2]. The term mode locking describes the locking of multiple axial modes in a laser cavity [3]. It is achieved by combining in phase a number of longitudinal modes of a laser which all have slightly different frequencies. A simple descriptive analogy is given here to explain the mechanism of mode locking. When modes of electromagnetic waves of different frequencies and random phases are added together, they produce a random distribution, average output of both the electric field and intensity in the time domain. Figure 3.1 shows three out of phase sinusoidal waves of frequency ω, 2ω and 3ω added together to produce a randomly fluctuating total field amplitude. The intensity variation is provided by squaring the amplitude.

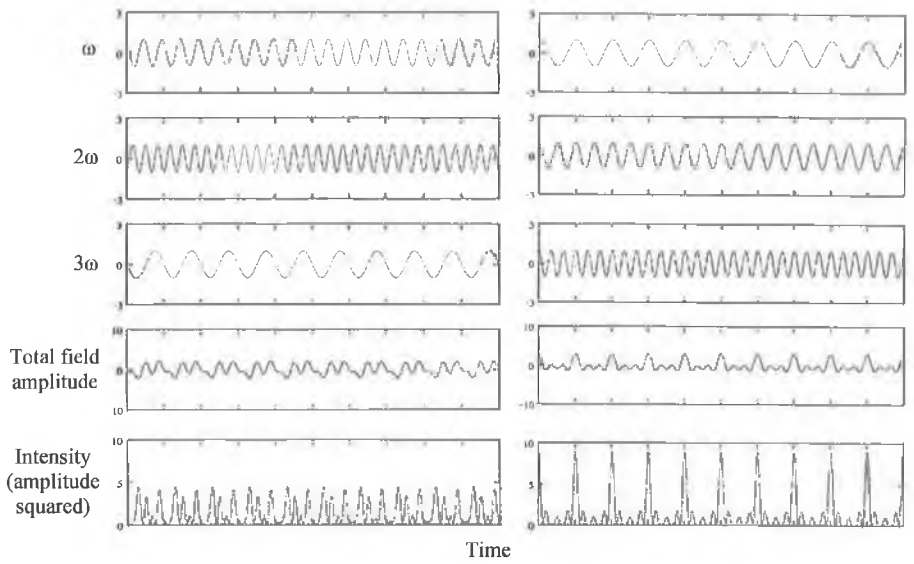

Fig. 3.1 Amplitude and intensity of (a) out-of-phase waves added together (b) in-phase waves added together [4]

When the same three frequencies or modes are added in phase, i.e. when all their phases are zero at the same spatial location as can been seen in Figure 3.1 (b), they combine to produce a total field amplitude and intensity output that has a characteristic repetitive pulsed nature. Mode locking may be carried out either actively such as using an acousto-optic device driven by an RF signal, or passively via a non-linear optical shutter that opens when the laser pulse arrives. As a result of achieving such phasing or mode locking, it has become a powerful method for generating ultra short pulses [5, 6].

3.1.2 Q-Switching

Q-switched lasers are a useful technology that allow high peak powers and high repetition rates [7]. Looking at Figure 3.2 we can see the basic dynamics of Q-switching [8]. The cavity loss is initially set at some artificially high value while the population inversion, and therefore the gain and stored energy, in the laser medium are pumped up to a level much higher than normal. This is achieved by blocking or removing one of the mirrors to prevent the build up of oscillation while the pumping process increases the population inversion to a very high level. Once a large inversion has been developed, the cavity feedback mechanism is restored which switches the cavity Q factor back to its usually large value. The result is a very short, intense burst of laser light which dumps all the accumulated population inversion in a single short laser pulse.

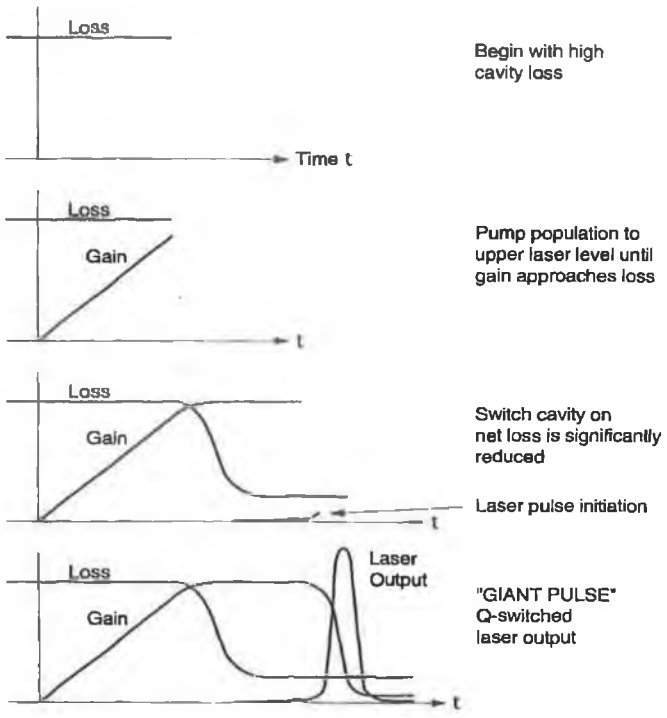

Fig. 3.2 Evolution of a Q-switched pulse [8]

Q-switching may be achieved either actively or passively. Active switching includes the use of rotating mirrors, electro-optic or acousto-optic shutters while passive switching uses saturable absorbers [5].

3.1.3 Pulse Shaping using External Modulators.

As has already been mentioned, another suitable technique for generating short optical pulses involves using continuous wave (CW) light from a laser diode coupled into an external modulator that is sinusoidally driven and suitably biased. Short, near transform limited pulses are shaped out of CW light due to the fact that the modulator response to an applied voltage is non-linear [9]. The greater the degree of non-linearity (slope of the transfer characteristic) the shorter the achievable pulses due to a higher compression factor. The shaping of optical pulses is most often performed using either electro-optic Mach-Zehnder modulators (MZMs) [10] or electroabsorption modulators (EAMs) [11]. The operation of both types has been described in section 1.3.1.3. Here we will discuss the method used to generate pulses using the Mach Zehnder modulator [12]. Pulse shaping using an EAM is discussed at the end of this chapter. Figure 3.3 below shows the transfer characteristics of the MZM and the EAM.

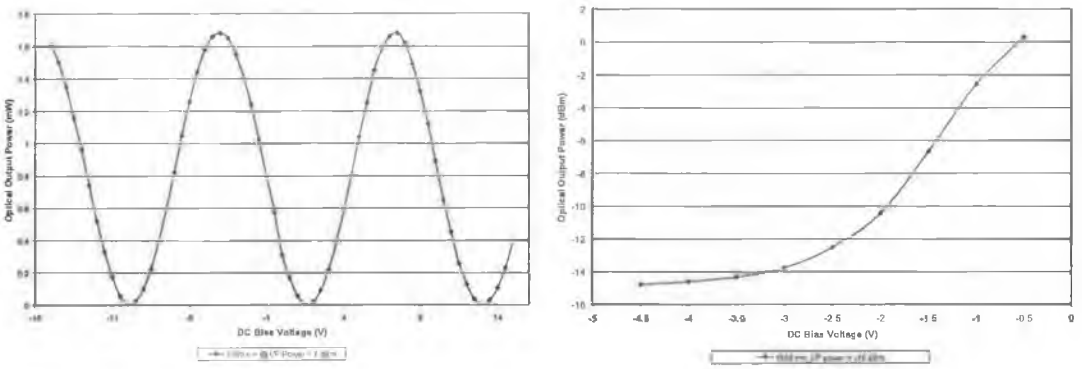

Fig. 3.3 Transmission curve for MZM (left) and EAM (right)

The transfer curve of an MZM as a function of applied voltage has a sinusoidal shape. The bias voltage applied to the modulator may be set to any point along the transmission curve depending on the desired application. Pulses are carved out of CW light by biasing the modulator near its null point and driving it with a sinusoidal electrical signal. Another application involves biasing at the null point and driving the modulator at twice the switching voltage which results in the shaping of pulses that have a repetition rate of twice the frequency of the applied electrical signal. A disadvantage of this technique is that a high driving voltage is needed. Comparing the two different types of modulators; lithium niobate modulators have low wavelength chirp but one of its drawbacks includes high operating voltages [11]. Electro absorption modulators, however, could be driven at lower voltages and are easy to integrate with a light source compared to lithium niobate modulators. The major disadvantages of both types are the high insertion loss. Also, the need for a modulator for the shaping of pulses, which is not necessary when using other techniques, could be considered a disadvantage in terms of the additional cost.

3.1.4 Gain Switching

Gain switching of a laser diode is one of the simplest techniques available for producing high repetition rate optical pulses. Its advantages include easily tuneable repetition rates, stability, compactness and simplicity [13]. The first indication that very short optical pulses can be generated by a directly modulated laser was first observed from relaxation oscillation when turning on a laser from below threshold. It was noticed that the optical pulse width was much shorter than the applied electrical signal [14]. Gain switching is achieved by applying a large amplitude RF signal to a laser biased below threshold to excite the 1st spike of relaxation oscillation and then terminate the electrical pulse before the onset of subsequent spikes. This results in the generation of optical pulses that are much shorter than the applied electrical signal. Gain switching is very similar to laser spiking and the same mechanisms of spiking

may be used to describe the gain switching process, and can be followed in Figure 3.4. Once the electrical signal has been applied the carrier density, N(t), passes up through the threshold value N_{th} at the starting time t_1, but the photon number, n(t), within the cavity is still zero at this time. As soon as the carrier density, N(t), passes through the threshold value, N_{th}, at time t_1, the gain begins to exceed the losses and the photon number begins to build up exponentially from noise. As the photon number, n(t), increases, the optical signal in the cavity becomes large enough to start burning up the injected carriers faster than the pump (electrical signal) can supply them. As a result, beyond the time t_2 the carrier density, N(t), stops increasing and begins to be pulled down rapidly. However the carrier density, N(t), is still greater than the threshold value, N_{th}, so the net gain within the cavity is still greater than the losses and as a result the photon number continues to rise. When the carrier density, N(t), reaches the threshold, N_{th}, value, thereby equalling the gain and loss in the cavity, the photon density, n(t), reaches its peak value at time t_3 and starts to drop back downward. At this point there is still a large optical signal travelling around inside the cavity, burning up excited carriers but the carrier density, N(t), continues to be driven below the threshold level, N_{th}. Also at this point there is a net loss within the cavity and the photon number, n(t), begins to suddenly drop down. When the photon number reaches t_4, the carrier density reaches a minimum value. If the electrical pulse is terminated as the carrier concentration falls, this prevents the second peak of relaxation oscillation from occurring resulting in the output of picosecond optical pulses.

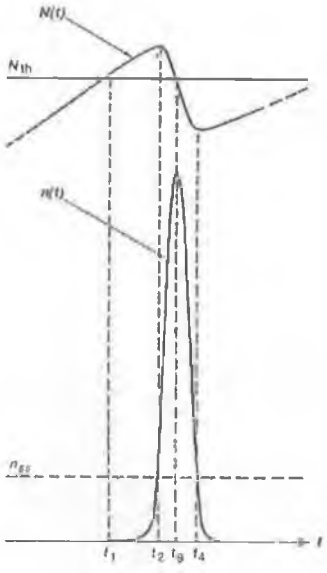

Fig 3.4 Carrier and photon density variation during gain switching cycle [8]

The mechanism behind gain switching can be described by analysing the rate equations for a single mode laser that connect the photon density P, and electron density N, in the cavity [15].

$$\frac{dN}{dt} = \frac{J}{qd} - g(N - N_t)P - \frac{N}{\tau_n} \tag{3.1}$$

$$\frac{dP}{dt} = g\Gamma(N - N_t)P - \frac{P}{\tau_p} + \beta\Gamma\frac{N}{\tau_n} \tag{3.2}$$

J	=	Injected current density
q	=	Electron charge
d	=	Active layer thickness
g	=	Gain coefficient
N_t	=	Carrier density at transparency
Γ	=	Optical confinement factor
β	=	Fraction of spontaneous emission coupled into the lasing mode
τ_n	=	Electron lifetime
τ_p	=	Photon lifetime

Equation 3.1 describes the evolution of the carrier density within the active region. The $\frac{J}{qd}$ term describes the injected carrier density into the active region. This value will increase with larger injection currents and for smaller cavities. The second term, $-g(N-N_t)P$, accounts for stimulated emission. The $-\frac{N}{\tau_n}$ term describes the spontaneous emission due to the recombination of carriers. The evolution of the photon density is described in equation 3.2. The first term on the right hand side, $g\Gamma(N-N_t)P$ describes the photon growth rate due to stimulated emission. The change in sign compared to equation 3.1 is due to photons produced by stimulated emission while carriers are lost. The second term, $-\frac{P}{\tau_p}$ accounts for the loss of photons from the cavity, described by the photon lifetime and is due to absorption, scattering and emission through one of the mirrors. The last term, $\beta\Gamma\frac{N}{\tau_n}$

represents the fraction of spontaneous emission that yields a photon which contributes to the lasing mode.

3.1.4.1 Characteristics of a Gain Switched Pulse.

The duration and peak power of the pulse depends on a few different parameters such as structure of the laser, the material, relaxation oscillation frequency, amplitude of applied current, and the bias current [5]. However, typical pulse widths achievable from gain switching range from 10-60 ps. A gain switched pulse may be roughly described as a combination of two exponential curves of a rise and fall time, where the decay time is about 1.3 to twice the rise time [15]. The rise time of the pulse is inversely proportional to the net charge Q transferred to the active region by the electrical pulse while the fall time depends on how far down below threshold the carrier density is pulled during the formation of the optical pulse [14]. It has been shown that the dc bias is an important factor in determining the quality of the gain switched pulse. There is an optimum dc bias level for which the pulse width (FWHM) is minimised and the amplitude is at a maximum, this is usually just below the threshold current of the laser. Biasing further below threshold adds a number of disadvantages such as increasing the duration of the optical pulse and decreasing the amplitude, also there is an increase of both frequency chirp and noise and a delay in the emission of subsequent pulses [15]. Biasing above threshold would reduce frequency chirping but also reduces the signal on/off ratio resulting in an extinction ratio penalty [15]. Therefore, biasing just below the threshold value of the laser allows for the best performance. One of the main reasons for not being able to reduce the pulse width is due to the difficulty in maintaining a large initial inversion before emission of the optical pulse [16].

3.1.4.2 Gain Switched Optical Spectra and Frequency Chirp

An important parameter of gain switched pulses is their optical bandwidth. Gain switching of a laser diode results in the spectrum being broadened and may be clearly seen when compared to the spectrum of the same laser operating in CW mode. This broadening could lead to a dispersion penalty in an optical communications system as discussed in the previous chapter. During the emission of a gain switched pulse the carrier concentration experiences large variations and so the refractive index within the cavity also varies. Since the wavelength is related to the carrier concentration, due to the effect of free carriers on the refractive index of the semiconductor material, the wavelength also changes. This wavelength chirping $\Delta\lambda$ may be described by the following equation [14]

$$\Delta\lambda = \frac{\lambda}{\mu}\frac{d\mu}{dn}\Delta n \tag{3.3}$$

Δn is the variation of the carrier density within the cavity. $d\mu / dn$ describes the dependence of the refractive index on the carrier concentration and typically has a negative value meaning that the wavelength shifts towards longer wavelengths (red shift) [17]. Due to this wavelength chirp, gain switched pulses have a time bandwidth product that is far from transform limited. Also it is important to note that the chirp across the centre of the pulse is linear while the chirp in the wings of the pulse is non-linear. So for practical applications of gain switched pulses in communication systems, some form of chirp compensation is needed to counteract the effects of both the linear and non-linear chirp. This is usually carried out using either dispersion compensating fiber (DCF) or chirped fiber Bragg gratings [18]. Another side effect of the gain switching process is the reduction in the side mode suppression ratio (SMSR). As explained in the previous chapter, the SMSR is the ratio between the power in the strongest mode and the second strongest mode. During gain switching the SMSR is degraded. This reduction in the ratio is due to large fluctuations in the photon density caused by the laser being pulled below threshold. This causes the side modes of the laser to be strongly excited lowering the SMSR [19]. This degraded SMSR will lead to an increase of noise on the pulses due to the interaction of mode partition noise effect with either fiber dispersion or spectral filtering. This effect will be described further in the next chapter. A simple and cheap technique to improve the SMSR and to a small degree the chirp of a gain switched pulse source is to self seed [20] or inject light from an external source into the gain switched laser [21]. This will be demonstrated later in this chapter.

3.4.1.3 Timing Jitter

Timing jitter is another important parameter of optical pulses as it can have a dramatic effect on the performance of a communication system when a gain switched pulse source is used. Timing jitter may be classed as either correlated or uncorrelated. Correlated jitter is mainly caused by the drive circuits and is considered to be negligible [22]. Uncorrelated jitter however is the major contributor to the overall timing jitter and is related to the spontaneous noise and pulse turn on dynamics. The time between when the laser is switched on and the optical emission is called the turn on delay time and the noise that manifests itself in the turn on delay time jitter (TOJ) originates from the fluctuations in the photon density during the build up of the optical pulse, caused by the random nature of spontaneous emission [23]. The

effects of jitter may be addressed in a number of ways. Two of the simplest methods are self-seeding [24] or external injection [25] of the gain switched laser, both of which has been shown to partially reduce the TOJ.

3.2 Experimental Results

3.2.1 Gain Switching of a DFB Laser Diode.

Gain switching may be carried out by driving the laser with either large amplitude short electrical pulses or with a large sinusoidal current. The former has been reported to result in narrower optical pulses [26] but it is difficult to generate electrical pulses at the desired repetition rates for use in high-speed OTDM systems. As a result, the use of sinusoidal currents at high frequencies is more attractive. This section outlines the procedure and results of gain switching a DFB laser diode with a sinusoidal current. A schematic representation of the setup used is shown in Figure 3.5. The laser used was a commercially available InGaAsP DFB (KELD 1551 CCC) device. When biased at 60 mA it had a central wavelength of 1542 nm at 25°C. The first step was to take a dc characterization of the device. By plotting the optical output power versus the bias current the threshold current of the laser was found to be about 19 mA and was initially biased just below this point and later changed to optimise the output pulses. A signal generator produced a 2.5 GHz sine wave which was passed through a 50:50 electrical power splitter. Half of the modulating signal was used to trigger an oscilloscope and the remaining half was electrically amplified (to a power of about 29 dBm) before being coupled into a bias tee to combine the electrical signal with a variable dc bias and applied to the laser.

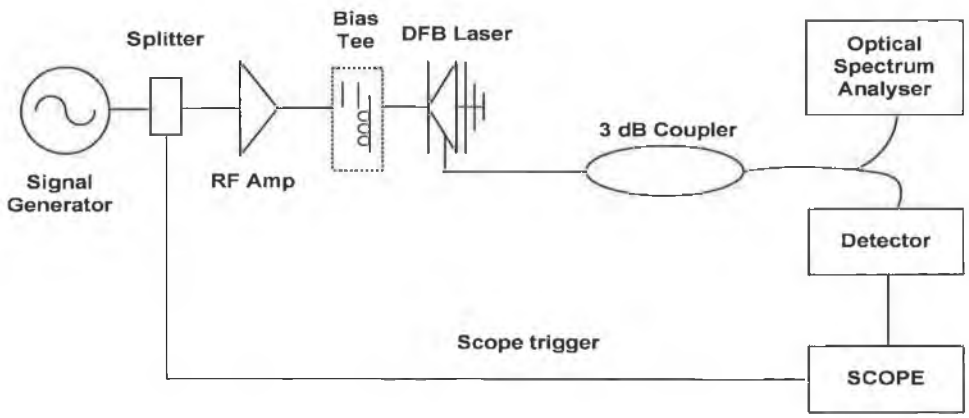

Fig. 3.5 Experimental setup for gain switching a DFB laser

The output signal was then coupled into a fiber via a Graded Index (GRIN) lens that had an antireflection coating to prevent back reflections entering the laser. This signal was then split by a 3 dB coupler to allow characterisation in both the spectral and temporal domains. One arm was coupled into an Anritsu MS9717A optical spectrum analyser (OSA) which had a resolution of 0.07 nm and the other arm was passed into a high-speed photodetector and then a 50 GHz oscilloscope (HP54750A). The dc bias and the modulation frequency were optimised to obtain the best possible pulse in terms of duration and noise. The resulting optical pulses are shown in Figure 3.6.

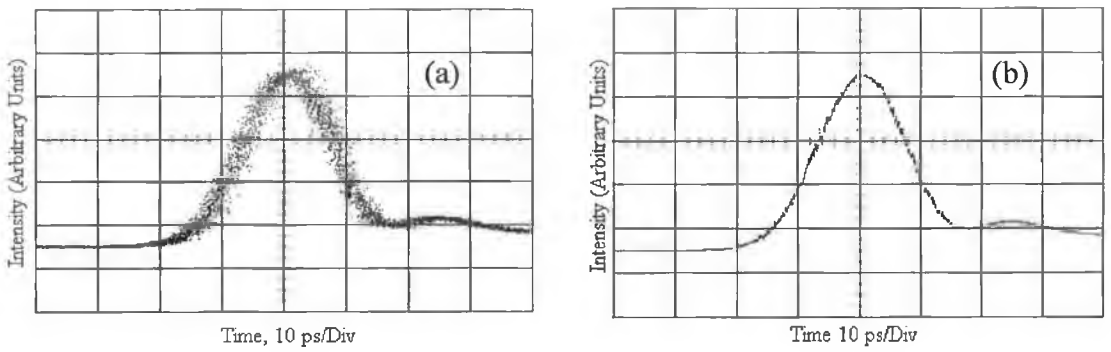

Fig. 3.6 Gain switched pulses (a) non averaged (b) averaged over 16

From the non averaged pulse the jitter is quite noticeable and measured to be about 3 ps. The measured pulse width is 17 ps, but to calculate the actual pulse width, the temporal resolution of the measurement system must be taken into account, which in this case was about 12 ps. The resolution of the measurement system accounts for the rise times of both the photodetector and oscilloscope. The actual deconvolved pulse width, τ_A, is then given by the sum of squares formula:

$$\tau_A = \sqrt{\left(\tau_M^{\,2} - \tau_R^{\,2}\right)} \qquad (3.4)$$

where τ_M is the pulse width measured on the oscilloscope and τ_R is the temporal resolution of the measurement system. The deconvolved pulse width was found to be 12ps.

Using an optical power meter, a reading of the average power of the pulse was taken at the output of the optical coupler and measured to be 0.18 mW. From this it was possible to calculate the peak power, P_{Peak}, of the optical pulse using the deconvolved pulse width, $\Delta\tau$, and the period of the modulation frequency, T.

$$P_{Peak} = \frac{P_{Avg} \times T}{\Delta\tau} \tag{3.5}$$

The peak power of the pulse was calculated to be 6.02 mW.

The optical spectrum for the laser running in CW mode and under modulation is shown in Figure 3.7 (a) and (b) respectively. It can be clearly seen that when the laser diode is modulated the longitudinal modes of the gain switched spectrum are broadened due to frequency chirp.

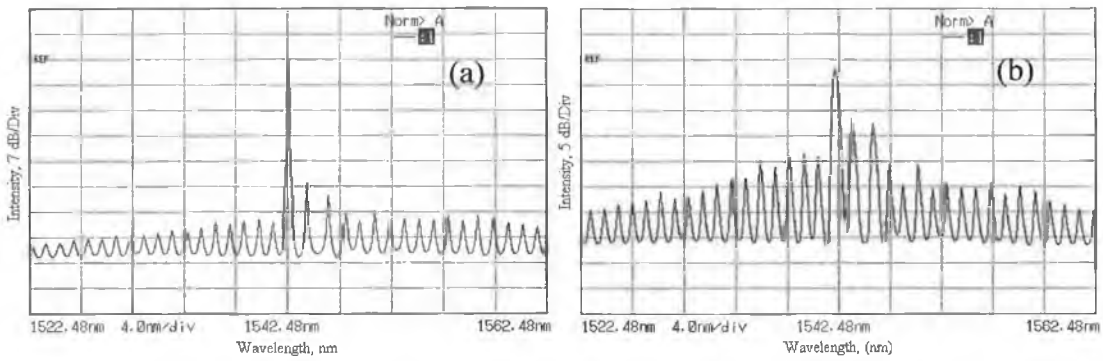

Fig 3.7 CW spectra (a) and gain switched spectra (b)

Under modulation the spectral width increased to 0.5 nm (63 GHz at 1542 nm). The resulting time bandwidth product (TBP) was 0.75. A side effect of the gain switching process is the reduction in the side mode suppression ratio (SMSR). Under CW operation the SMSR is approximately 35 dB, however, once modulated the SMSR is degraded to about 9 dB.

As we can see, there are a few complications that accompany the gain switching process. Problems with temporal jitter, an increased spectral width and degraded SMSR must be addressed before gain switched pulses can be used in an optical communication system. Two of the most common techniques available to counter these ill effects are self seeding and external injection. Both involve injecting an optical signal back into the laser cavity during the build up of a pulse, and both produce cleaner optical pulses (in terms of jitter), improved SMSR and a reduction in the spectral width.

3.2.2 Self Seeding of a Gain Switched DFB Laser.

Self seeding involves reflecting back a small potion (0.2-6%) of the pulse back into the cavity [14, 27] using a wavelength selective element to seed the desired mode. The reflected

pulse must arrive back at the laser at just the right time (when the carrier density is starting to build up) to obtain a large SMSR. Figure 3.8 below shows the setup used to self seed the DFB laser. The gain switching section was carried out using the same setup as before while the self seeding section comprised of an external cavity containing a tunable Fiber Bragg grating (FBG) and a polarisation controller (PC). The laser used was the same as before (InGaAsP DFB laser). An electrical signal amplified to a power of about 29 dBm at a frequency of 2.5 GHz was initially applied to it via a bias tee that combined the RF signal with a variable dc bias. The dc bias was varied to optimise the output pulses and set to about 16.3 mA. The output signal was coupled into a fiber via a fiber GRIN lens and then split using a 50:50 optical coupler. One arm of the coupler was connected to the FBG which reflected the signal back into the laser.

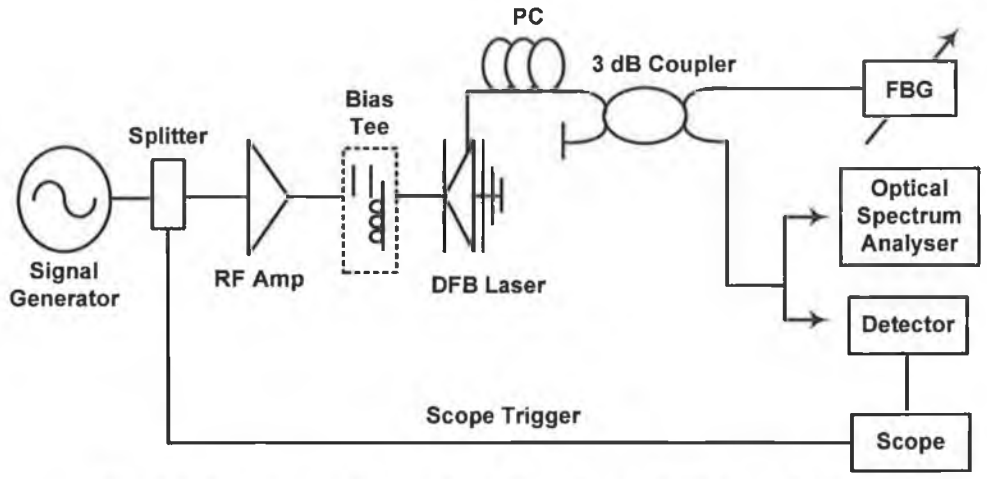

Fig. 3.8 Experimental setup for self seeding a DFB laser diode

To obtain optimum self seeded gain switched (SSGS) pulses, the central wavelength of the fibre grating was tuned to the main longitudinal mode of the gain switched laser. The modulation frequency was then varied to ensure that the signal re-injected back into the cavity arrived as an optical pulse was building up. A suitable frequency was found to be 2.47 GHz. The PC was also adjusted to optimise the re-injected signal. The SSGS pulses were then analysed in the spectral and temporal domains using the lower output arm of the optical coupler. The spectral results of gain switching and self seeding are show in Figure 3.9 (a) and (b) respectively.

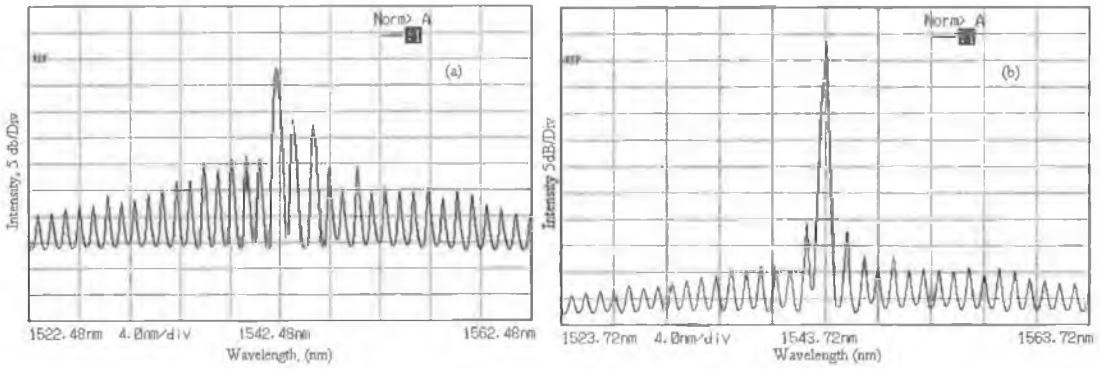

Fig. 3.9 (a) Gain switched spectra and (b) self seeded gain switched

The broadened spectrum (compared to the cw case) and reduced SMSR (9.6 dB) of the gain switched spectrum can be seen in Figure 3.9 (a). The improved SMSR (33.9 dB) of the SSGS spectrum seen in Figure 3.9 (b) is due to the feedback signal causing an initial excitation level well above the spontaneous emission noise level for the main mode, resulting in the output being strongly single moded with a high SMSR [20]. The visible reduction in the linewidth to 0.34nm (43 GHz @ 1543nm), and hence the time bandwidth product (0.6), is brought about by the reduction in the frequency chirp. This is caused by the injected optical feedback signal lowering the overall variation of the carriers within the cavity during the build up of the pulse.

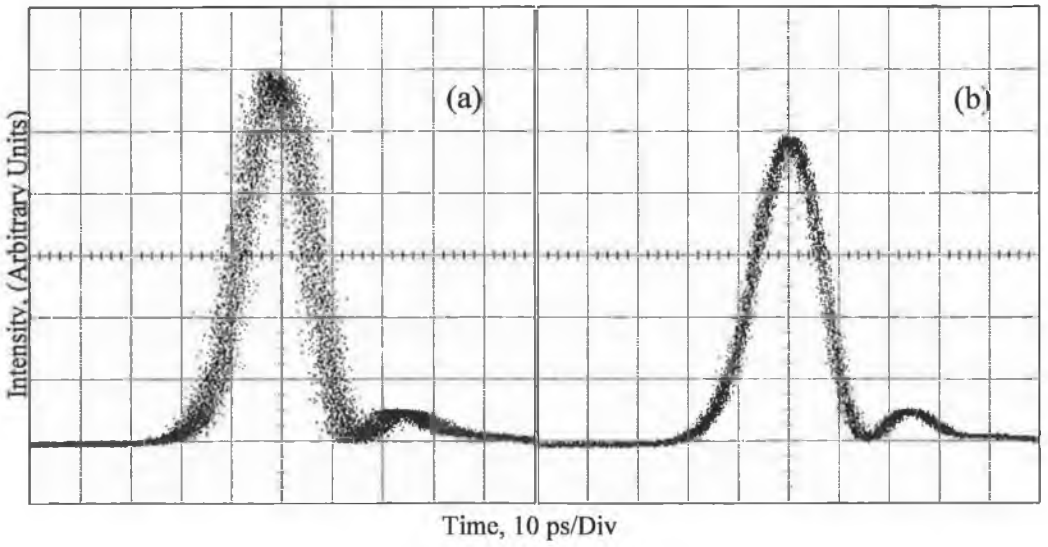

Fig 3.10 (a) Gain switched pulse, (b) SSGS pulse

Figure 3.10 (a) shows the gain switched pulse with a FWHM of 12.3 ps (deconvolved) and an rms jitter of about 3 ps. The average power of the pulse, measured at the lower output arm of the 3 dB coupler was about 0.19 mW, and from this the peak power of the pulse was calculated to be 6.18 mW. Figure 3.10 (b), illustrates the self seeded gain switched pulses

and it can be seen that the pulse duration has increased to 14 ps, while the rms jitter has been reduced to 1.6 ps. The average power decreased slightly to 0.18 mW and the peak power to 5.4 mW. Both traces are non-averaged. Both the reduction in the timing jitter and the increase of the SMSR are due to the same fundamental mechanism. As mentioned before, uncorrelated timing jitter stems from random fluctuations of the spontaneous emission during the build up of the pulse. The optical feedback increases the photon number in the relevant mode which decreases the effects of spontaneous emission. This reduces the random fluctuations of the photon density which manifests as a smaller timing jitter in the output pulses [28].

A major disadvantage of self seeding is that the length of the cavity has to be continually tuned so that the pulse repetition frequency is an integer multiple of the cavity round trip time. This ensures that the seeding signal arrives back at the laser cavity during the build up of the next optical pulse. An alternative technique that requires no adjustment of the repetition frequency or cavity length involves external injection of light from a CW source into a gain switched laser [29, 30].

3.2.3 External Injection Seeding of a DFB Laser.

The experimental setup used to externally inject light from a master laser to a slave laser is shown in Figure 3.11. The laser diodes used were commercially available NEL DFB's contained in a hermetically sealed high-speed package. The gain switched laser had a threshold current of about 19 mA, an output power of 4 dBm when biased at 3 times the threshold and a central emission wavelength of 1551 nm. Gain switching was carried out at 10 GHz by applying the electrically amplified signal to the laser that was to be modulated via a bias tee. The bias tee was used to combine the electrical RF signal with a dc bias of 17.5 mA. CW injection was provided by a second DFB laser which injected light into the gain switched laser via a circulator and a PC. This master laser had a central wavelength of 1550 nm, was biased at 23 mA and had an isolator incorporated into the attached fiber pig-tail, preventing any light from entering it. By varying the temperature of the master laser it was possible to attain wavelength tunability (over a range of about 2 nm). This allowed the emitted wavelength to be match to that of the slave laser. The PC was used to ensure that the light being injected into the slave laser was aligned with its optical axis thereby maximising the output SMSR.

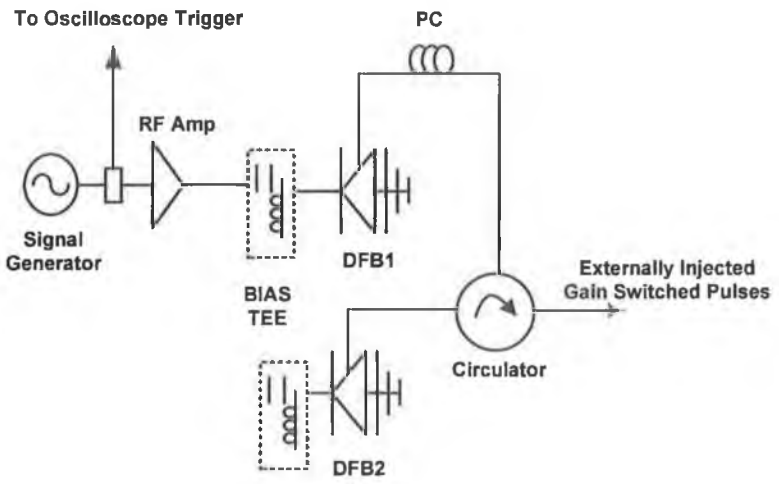

Fig 3.11 Schematic of external injection setup

Taking into account the losses due to the circulator, PC and coupling of light into the modulated laser, the optical power injected was estimated to be about -20 dBm. The resulting externally injected gain switched pulses were observed on an oscilloscope and optical spectrum analyser via the output arm of the circulator and can be seen in Figures 3.12 and 3.13 respectively.

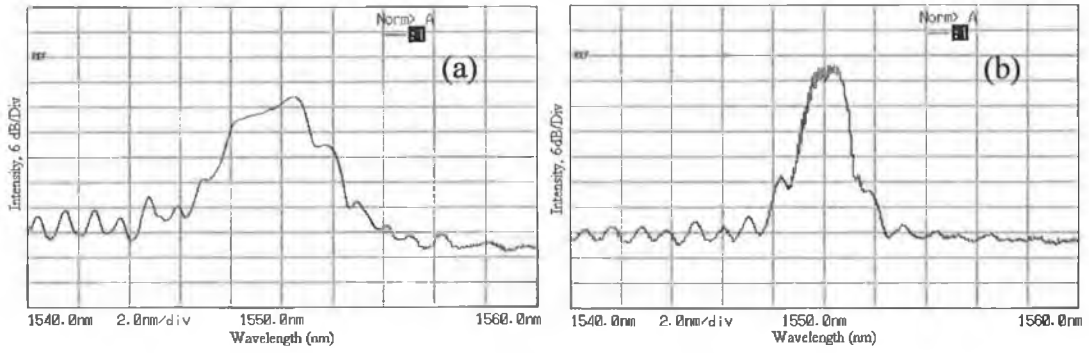

Fig. 3.12 Gain switched spectra (a) without and (b) with external injection

With optimum light injection an improvement in the SMSR from 11 dB under gain switching, to 28 dB with external injection was achieved. This can be explained as follows. As light is injected into the cavity, the carrier concentration in the modulated laser decreases since the gain threshold of the mode whose frequency coincides with the frequency of the injected photons becomes lower. All other modes then remain far below their threshold gain [31]. The spectral width before and after injection were measured at 1.4 nm and 1.2 nm respectively.

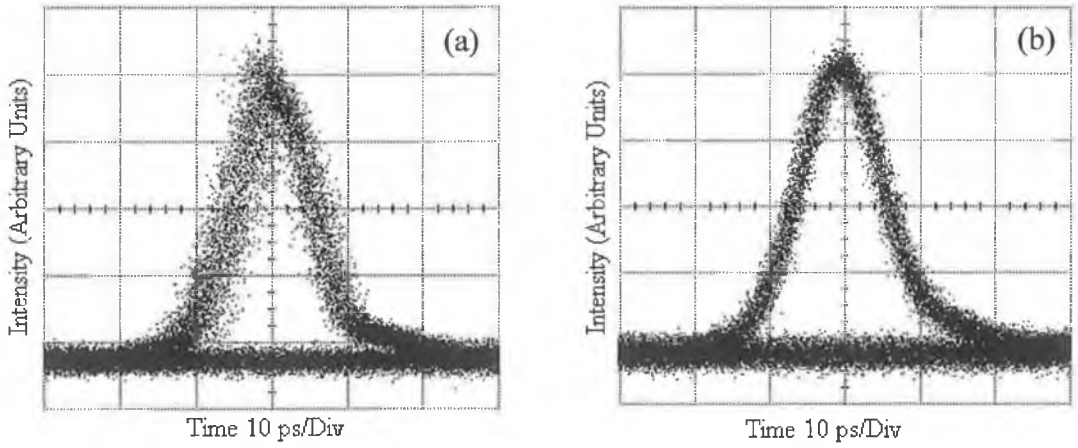

Fig. 3.13 (a) Gain switched pulse and (b) externally injected pulse

Figure 3.13 shows the zero optical level to indicate the good extinction ratio (>20 dB) of the generated pulses. Before injection the rms jitter was measured at 3.3 ps, and was reduced to 1.4 ps with injection. As with self seeding, the external injected signal provides an excitation above the spontaneous emission level within the laser cavity, reducing the relative fluctuations in the photon density thereby reducing the timing jitter of the optical pulses [32]. The deconvolved pulse width before injection was about 9.5 ps and after injection was 11 ps. After injection the TBP was 1.63, while the peak power was 4.7 mW.

3.2.4 Gain Switching of a Fabry Perot Laser Diode.

To gain switch the FP laser we used the same experimental setup as was used to gain switch the DFB laser, Figure 3.14. The FP laser used was a commercially available InGaAsP device which had a threshold current of 19 mA and a central wavelength of 1541 nm. The 2.5 GHz electrical signal from the signal generator was passed through a 50:50 electrical power splitter. One half of the modulating signal was used to trigger a sampling oscilloscope and the remaining 50% was electrically amplified before being coupled into a bias tee to combine the electrical signal with a variable dc bias and then applied to the laser. The output signal was then coupled into a fiber via a graded index (GRIN) lens that had an antireflection coating to prevent back reflections entering the laser. The optical pulses were then characterised in the spectral and temporal domains by passing the signal through a 3 dB optical coupler; one arm was passed to an OSA and the other into a high-speed photo detector which was coupled to a 50 GHz oscilloscope. Both the dc bias and the modulation frequency were optimised to obtain the best possible pulse in terms of duration and noise. The resulting optical pulses are shown in Figure 3.15 (a) and (b).

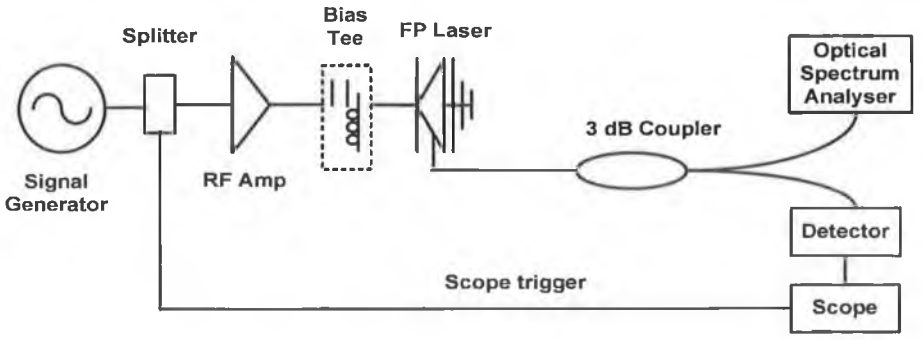

Fig. 3.14 Experimental setup for gain switching an FP laser

Figure 3.15 (a) shows a non averaged pulse and figure (b) shows a pulse averaged over 16. The FWHM pulse width was measured to be 32 ps, which after taking into account the resolution of the measurement system, gave a deconvolved pulse width of 29.6 ps. RMS jitter was measured at about 2 ps.

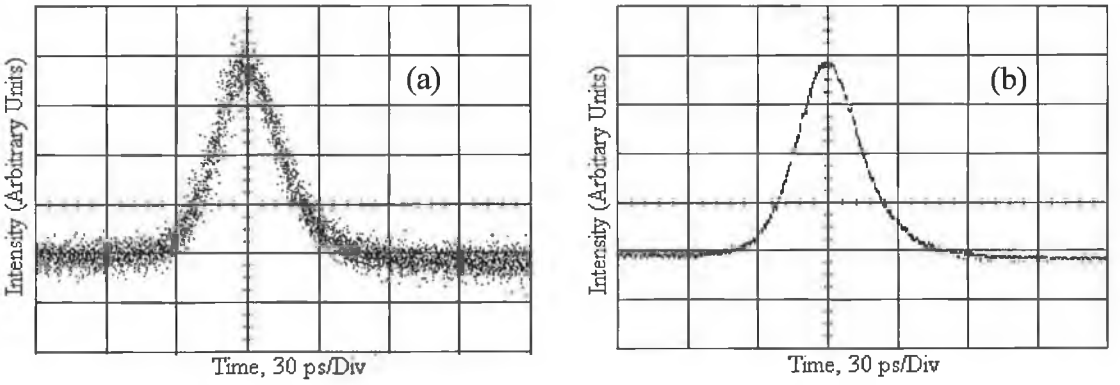

Fig. 3.15 Gain switched pulses from FP laser (a) non averaged (b) and averaged

The optical spectra for the laser running in CW mode and under modulation are shown in Figure 3.16 (a) & (b) respectively. When the laser diode is modulated it can be seen that the longitudinal modes of the gain switched spectrum are broadened due to frequency chirp. Under modulation the spectral width of each mode increased to about 0.7nm (88.4 GHz at 1541 nm).

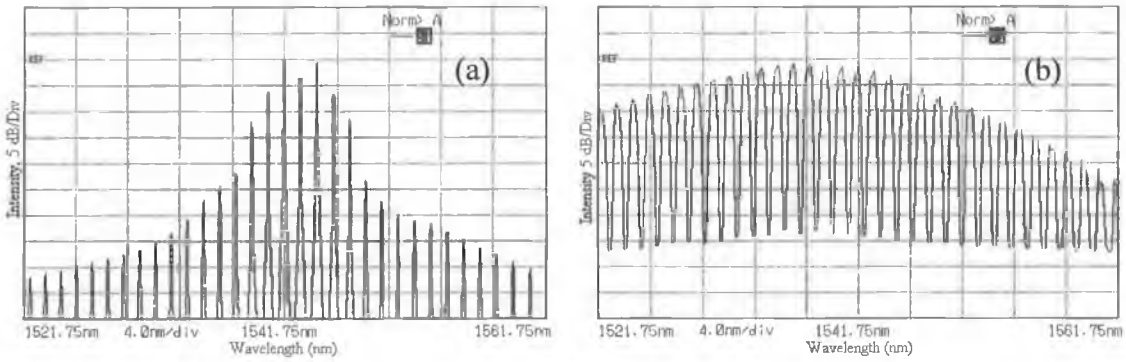

Fig 3.16 Optical spectra of FP laser (a) CW (b) gain switched

From these results we can see that gain switching an FP laser produces a pulse train with a multimode spectrum. While these pulses exhibit less temporal jitter than a DFB laser, the multimode spectrum would still cause a problem if these pulses were used in an optical communication link. As the pulse travels in a dispersive fiber medium, each mode travels at a different speed resulting in temporal broadening. As well as the benefits self seeding offers in terms of improving the timing jitter and to a small degree the chirp, it has also been shown that self seeding of an FP laser improves the SMSR by increasing the number of photons in a particular mode which lowers the gain threshold of that mode thereby increasing its output power in comparison to the side modes. In essence, self-seeding an FP laser can switch the output from multimode to single mode emission [33].

3.2.5 Self Seeding of an FP Laser.

Self seeding a gain switched FP laser is one of the simplest and cheapest ways to generate wavelength tunable single mode optical pulses and there have been many reported experiments using this technique [34, 35]. The laser diode is seeded with optical feedback of a suitable wavelength and once the feedback arrives during the build up of an optical pulse, a single moded pulse is emitted. Figure 3.17 below outlines the setup used to generate self seeded gain switched pulses. The same FP laser used for gain switching was again used here. Gain switching was carried out by applying a 2.5 GHz modulating signal and a dc bias current of 13.3 mA to the laser diode. Self seeding was realised by using an external cavity consisting of a PC, a 3 dB optical coupler and a tunable fiber Bragg grating (FBG) which had a 3 dB bandwidth of 0.37 nm.

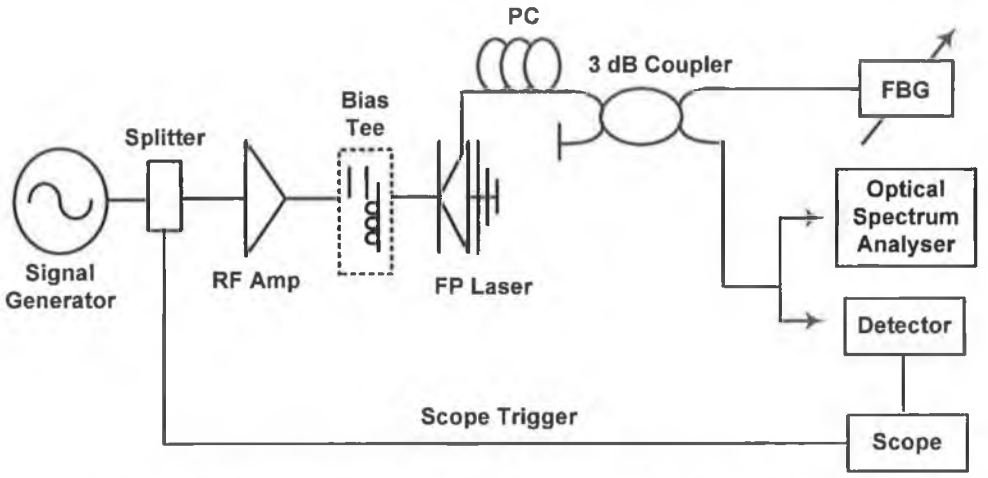

Fig 3.17 Experimental setup for generating SSGS pulses

The central wavelength of the fibre grating was tuned to one of the longitudinal modes of the gain switched laser. The modulation frequency was then varied to ensure that the signal re-injected back into the cavity arrived as an optical pulse was building up. An operating frequency of 2.532 GHz was found to be suitable. The amount of light re-injected, and therefore the SMSR of the output pulses, could also be varied by adjusting the PC. The generated self-seeded gain switched (SSGS) pulses were then characterised both in the temporal domain and spectral domain using the lower output arm of the 50:50 coupler.

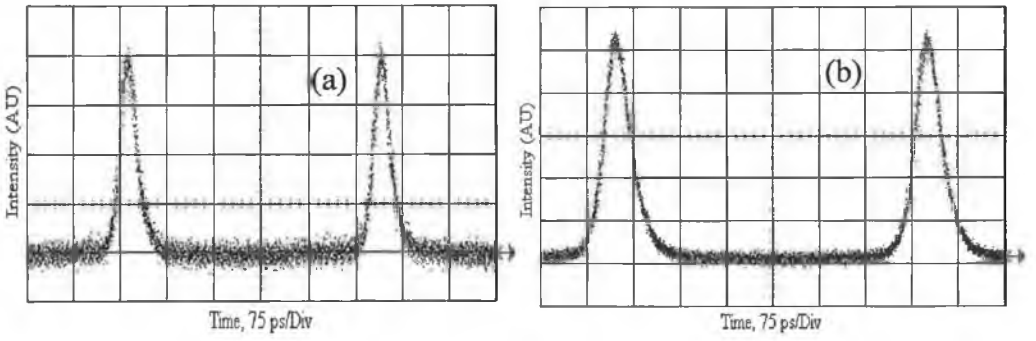

Fig. 3.18 (a) Gain switched pulse, (b) self seed gain switched pulse

Figure 3.18 (a) shows the gain switched pulse before self seeding with a deconvolved pulse width of 28.5 ps. Adjusting the PC to maximise feedback into the FP cavity, resulted in the output pulses shown in Figure 3.18 (b) which had a deconvolved pulse width of 30 ps. This broadening of the self seeded pulse is due to the laser medium being driven more rapidly into saturation, as a result the laser switches sooner and the gain at the switching time is lower than the gain of the CW case. Therefore the gain variation during the emission of the pulse is

reduced, leading to a larger pulse width. We also can see that the jitter has been reduced from 2 ps to 1.3 ps due to self seeding. The SSGS pulses had a peak power of 4.5 mW.

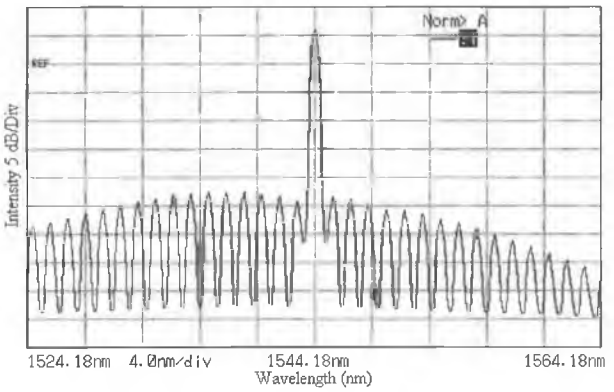

Fig. 3.19 Single moded SSGS spectra

From Figure 3.19, we can see that the spectral mode selected with the FBG was at a wavelength of 1544.18 nm and had a spectral width of about 0.3 nm (37 GHz at 1554 nm) resulting in a TBP of 1.13. A clear improvement in the SMSR (30.35 dB) can be seen when compared to the modulated spectrum of Figure 3.16 (b).

3.2.6 Pulse Shaping using an External Modulator.

The external modulator used was an electroabsoprtion modulator (EAM2010B-HG) which had a modulation bandwidth of 10 GHz and a switching voltage of about 2.5 volts. The static (DC) transfer characterisation was obtained by using the experimental setup shown below (Figure 3.20).

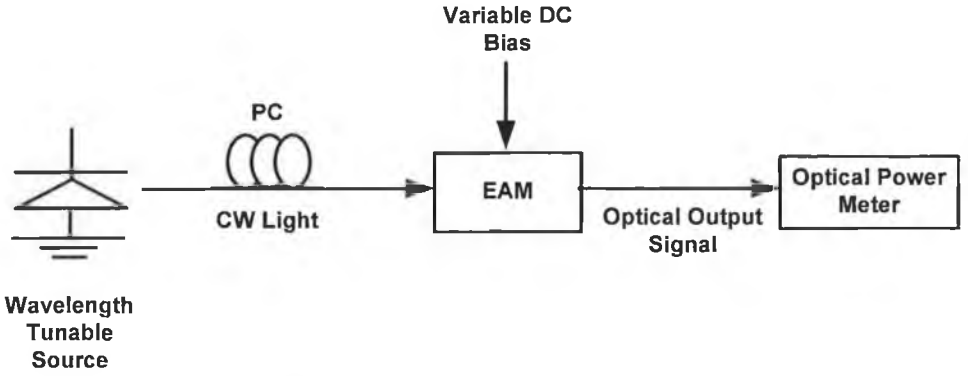

Fig 3.20 Setup used for DC characterisation of EAM

CW light from a wavelength tunable source set to 1550 nm was coupled into the EAM via a polarisation controller (PC). The output power from the wavelength tunable source was set to -10 dBm due to presence of two semiconductor optical amplifiers (SOAs) integrated into

the modulator and placed before and after the electroabsorption modulator. The polarisation controller was then adjusted to maximise the output power. The bias applied to the modulator was then varied from -4.5 v to -0.5 volts and the output power noted at each discrete bias. The results were then plotted and can be seen in Figure 3.21.

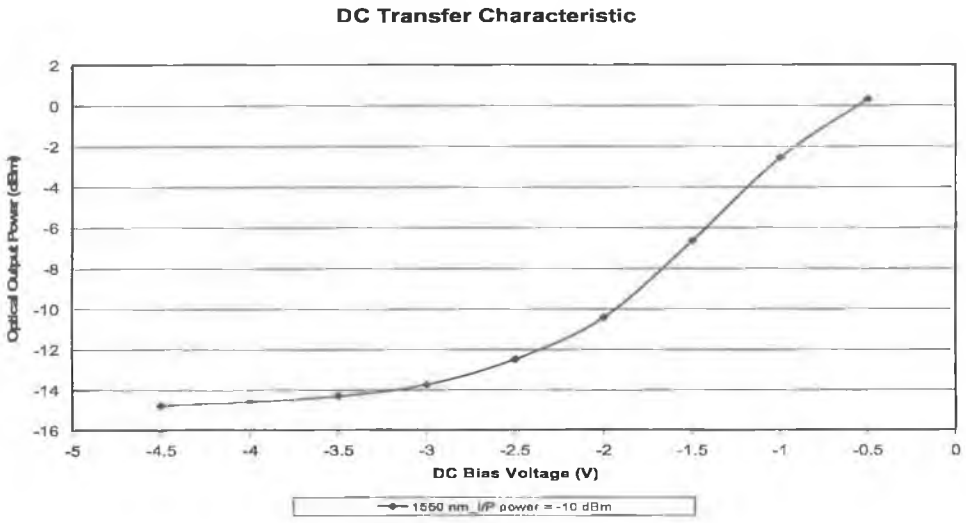

Fig. 3.21 Transfer characteristic for EAM modulator

It can be seen from the graph that a switching voltage of about 2.5 V gives an extinction level of 14 dB. Once we had characterised the modulator, we generated pulses using the setup in Figure 3.22.

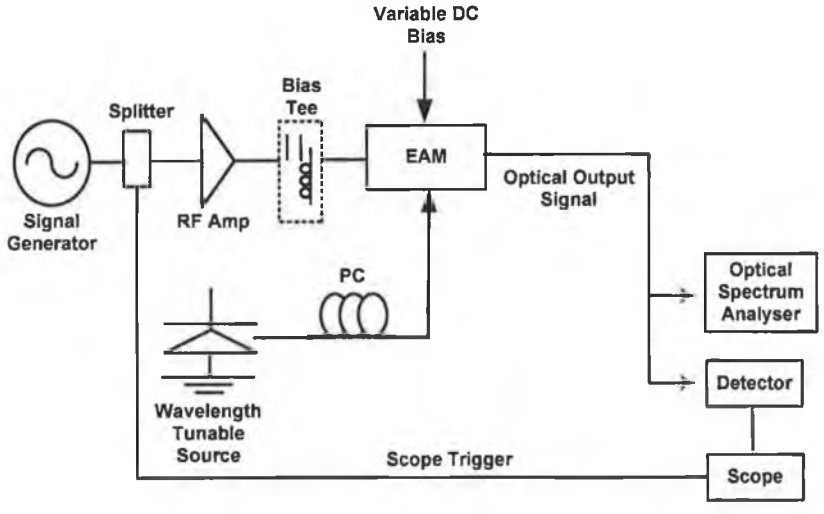

Fig. 3.22 Experimental setup for pulse shaping using an external modulator.

Using the same CW source, light was coupled into the modulator via the PC. The dc bias to the modulator was set to -2 V (the centre of the transfer characteristic) and a 10 GHz sine wave was split using a 50:50 electrical power splitter. 50% was used to trigger the

oscilloscope and the other 50% arm was electrically amplified before being coupled into a bias tee. The bias tee was used to couple the dc bias and the applied RF signal before applying both to the modulator. The RF level applied to the EAM was around 2.01 V peak-to-peak. The currents to SOA 1 and SOA 2 were set to 50.77 mA and 77.32 mA respectively. If the EAM is biased appropriately the non-linear profile of the transfer characteristic shapes pulses from the applied sine wave. The generated pulses were then observed on an oscilloscope via a 50 GHz photodiode, and an optical spectrum analyser.

The pulses observed on the scope can be seen in Figure 3.23. At a wavelength of 1544 nm the FHWM pulse width was measured to be 29.7 ps and 28.8 ps at a wavelength of 1549 nm. The peak power at 1545 nm was 1.92 mW, while, at 1549 nm it was 4.36 mW. Both pulse trains had a period of 100 ps which was due to the modulation frequency of 10 GHz.

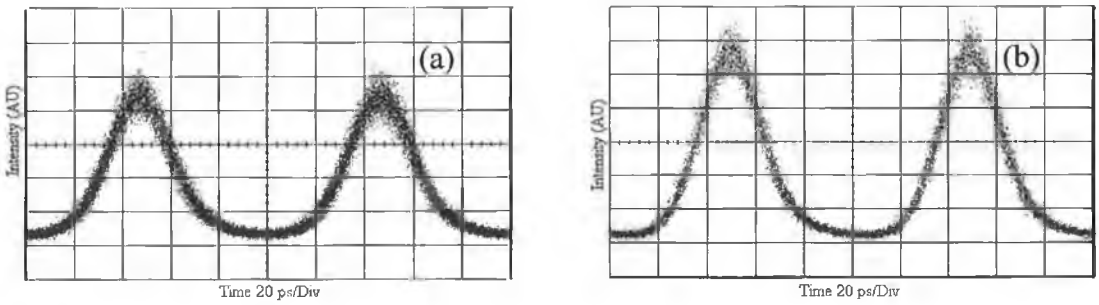

Fig 3.23 (a) 1545 nm pulse (b) 1550 nm

The associated spectra for 1544 nm and 1549 nm are presented in Figure 3.23 (a) and (b) respectively. The 3 dB spectral width at 1544nm was measured to be 0.13 nm (16 GHz @ 1544 nm) and at 1549 nm it was 0.14 nm (17 GHz @ 1549 nm). The resulting TBP for pulses at 1544 nm was 0.47 and at 1550 nm was 0.51.

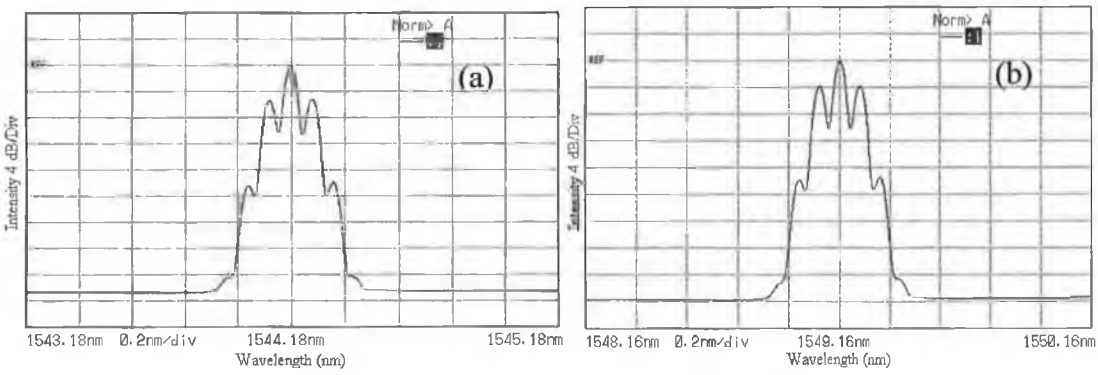

Fig. 3.24 Spectra at (a) 1544 and (b) 1549 nm

Summary

This chapter has shown that gain switching of a DFB or FP laser is one of the simplest and cost effective methods for generating picosecond optical pulses. However these pulses usually have high levels of jitter and poor spectral quality which has a detrimental effect on the use of these pulses in high-speed communication. Two methods that are used to reduce these side effects are self seeding and external injection and when applied to an FP laser, it allows for a cheap and easy way to generate tunable optical pulses. Table 3.1 below summarises the key results from this chapter. By gain switching a DFB laser and self seeding it, we have demonstrated the generation of 14 ps pulses at 2.5 GHz with an average power of about 0.18 mW. These pulses exhibit a high SMSR of 33 dB, a timing jitter of 1.6 ps and a TBP of 0.6. Externally injecting light from a second laser into a gain switched DFB laser resulted in the generation of pulses with durations of 11 ps at 10 GHz that had an average power of 0.47 mW. The timing jitter of these pulses was around 1.4 ps and the TBP was 1.63 while the SMSR was 28 dB. Next we looked at SSGS pulses generated using an FP laser at a repetition rate of 2.5 GHz. The FWHM pulse width was about 30 ps at an average power of 0.32 mW and had a timing jitter value of 1.3 ps. A SMSR of 30 dB and a TBP of 1.13 was displayed by pulses generated using this technique. Finally we examined the method of pulse shaping using an external modulator to generate pulses at 10 GHz and at two different wavelengths, 1544 and 1549 nm. At 1544 nm, the pulse duration was about 29 ps, the TBP was 0.47 and the average power was 0.55 mW. At 1549 nm, the pulse width was about 28 ps, the TBP was 0.51 and the average power was about 1.29 mW.

	Spectral Width (nm)	Pulse Width (ps)	TBP	SMSR (dB)	Jitter (ps)	Peak Power (mW)	Average Power (mW)
GS DFB @ 2.5GHz	0.5	12	0.75	9.66	3	6.02	0.18
GS DFB @ 2.5GHz	0.5	12.3	0.75	9.66	3	6.18	0.19
SSGS DFB @ 2.5GHz	0.34	14	0.6	33.9	1.6	5.4	0.18
GS DFB @10 GHz	1.4	9.5	1.66	11	3.3		
EIGS DFB @10 GHz	1.2	11	1.63	28	1.4	4.7	0.47
GS FP @ 2.5 GHz	0.7	29.6	2.6	9.66	2		
SSGS FP @2.5 GHz	0.3	30	1.13	30.35	1.3	4.5	0.32
EAM @ 10 GHz 1554nm	0.13	29.7	0.47	32	1.8	1.92	0.55
EAM @ 10 GHz 1549nm	0.14	28.8	0.51	32	1.9	4.36	1.29

Table 3.1: Pulse parameters from gain-switching, self-seeding, external injection and pulse shaping using an external modulator

Reference

[1] D.M Spirit, A. D. Ellis, and P. E. Barnsley, *"Optical Time Division Multiplexing: Systems and Networks."* IEEE, Communications Magazine, pp 56-62, December 1994.

[2] S. Kawanishi, *"Ultrahigh-Speed Optical Time-Division-Multiplexed Transmission Technology Based on Optical Signal Processing"*, IEEE J. Quantum Electro., vol. 34, vol. 11, pp 2064-2079, 1998.

[3] H. A. Haus, *"Mode-Locking of Lasers"*, IEEE J. Select. Topics of Quantum Elec. vol. 6. no. 6, pp 1173-1185, 2000

[4] W. T. Silfvast, *"Laser Fundamentals"*, Cambridge University Press, 1st Ed., 1996.

[5] K.Y.Lau, *"Short-pulse and high-frequency signal generation in semiconductor lasers"*, IEEE J.Lightwave Technol., vol. 7, no. 2, pp. 400–419, 1989.

[6] J. A. Leegwater, *"Theory of Mode-Locked Semiconductor Lasers"*, IEEE J. Quantum Elec., vol. 32, pp. 1782-1790, 1996.

[7] C. Rulliere, *"Femtosecond Laser Pulses Principles and Experiments"*, 2nd Ed., Springer, 2005.

[8] A. E. Siegman, *"Lasers"*, University Science Books, 1st Ed., 1986.

[9] S. Kawanishi, *"Ultrahigh-Speed Optical Time-Division-Multiplexed Transmission Technology Based on Optical Signal Processing"*, IEEE J. of Quantum Electron., vol. 34, no. 11, pp. 2064–2079, 1998.

[10] R. C. Alferness, *"Waveguide Electro-optic Modulator"*, IEEE Transactions on Microwave Theory and Techniques", vol. mtt-30, pp. 1121-1137, 1982.

[11] K. Nagai and H. Wada, *"40Gb/s EA modulator"*, OKI Technical Review, Issue 190 vol. 69, no. 2, 2002.

[12] J. J. Veselka and S. K. Korotky, *"Pulse Generation for Soliton Systems Using Lithium Niobate Modulators"*, IEEE J. Selec. Topics of Quantum Electron., vol. 2 pp. 300-310, 1996.

[13] P. Gunning, R. Kashyap, A.S. Siddiqui and K. Smith, *"Picosecond pulse generation of < 5ps from gain-switched DFB semiconductor laser diode using linearly step-chirped fibre grating"*, Electron. Lett., vol. 31, no. 13, pp 1066-1067, 1995.

[14] P. Vasil'ev, *"Ultrafast diode lasers: Fundamental and Applications"*, Artech House, 1st Ed., 1995.

[15] P. M. Downey, J. E. Bowers, R. S. Tucker and E. Agyekum, *"Picosecond Dynamics of a Gain Switched InGaAsP laser"*, IEEE J. of Quantum Elec., no. 6, pp 1039-1047, 1987.

[16] K. Y. Lau, *"Gain switching of semiconductor injection lasers"*, Appl. Phys. Lett., vol. 52, no. 4, pp 257-259, 1998.

[17] M. Osinski, & M. J. Adams *"Picosecond Pulse Analysis of Gain Switched 1.55m InGaAsP Lasers"*, IEEE J. Quantum Electron., vol. 21, pp 1929-1936, 1985.

[18] J. M. Dudley, L. P. Barry, J. D. Harvey, M. D. Thomson, B. C. Thomsen, P. G. Bollond, & R. Leonhardt, *"Complete Characterization of Ultrashort Pulse Sources at 1550 nm"*, IEEE J. Quantum Electron., vol. 35, pp 441-450, 1999.

[19] D. Marcuse and T-P. Lee, *"On Approximate Analytical Solutions of Rate Equations for Studying Transient Spectra of Injection Lasers"*, IEEE J of Quantum Electron., vol. QE-19, pp. 1397-1406, 1983.

[20] L. P. Barry, J. Debeau & R. Botittin, *"Simple Technique to Improve the Spectral Quality of Gain Switched Pulses from a DFB Laser"*, Electron Lett., vol. 30 pp. 2143-2145, 1994.

[21] S. Nogiwa, Y. Kawaguchi, H. Ohta & Y. Endo, *"Generation of Gain-Switched Optical Pulses with very Low Timing Jitterby using External CW-Light Injection Seeding"*, Electron Lett., vol. 36 pp 235-236, 2000.

[22] M. Jinno, *"Correlated and Uncorrelated Timing Jitter in Gain Switched Laser Diodes"*, IEEE Photon. Technol. Lett., vol. 5, pp 1140-1143, 1993.

[23] M. Schell, W. Utz, D. Huhse, J. Kassner & D. Bimberg, *"Low jitter single-mode pulse generation by a self seeded, gain-switched Fabry-Perot semiconductor laser"*, Appl. Phys. Lett., vol. 65, pp 3045-3047, 1994.

[24] M. Schell, D. Huhse, W. Utz, J. Kaessner, D. Bimberg & I. S. Tarasov, *"Jitter and Dynamics of Self-Seeded Fabry-Perot Laser Diode"*, IEEE, J. Select. Topics Quantum Elec., vol 1, pp 528-534, 1995.

[25] P. Gunning, J.K. Lucek, D. G. Moodie, K. Smith, R. P. Davey, S. V. Chernikov, M. J. Guy, J. R. Taylor, and J. S. Siddiqui, *"Gain Switched DFB laser Diode Pulse Source using Continuous Wave Light Injection for Jitter Suppression and an Electro-absorption Modulator for Pedestal Suppression"*, Electron. Lett. vol. 32, pp 1010-1011, 1996.

[26] J. P. Van Der Ziel & R. A. Logan, *"Generation of Short Optical Pulses in Semiconductor Lasers by Combined dc and Microwave Current Injection"*, IEEE, J. of Quantum Electron., vol. 18 pp 1340-1350, 1982.

[27] D.Huhse, M.Schell, W.Utz, J.Kaessner, and D.Bimberg, *"Dynamics of Single Mode Formation in Self-Seeded Fabry-Perot Laser Diodes"*, IEEE Photon. Technol. Lett., vol. 7, no. 4, pp. 351–353, 1995.

[28] M. Schell, W. Utz, D. Huhse, J. Kassner and D. Bimberg, *"Low jitter single-mode pulse generation by self-seeded, gain-switched Fbary-perot semiconductor laser"*, Appl. Phys. Lett., vol. 65, pp. 3045-3047, 1994.

[29] A. M. Clarke, P. M. Anandarajah and L. P. Barry, *"Generation of Widely Tunable Picosecond Pulses with Large SMSR by Externally Injecting a Gain-Switched Dual Laser Source"*, IEEE Photon. Technol. Lett., vol. 16, pp 2344-2346, 2004.

[30] D. Seo and H. Liu, *"Wavelength-tunable nearly transform limited pulse generation by external injection-seeding of a gain-switched Fabry- Perot laser"*. Electron. Lett., vol. 33, pp 2129-2130, 1997.

[31] S. Mohrdiek, H. Burkhard & H. Walter, *"Chirp Reduction of Directly Modulated Semiconductor Lasers at 10 Gb/s by Strong CW Light Injection"*, IEEE J. Lightwave Technol. vol. 12, pp 418-424, 1994.

[32] D.-S. Seo, D. Y.Kim, and H.-F. Liu, *"Timing jitter reduction of gain-switched dfb laser by external injection-seeding"*, Electron. Lett., vol. 32, no. 1, pp. 44–45, 1996.

[33] S. Li, K. S. Chiang, W. A. Gambling, Y. Liu, L. Zhang, and I. Bennion, *"Self-Seeding of Fabry–Perot Laser Diode for Generating Wavelength-Tunable Chirp-Compensated Single-Mode Pulses with High-Side mode Suppression Ratio"*, IEEE Photon. Technol. Lett., vol. 12, pp 1441-1443, 2000.

[34] J. Debeau, L. P. Barry and R. Boittin, *"Wavelength Tunable Pulse Generation at 10 GHz by Strong Filtered Feedback using a Gain-Switched Fabry Perot Laser"*, Electron. Lett., vol. 30, pp 74-75, 1994.

[35] J.W. Chen adnd D. N. Wang, *"Self-Seeded, Gain Switched Optical Short Pulse Generation with High Side Mode Suppression Ratio and Extended Wavelength Tuning Range"*, Electron. Lett., vol. 39, pp 679-681, 2003.

4. Optimisation of Gain Switched Optical Pulse Parameters for Implementation in High-Speed Communication Systems

Introduction

Since the end of the seventies, the generation of ultra short optical pulses from semiconductor laser diodes has been the subject of intense research activity [1]. As a result, many practical applications have been developed, ranging from military and medical uses to signal processing, optical spectroscopy and metrology to name but a few. One application that was the main driving force behind the development of such pulse sources is the field of telecommunications. In terms of communication applications these pulses sources are extremely important for use in future optical time division multiplexed (OTDM), and hybrid WDM/OTDM optical systems [2]. Over the past few years the ceiling of the base data rate has been 10 Gb/s, with most systems employing Non-Return-to-Zero (NRZ) coding at the transmitter. However, with the move to higher data rates of 40 Gb/s and above, it may become necessary to use Return-to-Zero (RZ) coding. The RZ coding is far less susceptible to non-linearity and dispersion effects in the transmission fiber, resulting in a higher signal-to-noise ratio (SNR) and a lower system bit error rate giving a better overall system performance [3,4,5,6]. This is due to the fact that RZ pulses take advantage of soliton-like pulse compression in SMF and improved receiver sensitivity. The reduced channel spacing and increased line rate necessary to achieve higher aggregate data rates, places stringent requirements on the optical RZ transmitter to generate pulses with acceptable temporal and spectral purity. As discussed in the previous chapter, there are numerous methods available to generate picosecond optical pulses, such as pulse shaping of continuous wave (CW) light using an external modulator, mode locking of a semiconductor or fiber ring lasers [7] and gain switching.

The technique of gain switching, when compared with the above-mentioned alternatives, offers efficient wavelength stable performance and the ability to produce high repetition rate pulses [8]. Some of the important temporal characteristics of these pulse sources include; the pulse width, temporal jitter and temporal pedestal suppression ratio (TPSR). While important spectral parameters include; the spectral width, side mode suppression ratio (SMSR) and chirp. We discussed some of these characteristics in the previous chapter. In this chapter, a detailed experimental analysis of the SMSR, chirp and TPSR of the generated gain switched pulse will be carried out.

In the following section we focus on analysing the effects of the SMSR of SSGS pulses when employed in hybrid WDM/OTDM networks. The SMSR is defined as the ratio of power emitted in the strongest mode to that emitted in the second strongest mode and usually expressed in decibels. This investigation into the effect of the pulse SMSR on the performance of SSGS pulses in optical communication systems is carried out by examining pulses portraying different SMSR that are propagated through an optical filter. A pulse with a low SMSR that is filtered will have a large amount of amplitude jitter added to the pulse which will degrade the SNR.

4.1 Effects of SMSR on Self Seeded Gain Switched Pulses.

The generation of gain switched pulses using both DFB and FP lasers has been demonstrated in the previous chapter. The main advantages of gain switching an FP laser diode as opposed to a DFB are the cost effectiveness and ease of wavelength tunability. One of the desired features of an optical pulse source is to be wavelength tunable, which enhances the flexibility of WDM networks. Self seeding a gain switched Fabry Perot (FP) laser is one of the simplest, most reliable and attractive options to generate wavelength tunable picosecond optical pulses [9, 10]. As we have seen in the previous chapter, this essentially involves gain switching an FP laser, and then feeding back one of the laser modes into the FP diode using a wavelength selective external cavity. Provided that the optical signal re-injected into the laser arrives during the build-up of an optical pulse in the FP laser, then a single-moded, low jitter output pulse can be obtained [11].

We carried out a detailed investigation on the increase in the noise of filtered SSGS pulses [12] with degrading inherent SMSR. Here, we define the inherent SMSR, as the SMSR directly at the output of the SSGS laser or, alternatively, as the SMSR of the SSGS laser before filtering. Generally, filtering of SSGS pulses is used to either select out a particular wavelength in multi-wavelength systems, to improve the SMSR of the SSGS pulses, or to remove amplified spontaneous emission (ASE) power from an erbium doped fiber amplifier (EDFA) which may have been placed after the SSGS setup. Although many of the previously reported wavelength tunable SSGS pulse sources use output filtering on pulses that have low inherent SMSRs of about 15 – 20 dB, to achieve a final SMSR > 30 dB [13, 14, 15], our results show that such pulses may be unsuitable for use in either WDM or OTDM systems. The reason for this lies in the build up of noise on the filtered optical pulses due to the mode partition effect. Hence, it is vital that any pulse source based on the SSGS technique possesses a large enough inherent SMSR, especially before optical filtering to prevent the degradation of SNR due to mode partition noise (MPN). Therefore, it is

important when characterizing such pulses for use in optical systems, that both the SMSR and the amplitude noise of these pulses should be accurately described, as there maybe a direct relationship between them.

4.1.1 Experimental Results

Figure 4.1 shows the experimental set-up used. The FP laser used was a commercially available InGaAsP device, which had a threshold current of about 25 mA, a longitudinal mode spacing 1.1 nm and a central wavelength of 1542 nm. A 2.5 GHz sine wave produced from a signal generator was passed through a 50:50 electrical splitter. One part was used to trigger an oscilloscope while the other was electrically amplified to a power of about 29 dBm before being coupled into a bias tee that was used to combine the electrical signal with a variable dc bias of about 17 mA. The resulting optical signal from the laser was coupled into a GRIN lens fiber pigtail that had an antireflection coating to prevent back reflection entering the laser. Self seeding of the gain switched laser diode was achieved by using an external cavity containing a Polarization Controller (PC), a 3 dB optical coupler and a tunable fibre Bragg grating (FBG) (HWT 4399901) that had a bandwidth of 0.4 nm. To achieve optimum SSGS pulse generation, the central wavelength of the FBG was initially tuned, via a piezoelectric controller, to one of the longitudinal modes of the gain switched laser. To ensure that the signal re-injected into the laser from the external cavity, arrived as an optical pulse was building up in the laser, we varied the frequency of the sinusoidal modulation. The same result could have been achieved by incorporating an optical delay line to vary the round trip time of the signal within the cavity. An operating frequency of 2.488 GHz was found to be suitable. This rate was the 58^{th} harmonic of the fundamental frequency, which was calculated to be ~ 48.49 MHz. The level of feedback, taking into account the losses incurred in the external cavity and coupling, was measured to be approximately -15 dBm.

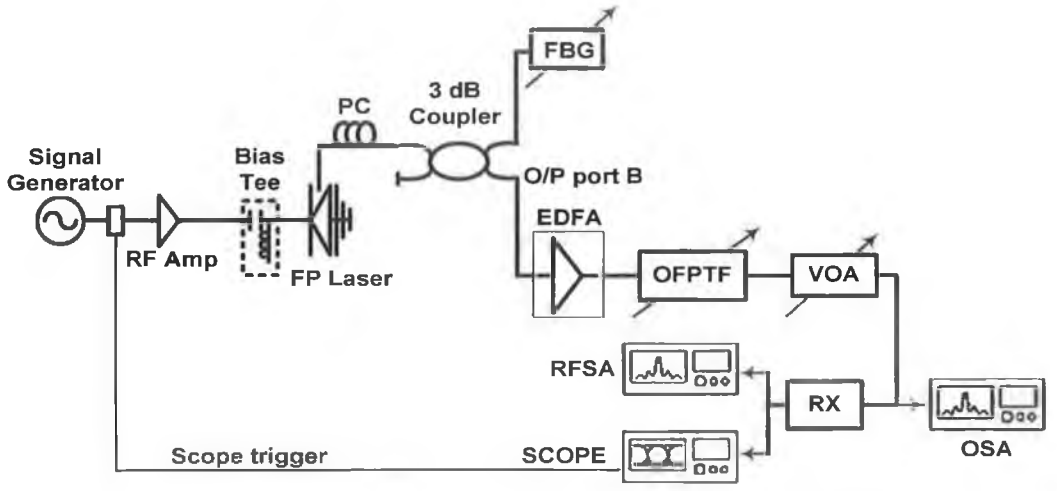

Figure 4.1: Experimental set-up for the characterisation of degraded SSGS pulse after filtration

By tuning the FBG and the modulation frequency, the amount of light re-injected into the laser and therefore the SMSR of the optical pulses could be varied. However, by also varying the PC, the optic axis of the re-injected light could be matched to that of the light from the laser meaning that the power coupled into the lasing mode could be changed. This effectively changes the SMSR of the optical pulses and we utilised this fact to represent pulses with various levels of side mode suppression. The resulting SSGS pulses were available at the lower output arm of the 3 dB coupler, labeled output port B in Figure 4.1. The SMSR portrayed by these pulses is called the inherent SMSR. These pulses were then amplified with the aid of an EDFA after which they are filtered using an optical Fabry Perot tunable filter (OFPTF) to improve the output SMSR. The OFPTF (Santec-300) had a FWHM passband of about 0.7 nm (84 GHz) and an extinction ratio of about 20 dB. In order to characterize the noise on the filtered SSGS pulses as a function of the input SMSR, the output SMSR had to be kept constant. Due to the large extinction ratio of the filter, the inherent SMSR of the pulses could be improved by about 20 dB by passing the signal through the centre of the filters passband. Depending on whether the inherent SMSR was weak or strong, the filters passband was tuned towards or away from the central wavelength of the SSGS pulses. When the inherent SMSR of the SSGS signal was high (30 dB) the output SMSR was maintained at 35 dB by tuning the filter away from the central wavelength of the SSGS signal. On the other hand, when the inherent SMSR of the SSGS signal was low (15 dB) the output SMSR was maintained at 35 dB by tuning the filter to the central wavelength of the SSGS signal. The lower and the upper SMSR limits were set by the extinction ratio of the filter, which meant that the inherent SMSR could be varied between a range of 15 – 30 dB while still maintaining an output SMSR of 35 dB. However, this tuning

of the filters passband towards and away from the central wavelength meant that the output power of the filtered SSGS signal would vary because the signal would experience various levels of attenuation at different portions of the filter's transfer characteristic. To overcome this problem and ensure that the power falling on the detector was always kept constant, a variable optical attenuator (VOA) that incorporated an inline power meter was added after the filter. The output pulses were then characterized in the temporal domain using a 50 GHz photodiode in conjunction with a 50 GHz sampling oscilloscope (HP54750A). An Anritsu (MS9717A) optical spectrum analyzer (OSA) was used to characterize the output pulses in the spectral domain. The high-speed detector was alternated between the oscilloscope and an Anritsu (MS2668C) RF spectrum analyzer (RFSA), which was used to measure the RF noise spectrum.

With the PC adjusted to allow maximum feedback into the FP laser, the resulting SSGS pulses before optical filtration are shown in Figure 4.2 (a). The deconvolved output pulse width was calculated to be around 26 ps, assuming a total response time of about 9 ps for the combination of the photodiode and the oscilloscope. Figure 4.2 (b) shows the spectral output from which we can determine that the FP mode selected using the FBG was at a wavelength of 1547.08 nm. From this figure it can be seen that the inherent SMSR of the signal was 37 dB, and the 3 dB spectral width was about 0.3 nm (37 GHz @ 1546 nm). These pulses would be suitable for use in a high-speed communication system. However in certain cases the inherent SMSR may not be as high. A weaker SMSR may have been brought about due to various reasons such as an inefficient seeding mechanism, temperature and current drifts or aging of components. Tuning of the wavelength to a mode further away from the peak of the gain curve could also result in a pulse with a poorer SMSR. Here we degraded the SMSR to represent pulses which have a poor inherent SMSR brought about by the above mentioned cases.

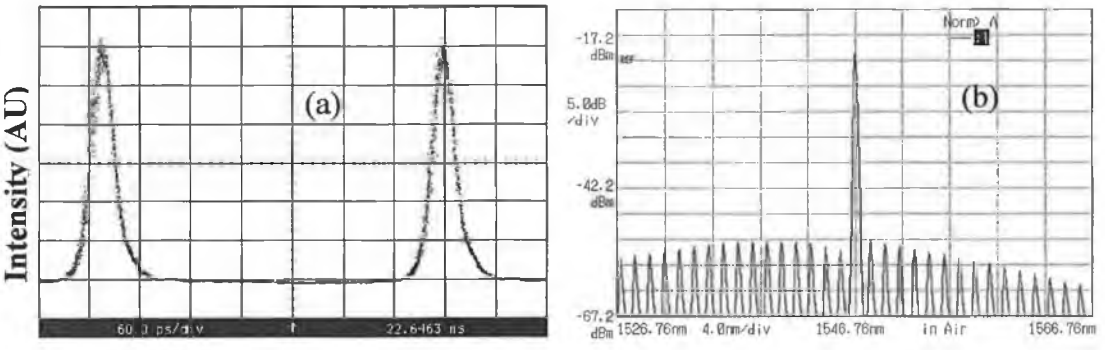

Figure 4.2: (a) Optical pulse with inherent SMSR of 37 dB (b) Optical spectrum with inherent SMSR of 37 dB

To vary the SMSR of the generated optical pulses from 30 dB down to 15 dB, we simply had to adjust the PC in order to reduce the amount of light fed back into the laser diode. As we saw before, the reduction in feedback and SMSR also resulted in a slight decrease in the pulse duration and a slight increase in the spectral width. Figure 4.3 (a) and (b) show the SSGS pulses after optical filtration when the inherent SMSR was set at 30 and 15 dB respectively and the output SMSR maintained at a constant value of 35 dB. It can be seen clearly that the noise level on the filtered output pulse which had a corresponding inherent SMSR of 30 dB, (Figure 4.3 a), is lower than that of the output pulse which had a corresponding inherent SMSR of 15 dB, (Figure 4.3 b).

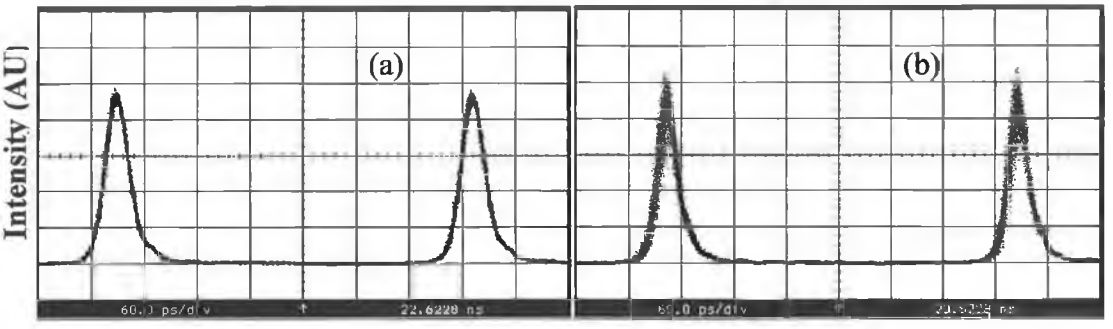

Fig. 4.3: Filtered optical pulses with inherent SMSR of (a) 30 dB and (b) 15 dB

The corresponding spectra depicting the inherent SMSRs (high and low) are shown in Figure 4.4 (a) and (b) respectively while the filtered output spectra are shown in Figure 4.5 (a) and (b) respectively. The filtered output spectra show that even though the inherent SMSR is varied between 15 and 30 dB, by tuning the filter towards or away from the central wavelength of the SSGS signal, the output SMSR could still be maintained at a constant level of 35 dB.

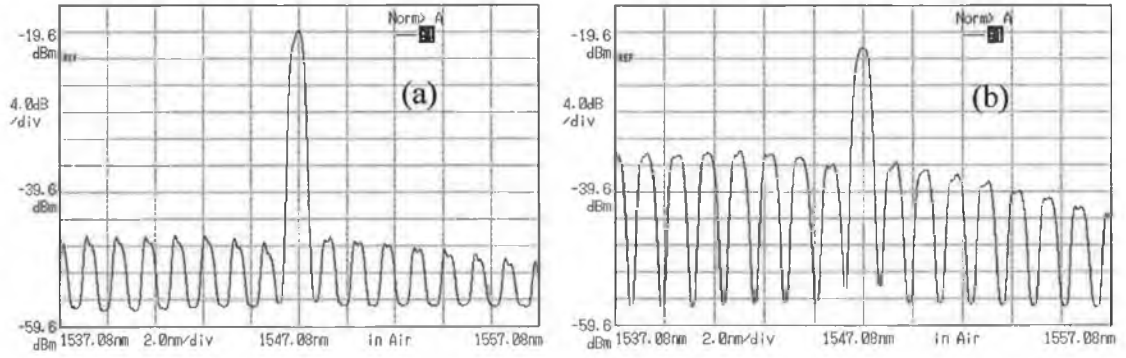

Fig. 4.4: Input optical spectra with inherent SMSR of (a) 30 dB and (b) 15 dB

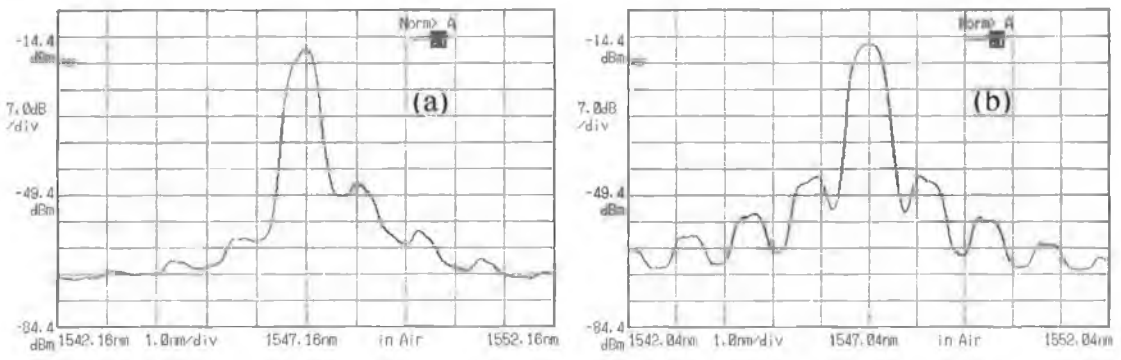

Fig. 4.5: Filtered optical spectra with output SMSR maintained at 35 dB and inherent SMSR of (a) 30 dB & (b) 15 dB respectively

The increase in noise as the inherent SMSR is reduced is associated with the mode partition effect of the FP laser which essentially involves the energy of each laser mode fluctuating with time, due to a constant transfer of energy between the laser modes [16]. Since only the main mode is transmitted through the optical filter, any temporal fluctuations in the energy level of this mode will manifest itself as amplitude noise on the transmitted pulse. Clearly as the SMSR is reduced, the energy in the side modes increases and the fluctuation of the energy in the main mode increases, resulting in additional amplitude noise on the transmitted pulse. This can cause a degradation of the signal to noise ratio.

Having observed the addition of amplitude noise on the transmitted pulses, we next carried out a more quantitative analysis of the increased noise floor. By performing RF spectral measurements on the detected pulses, we could conduct a more detailed investigation into the noise introduced on the filtered SSGS pulses as the SMSR is degraded. The latter was carried out, with the aid of an RFSA, within a span of 8 GHz over a range of 2 – 10 GHz at a resolution band-width (RBW) of 1 MHz. The measurement carried out over this range included the fundamental and the first three harmonics of the pulse train and is shown in Figure 4.6 It can be seen that the power levels of each of the plots, corresponding to the various inherent SMSRs (30, 25, 20 and 15 dB), have been equalized with the aid of the VOA. It is important to remember that a pulse with a constant output SMSR of 35 dB was maintained. From the graph, we can clearly see an increase in the noise floor for decreasing values of the inherent SMSR. The noise floor measurements were taken at an offset of about 1 GHz from the carrier. When the inherent SMSR was set to 30 dB, represented by the black trace, the noise floor was measured at -88 dBm. However, when the inherent SMSR was degraded to a poorer level of 15 dB, shown as the red trace, the noise floor increased to -65 dBm.

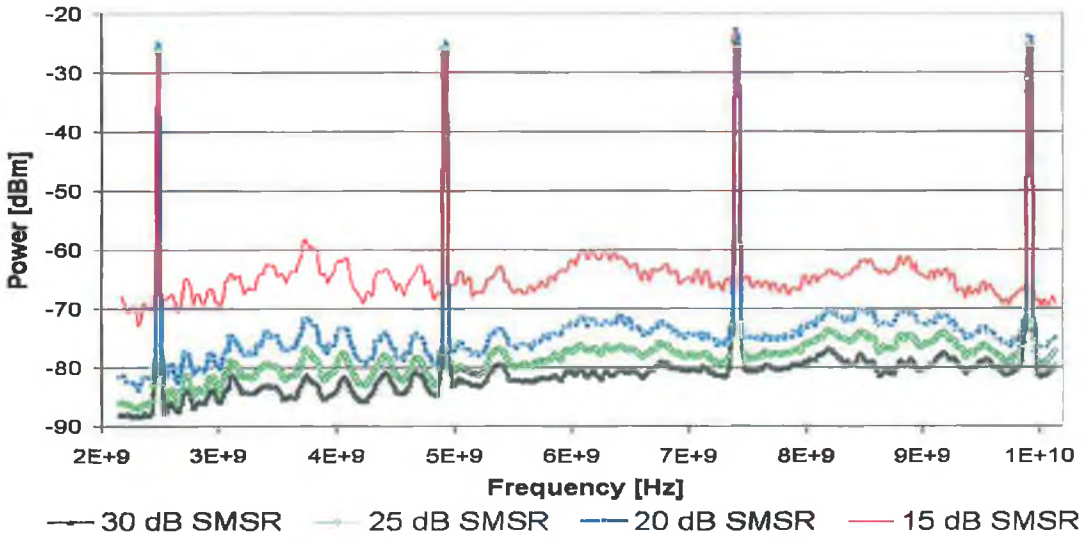

Fig. 4.6: RF spectrum of SSGS pulses exhibiting various inherent SMSRs

Table 4.1 below helps to quantify the corresponding changes in the noise floor measurements when a degrading sweep of the inherent SMSR from 30 to 15 dB in steps of 5 dB was taken. The table clearly shows that, for a 5 dB change in the inherent SMSR, the increase in the noise level is greater at lower inherent SMSRs. The table illustrates that when the inherent SMSR was degraded from 30 to 25 dB, the noise floor rose by 4.52 dB. Degrading from 25 to 20 dB raised the noise floor by 5.33 dB while degrading even further from 20 to 15 dB resulted in a dramatic increase of 13.16 dB. So it is clear that when the inherent SMSR is degraded from a strong case of 30 dB to a weaker case of 15 dB it results in the level of the noise floor increasing by about 23 dB even though the output SMSR is maintained at a level of 35 dB. This is due to the fact that there is a bigger increase in the percentage of power in the side modes which in turn leads to larger fluctuations in the main lasing mode.

Change in Input SMSR	Change in Noise Floor
30 – 25 dB	4.52 dB
25 – 20 dB	5.33 dB
20 – 15 dB	13.16 dB
30 – 15 dB	23.02 dB

Table 4.1: Change in noise floor with decreasing inherent SMSR (offset from carrier = 1 GHz)

Looking at the numbers closely reveals that going from an inherent SMSR of 30 – 25 dB is an increase of only about 0.3 % in power in the side modes, but going from 20 – 15 dB is an increase of approximately 2.3 % in power in the side modes thus making the increase in noise at weaker inherent SMSRs more noticeable. The larger fluctuations result in additional amplitude noise on the detected pulse. These results clearly quantify the major difference in the noise floor of an output filtered SSGS pulse that exhibits a weak inherent SMSR of 15 dB and a strong inherent SMSR of 30 dB.

The acquired noise on filtered SSGS pulses as the SMSR is reduced is due to MPN. MPN in digital transmission systems has been known for a long time and can severely affect the performance of an optical communication system, even when using distributed feedback lasers with non-ideal SMSR. It is mainly caused by the total optical power, in a multi-longitudinal mode laser diode, remaining relatively constant but the distribution of this power between the modes is a stochastic process [16]. In other words, there is a random change of energy in each mode due a constant transfer of energy between the modes. For a single mode laser that maintains a high SMSR, the power in the side modes may be considered insignificant and so the power fluctuations in the main mode are also negligible. However as the SMSR is reduced, the energy in the side modes increase and the fluctuations of the energy in the main mode increases. The spectral fluctuation of energy in the laser modes may thus manifest itself as an intensity fluctuation (noise) on the transmitted optical signal and this manifestation of noise in optical communication systems due to MPN can occur in two ways. Firstly, the effects of fibre dispersion in long haul links result in temporal fluctuations of received power because the fluctuating modes get separated in time due to the fibre dispersion [17]. Secondly, output optical filtering of the SSGS signal may result in fluctuations in the output power of the signal after the filter, which results in a degradation of the signal quality. Hence, an important parameter to characterize the level of MPN is the SMSR [18]. In order to reduce this MPN and prevent the build of noise on transmitted pulses, it is necessary to reduce the energy in the side modes. This can be done by ensuring that the inherent SMSR of SSGS pulses that undergo output filtration exhibit a high SMSR. In other words the total power in the side modes should be negligible. It is not sufficient to rely on optical filtration alone to improve the output SMSR.

4.2 Effects of Chirp on the Temporal Purity of Externally Injected Gain Switched Pulses.

While the gain switching technique has been accepted as one of the simplest and most reliable optical pulse source and the advantages in employing this method are numerous, one of its major drawbacks is the spectral purity of the generated pulses. The direct modulation of the laser diode causes a large variation in the carrier density over time within the active region of the device and so also varies the refractive index. As the wavelength is related to the carrier concentration, due to the effect of free carriers on the refractive index of the device, this in turn causes a variation in the output wavelength from the laser during the emission of the optical pulse. This results in a large linear frequency chirp across the centre of the pulse and a large non-linear chirp in the sides (wings) of the pulse. As this could degrade the performance of optical communication systems [19], it has been reported how this chirp can be used to compress the pulses using dispersion compensating fiber (DCF) [20] or linearly chirped fiber Bragg gratings (LC FBG) [21], to obtain near transform-limited pulses. However, using the compression techniques of DCF and LC FBG does not fully compensate for the non-linear chirp across the pulse and typically results in temporal pedestals on either side of the pulses. These pedestals can overlap into adjacent time slots leading to cross talk between neighbouring channels which in turn leads to a loss of signal integrity due to inter symbol interference (ISI), thus rendering such pulses unsuitable for use in practical systems. By using more complex arrangements involving non-linear loop mirrors or external modulators, after the linearly compressed pulse, it is possible to greatly reduce the pedestal [22].

We next describe the generation of temporally and spectrally pure short optical pulses. By this we mean pulses which have a temporal pedestal suppression ratio (TPSR) and spectral side mode suppression ratio (SMSR) greater than 30 dB. The generation of these pulses was achieved using a pulse source that comprised of a non-linearly chirped fiber Bragg grating (NC FBG) in conjunction with an externally injected gain switched DFB laser [23]. The design of the NC FBG was determined by carrying out a complete characterization of the gain switched pulse using the technique of frequency resolved optical gating (FROG) [24]. This characterization yields information on the parameters of the pulse that are required for the design of an NC FBG that must have a group delay profile that is opposite to that measured across the pulse. By employing the tailor made NC FBG after the gain switched laser, it is possible to achieve direct compression of the gain switched pulses and obtain near transform limited pulses. Experimental results, obtained by employing this novel technique, show 3.5 ps pulses (FWHM) at a repetition rate of 10 GHz and an associated spectral width of 130 GHz are generated. The resulting pulse and supporting spectral widths generated

using this technique yields near transform-limited pulses with a time bandwidth product (TBP) of 0.45. These pulses also exhibit an extinction of the temporal pedestals up to about 35 dB below the peak of the pulse. This excellent temporal pedestal suppression ratio (TPSR) is due not only to the grating filter having a non-linear group delay profile which is the inverse of that across the gain switched pulse measured directly from the output of the laser, but also by ensuring the grating filter has a specially adapted filter transfer characteristic. The NC FBG has a custom designed non-linear reflective profile that optimizes the output pulse spectrum to give a Gaussian shaped spectrum, thereby further enhancing the temporal quality of the pulses. The spectral and temporal characteristics of such a pulse source would make it suitable for use as a transmitter in 80 Gb/s OTDM or hybrid WDM/OTDM systems.

4.2.1 Experimental Setup

4.2.1.1 Externally Injected Gain Switched Laser

The experimental set-up used is shown in Figure 4.7. A 10 GHz sine wave was generated from a signal generator and then electrically split using a 50:50 electrical power splitter. One half of the electrical signal was used to trigger a sampling oscilloscope and the other was amplified with the aid of a high power RF amplifier. The amplified signal was then coupled into a bias tee that was used to combine the electrical RF signal with a dc bias to enable gain-switching of a commercially available NEL DFB laser. The laser was contained within a hermetically sealed high-speed package and had a threshold current of about 19.5 mA. The device had a 3 dB modulation bandwidth of 15 GHz, and an output power of 4 dBm, both measured at a bias current of three time the threshold current (3 I_{th} ~ 59 mA). Both the modulation frequency and dc bias were varied to optimize the gain switched pulses and an operating frequency of 10.3 GHz along with a dc bias of 48 mA (~2.5 I_{th}) were found to be suitable. The resulting pulses generated were at a wavelength of 1549.35 nm and wavelength tunability of the laser mode over a range of 2 nm could be achieved by temperature controlling the diode. To overcome the poor SMSR and timing jitter of the gain switched pulses, which in this case was about 5 dB and 2 ps respectively, we used external injection (via an optical circulator) from a second DFB (2). This master laser had a central wavelength of 1550 nm, was biased at 23.5 mA (~1.2 I_{th}) and had an isolator incorporated into the attached fiber pig tail, preventing any light from entering it. A polarization controller was also used to ensure that the light being injected was aligned with the optical axis of the modulated laser. The injected power, incident on the modulated laser diode, was measured to be about -20 dBm after taking into account the losses incurred in the optical injection path.

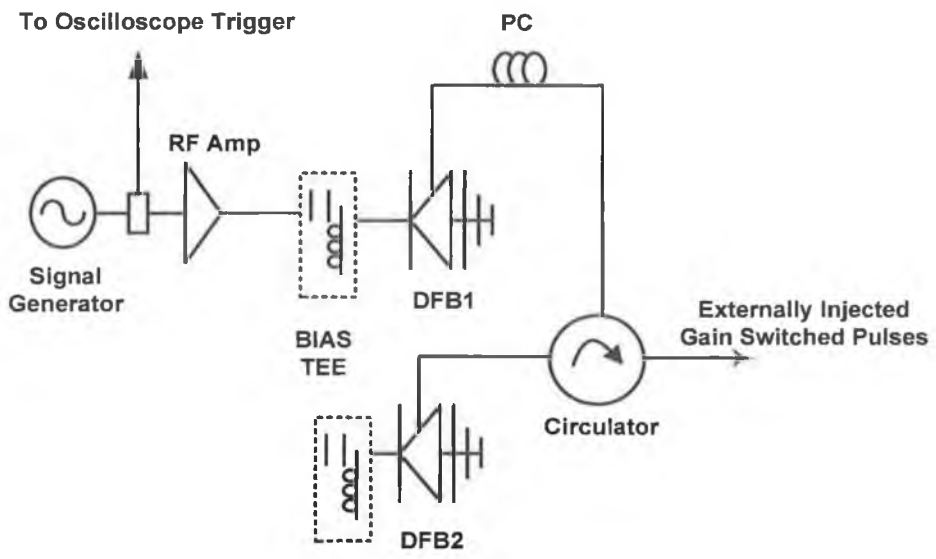

Fig. 4.7 Experimental setup used to generate externally injected gain switched pulses

Externally injecting light into the cavity of the modulated laser improves the SMSR to around 30 dB and reduces the timing jitter to <1 ps. The jitter was measured using an Agilent Digital Communications Analyzer which had a resolution of about 9 ps, taking into account the rise times of both the photodetector and the oscilloscope. The improvement in the SMSR is due to the injected optical signal reducing the gain threshold of the main mode of the modulated laser relative to side modes. The improvement in the timing jitter is due to the optically injected light providing an excitation above the spontaneous emission level, reducing the relative fluctuations in the photon density thereby reducing the timing jitter of the pulses. The actual jitter on the externally injected gain switched output is expected to be in the order of 200 fs or less as demonstrated in previous work [25]. The generated pulses were characterized using an optical spectrum analyzer (OSA), a high-speed oscilloscope in conjunction with a 50 GHz pin detector, and also the FROG measurement system. The optical spectra of the generated gain switched pulses are shown in Figure 4.8 (a) and (b) both without and with external injection respectively. It can be seen that the SMSR was degraded to about 5 dB without injection and the overlapping of the broadened modes prevents the side mode being distinguished from the main mode. However, with external injection, there was a vast improvement in the SMSR to greater that 30 dB. Also, from the same figure, the spectral width of the externally injected gain switched laser was determined to be about 140 GHz.

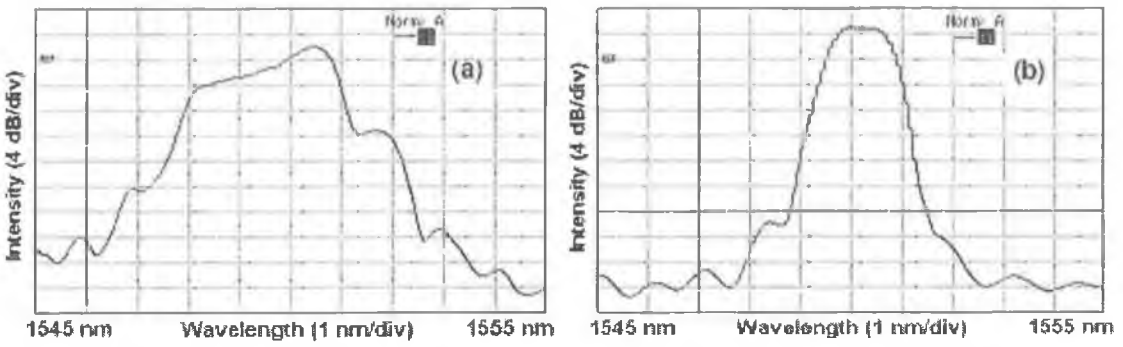

Fig. 4.8 Spectra of gain switched laser (a) without and (b) with external injection

The non-averaged oscilloscope trace of the detected pulse train from which the low temporal jitter can be noticed is shown in Figure 4.9. The ringing in this pulse is due to its duration being shorter than the response time of the detector, making it difficult to determine the actual pulse width, but it was estimated to be around 10 ps.

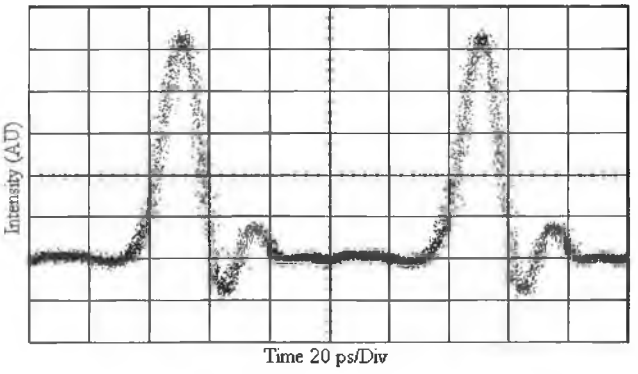

Fig. 4.9 Externally injected gain switched pulse

In order to accurately characterize this pulse it is necessary to use the frequency resolved optical gating (FROG) technique. A standard second harmonic generation (SHG) FROG based on the spectral resolution of the output from a non-collinear autocorrelator, as described in [24] was used. The complete electric field of the input optical pulse can be determined from the measured FROG spectrogram by using standard retrieval techniques [24]. To improve the SNR of the measurement, a short pulse Erbium Doped Fibre Amplifier (EDFA), specifically designed for the amplification of pulses with a duration in the order of 2 ps (FWHM), was placed before the FROG measurement set-up. From the FROG measurement, it is possible to accurately characterize the intensity and chirp profile across the optical pulses generated from the externally injected gain switched laser. Figure 4.10 shows the intensity and chirp profile across the pulses generated using this technique. It can be seen that the pulses had a duration (FWHM) of about 10.5 ps and that the frequency chirp, indicated by the dashed line in the figure, becomes non-linear in the wings of the pulse. The

time bandwidth product (TBP) of the pulse generated from the externally injected gain switching process was 1.5, which is far from the transform limit (0.44) for a Gaussian shaped pulse.

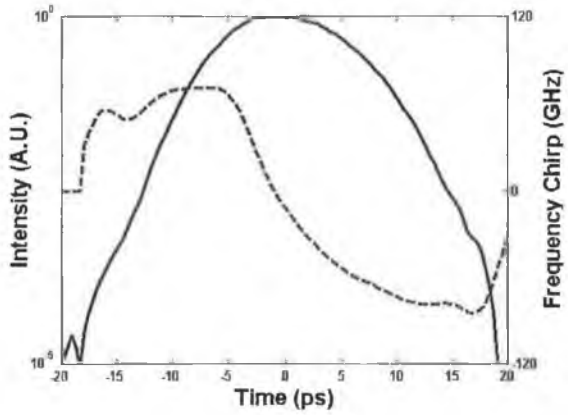

Fig. 4.10 FROG measurement of externally injected gain switched pulse depicting intensity (solid line) and chirp (dashed line).

4.2.1.2 Fabrication of a Non-Linearly Chirped FBG.

Once the measured non-linear chirp across the pulse was obtained we used it to design and fabricate an NC FBG. This process involved the creation of the group delay response for the FBG based on the group delay data derived from the FROG measurements of the externally injected gain switched pulse. The desired FBG group delay response was chosen to be simply the inverse to the pulse group delay response. This should ensure that when the pulse is reflected from the FBG it will have a constant group delay profile over the pulse bandwidth. For an optimised pulse source we not only require a constant group delay profile across the pulse bandwidth, but also require the pulse to exhibit a Gaussian spectrum. Generally, gain switched spectra tend to have a more rectangular shape as opposed to a Gaussian shape. The reflection profile of the NC FBG, shown in Figure 4.11, was constructed as the difference between the spectral amplitude of the gain switched output and a modelled Gaussian profile. As the gain switched spectra propagates through the grating, different spectral components of the pulse will experience various levels of attenuation due to the filter transfer characteristic. This should result in the compressed pulse portraying a Gaussian spectrum.

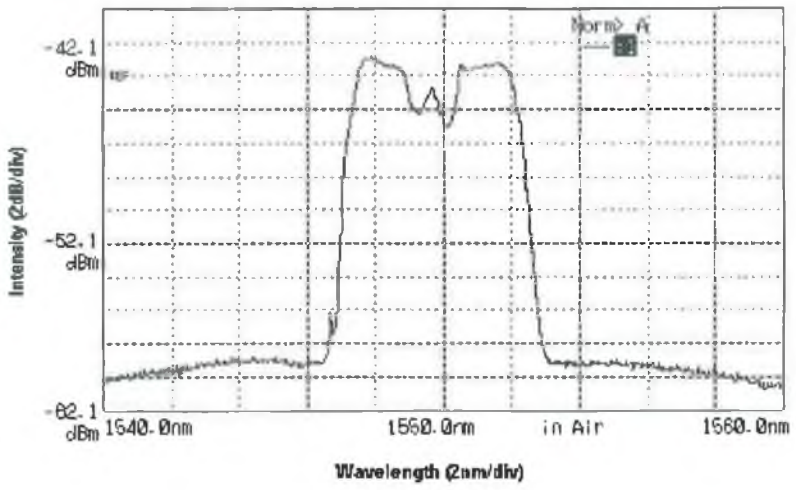

Fig. 4.11 Reflection profile of the NCFBG.

Once the desired spectrum and group delay profile of the FBG was obtained it was relatively straightforward to calculate an FBG design that could be implemented into the optical fibre by using an inverse scattering algorithm [26, 27, 28]. The actual FBG fabrication was carried out by an industrial partner using our design. The reflective and group delay profiles of the fabricated NC FBG are shown in Figure 4.12. We also fabricated a LC FBG which had a chirp profile that was opposite to a linear approximation of the chirp across the gain switched pulse.

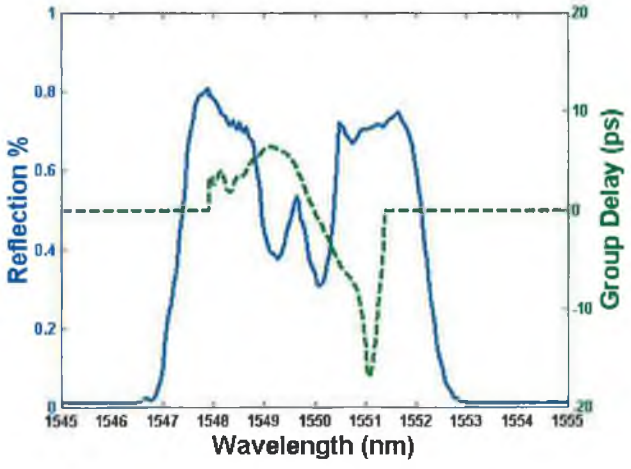

Fig. 4.12 Reflection (solid line) and group delay (dashed lines) profiles of the non-linearly chirped FBG.

4.2.1.3 Compression of Externally Injected Gain Switched Pulses.

By placing the NC FBG and LC FBG after the externally injected gain switched laser, as shown schematically in Figure 4.13, we subsequently characterised the pulse compression in the fibre gratings using the FROG technique. In the experimental work presented here, the

pulse recovery routinely gave retrieval errors of $G < 0.005$ on a 128×128 grid [24] which gave an indication into the accuracy of our retrievals. Figure 4.14 (a) and (b) show the measured intensity and chirp profile of the gain switched optical pulses after compression using the linearly and non-linearly chirped fibre gratings respectively. It can be seen that in both cases the gratings eliminated any frequency chirp across the centre of the pulses. However, when the linearly chirped grating was used, the non-linearity of the chirp from the gain switched laser resulted in significant pedestals on the leading and trailing edge of the pulse, Figure 4.14 (a). These pedestals, which are around 23 dB down from the peak of the pulse, can severely limit the performance of a high-speed OTDM system by creating interference noise between individual channels (through inter-symbol interference).
To avoid this problem and achieve better system performance, a TPSR of over 30 dB is required [29].

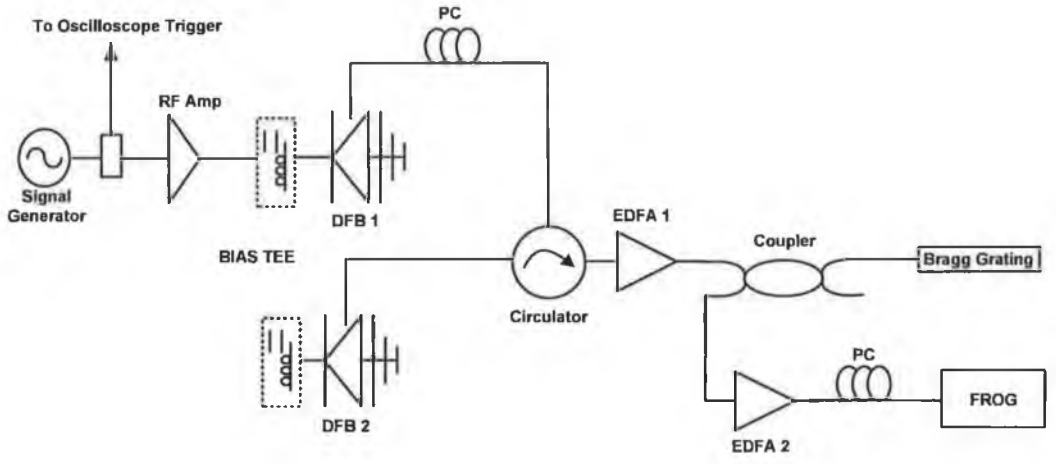

Fig. 4.13 Schematic of setup used to generate optimised pulses.

Figure 4.14 (b) shows the intensity and chirp profile of the compressed gain switched pulse using the non-linear chirped fibre Bragg grating. The compression produced a FWHM pulse width of 3.5 ps. It can clearly be seen that the resultant chirp across the pulse was flat and had a very small order of magnitude. From this figure it can also be seen that the pedestals were almost eliminated, with the TPSR measured to be >35 dB. This reduction in the temporal pedestal suppression ratio is not only due to the elimination of the chirp across the pulse but also to the output pulse spectrum having a Gaussian shape due to the non-linear reflection profile of the grating, as explained earlier.

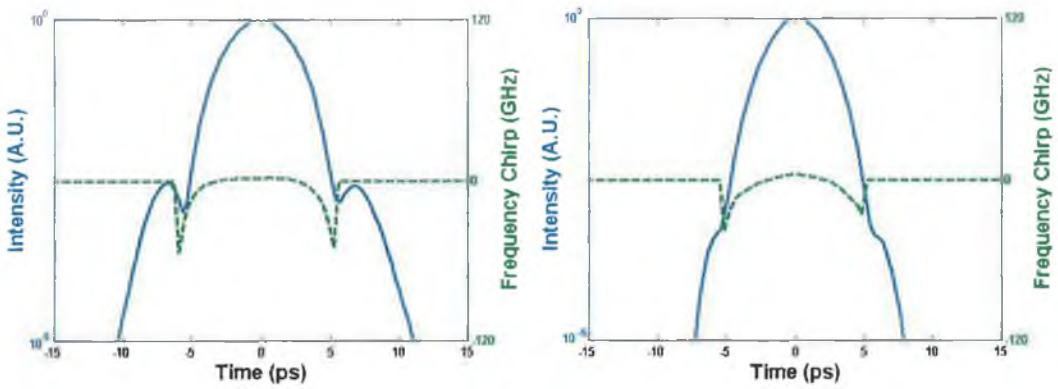

Fig. 4.14 Intensity (solid line) and chirp profiles (dashed line) of externally injected gain switched pulses after (a) linearly chirped and (b) non-linearly chirped FBGs.

It is important to note that, for a non-Gaussian spectrum, even if the group delay is entirely compensated for, the existence of temporal pedestals could still be possible. The Fourier transform of a rectangular spectrum, which results in a Sinc temporal pulse [30], could be used to justify the presence of such pedestals. Another important point to note is that a large ripple in the group delay profile of the compressing FBG could result in the creation of low intensity temporal pedestals. This group delay ripple (GDR) originates from the difference between the group delay designed for the grating and the group delay that is actually etched into the grating. A large difference between the two would result in the chirp not being compensated to the desired degree and the creation of temporal pedestals. In this experiment however, pedestals generated in such a manner were not observed. This was mainly due to the low level of GDR which had a standard deviation of less than half the compressed pulse width. The spectra and the group delay profiles of the input and output pulses to and from the NC FBG, are shown in Figure 4.15 (a) and (b) respectively. From Figure 4.15 (b), it is clear that the group delay had been completely compensated for by the tailor-made NC FBG and that the output spectrum was more Gaussian shaped and symmetric in comparison to the spectrum of the input pulse. This is due to the compensation by the non-linear reflection profile of the NC FBG.

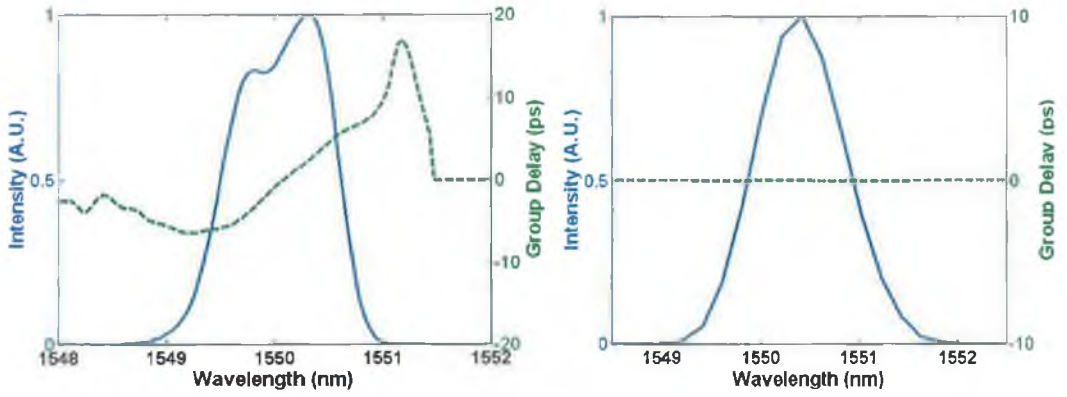

Fig. 4.15 Spectra (solid lines) and group delay profiles (dashed lines) of GS pulse (a) before NCFBG and (b) after grating.

The spectrum taken from the OSA of the pulse after passing through the NC FBG was in excellent agreement with the pulse spectrum obtained from the FROG measurement. Both spectra are shown in Figure 4.16 which also shows that the spectral width was around 130 GHz. The quoted pulse width of 3.5 ps and associated spectral width resulted in a TBP of 0.45 which is very close to the time bandwidth product of transform limited Gaussian pulses of 0.44.

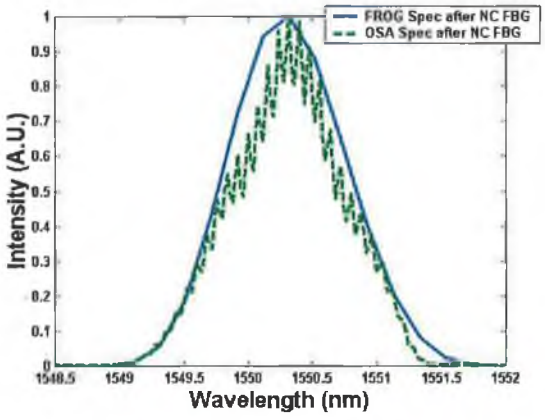

Fig. 4.16 Comparison of the spectrum obtained from the FROG (solid line) and the OSA (dashed line) after the NCFBG.

Summary

We have examined the effect of output filtration on SSGS pulses that exhibited various levels of SMSR. Our results categorically show that a reduction in the inherent SMSR of an SSGS pulse train from 30 – 15 dB would result in a 23 dB increase in the level of the noise floor of the detected pulse, leading to a reduced SNR.

It may be concluded that regardless of a high output SMSR, if the inherent SMSR of SSGS pulses are weak (< 25 dB) then the interaction of MPN with spectral filtering would result in

a large amount of amplitude noise on the output pulses. This noise or degradation of the SNR can leave such pulses totally unusable for transmission in a high-speed optical network. To avoid this it is vital that a source of SSGS pulses have an inherent SMSR of 30 dB or greater. It is therefore extremely important when characterizing optical pulses generated by the SSGS technique to simultaneously describe the SMSR and amplitude noise of the generated optical pulse train.

We have also demonstrated that a gain switched pulse which displays a large non-linear chirp across the wings of the pulse may be compensated for by using a non-linearly chirped fiber Bragg grating. The FROG measurement system was used to completely characterise the chirp across the initial gain switched pulse. From this complete characterization, a non-linearly chirped fiber Bragg grating that had a non-linear group delay profile opposite to the group delay of the input pulse was designed and fabricated. The fabricated grating also had a non-linear reflection profile to optimize the output spectrum of the generated pulses. This resulted in the generation of output pulses that displayed excellent temporal and spectral purity. The pulses were near transform limited 3.5 ps pulses that have an excellent TPSR of greater than 35 dB which would make this pulse source ideal for use in 80 Gb/s OTDM systems.

References

[1] C. Rulliere, *"Femtosecond Laser Pulses Principles and Experiments"*, 2nd Ed., Springer, 2005.

[2] T. Morioka, H. Takara, S. Kawanishi, O. Kamatani, K. Takiguchi, K. Uchiyama, M. Saruwatari, H. Takahashi, M.Yamada, T. Kanamori, and H. Ono, *"1Tbit/s (100Gbit/s times 10 channel) OTDM/WDM transmission using a single supercontinuum WDM source"*, Electron. Lett. vol. 32, pp. 906-907, 1996.

[3] R. Ludwig, U. Feiste, E. Dietrich, H. Weber, D. Breuer, M. Martin, and F. Kppers, *"Experimental Comparison of 40 Gbit/s RZ and NRZ Transmission Over Standard Single Mode Fibre,"* Electron. Lett., vol. 35, no. 25, pp. 2216–2218, December 1999.

[4] M. I. Hayee and A. E. Willner, *"NRZ Versus RZ in 10-40 Gb/s Dispersion-Managed WDM Transmission Systems,"* IEEE Photon. Technol. Lett., vol. 11, no. 25, pp. 991–993, December 1999.

[5] C. R. S. Fludger, Y. Zhu, V. Handerek, and R. J. Mears, *"Impact of MPI and Modulation Format on Transmission Systems Employing Distributed Raman Amplification,"* Electron. Lett., vol. 37, pp. 970–972, 2001.

[6] P. J. Winzer, M. Pfennigbauer, M. M. Strasser, and W. R. Leeb, *"Optimum Filter Bandwidths for Optically Preamplified NRZ Receivers,"* IEEE J. Lightwave Technol., vol. 9, pp. 1263–1273, 2001.

[7] S. Kawanishi, *"Ultrahigh-Speed Optical Time-Division-Multiplexed Transmission Technology Based on Optical Signal Processing"*, IEEE J. Quantum Electron. vol. 34, pp. 2064-2079, 1998.

[8] Y. J. Chai, K. A. Williams, R. V. Penty and I. H. White, *"High Quality Femtosecond Pulse Generation from a Gain Switched DFB Laser Using a Novel Self-Seeding Scheme"*, presented at the LEOS / CLEO Europe, Munich, Germany, 22-27 June, 2003.

[9] M. Cavelier, N. Stelmakh, J. M. Xie, L. Chusseau, J. M. Lourtioz, C. Kasmierski, and N. Bouadama, *"Picosecond (<2.5 ps) Wavelength Tunable (~20 nm) Semiconductor Laser Pulses with Repetiontion Rate up to 15 GHz"*, Electron Lett., vol. 28, pp. 224-226, 1992.

[10] J. W. Chen and D.N Wang, *"Self Seeded Gain Switched Optical Short Pulse Generation with High Side Mode Suppression Ratio and Extended Wavelength Tuning Range"*, Electron., Lett., vol. 39, pp. 679-681, 2003.

[11] M. Schell, W. Utz, D. Huhse, J. Kassner, and D. Bimberg, *"Low jitter single mode pulse generation by a self-seeded, gain-switched Fabry-Perot semiconductor laser"*, Appl. Phys. Lett. vol. 65, pp. 3045-3047, 1994.

[12] D. Curter, P. Pepeljugoski, and K.Y. Lau, *"Noise Properties of Electrically Gain-Switched 1.5 μm DFB Lasers after Spectral Filtering"*, Electron. Lett. vol. 30, pp.1418-1419, 1994.

[13] K. Lee, C. Shu and H. F. Liu, *"Subharmonic Pulse Gating in Self-Seeded Laser Diodes for Time- and Wavelength Interleaved Picosecond Pulse Generation"*, IEEE J. Quantum Electron. vol. 40, pp. 205-213, 2004.

[14] D. N. Wang and M. F. Lim, *"Tunable Dual-Wavelength Optical Short Pulse Generation by Use of a Fibre Bragg Grating and a Tunable Optical Filter in a Self Seeding Scheme"*, Appl. Opt. vol. 43, pp. 4106-4109, 2004.

[15] S. Li, K. S. Chiang, W. A. Gambling, Y. Liu, L. Zhang and I. Bennion, *"Self-Seeding of Fabry-Perot Laser Diode for Generating Wavelength-Tunable Chirp Compensated Single-Mode Pulses with High-Sidemode Suppression Ratio"*, IEEE Photon Technol. Lett., vol. 12, pp. 1441-1443, 2000.

[16] N. H. Jensen, H. Olesen, and K. E. Stubkjaer, *"Partition Noise in Semiconductor Lasers under CW and Pulsed Operation"*, IEEE J. Quantum Electron., QE-23, pp. 71-79, 1987.

[17] L.P.Barry, and P. Anandarajah, *"Effect of Side-Mode Suppression Ratio on the Performance of Self-Seeded Gain-Switched Optical Pulses in Lightwave Communications Systems"*, IEEE Photon. Technol. Lett., vol. 11, pp. 1360–1362, 1999.

[18] A. Valle, C. R. Mirasso and L. Pesquera, "Mode Partition Noise of Nearly Single Mode Semiconductor Lasers Modulated at GHz Rates", IEEE J. Quantum Electron. vol. 31, pp. 876-885, 1995.

[19] J. M. Dudley, L. P. Barry, J. D. Harvey, M. D. Thomson, B. C. Thomsen, P. G. Bollond, and R. Leonhardt, *"Complete Characterization of Ultrashort Pulse Sources at 1550 nm,"* IEEE J. of Quantum Electron., vol. 35, pp. 441–450, 1999.

[20] K. A. Ahmed, H. F. Liu, N. Onodera, P. Lee, R. S. Tucker, and Y. Ogawa, *"Nearly Transform Limited Pulse (3.6 ps) Generation From Gain-Switched 1.55 μm Distributed Feedback Laser By Using Fibre Compression Technique,"* Electron. Lett., vol. 29, no. 1, pp. 54–56, 1993.

[21] B. J. Eggleton, P. A. Krug, L. Poladian, K. A. Ahmed, and H. F. Liu, *"Experimental Demonstration of Compression of Dispersed Optical Pulses by Reflection from Self-Chirped Optical Fibre Bragg Gratings,"* Opt. Lett., vol. 19, pp. 877–879, 1994.

[22] P. Gunning, J. K. Lucek, D. G. Moodie, K. Smith, R. P. Davey, S. V. Chernikov, M. J. Guy, J. R. Taylor, and A. S. Siddiqui, *"Gain switched DFB Laser Diode Pulse Source Using Continuous Wave Light Injection for Jitter Suppression and an Electroabsorption Modulator for Pedestal Suppression,"* Electron. Lett., vol. 32, no. 11, pp. 1010–1011, 1996.

[23] A. Clarke, P. M. Anandarajah, D. Reid, G. Edvell, L. P. Barry, and J. D. Harvey, *"Optimized Pulse Source for 40-Gb/S Systems Based on a Gain-Switched Laser Diode in Conjunction With a Non-linearly Chirped Grating,"* IEEE Photon. Technol. Lett., vol. 17, no. 1, pp. 196–198, 2005.

[24] R. Trebino, K. W. DeLong, D. N. Fittinghoff, J. N. Sweetser, M. A. Krumbugel, and B. A. Richman, *"Measuring Ultrashort Laser Pulses in the Time Frequency Domain Using Frequency-Resolved Optical Gating"*, Rev. Sci. Instrum., vol. 68, pp. 3277–3295, 1997.

[25] S. Nogiwa, Y. Kawaguchi, H. Ohta, and Y. Endo, *"Generation of Gain Switched Optical Pulses with Very Low Timing Jitter by Using External CW-Light Injection Seeding,"* Electron. Lett., vol. 36, no. 3, pp. 235–236, 2000.

[26] A. Rosenthal and M. Horowitz, *"Inverse Scattering Algorithm for Reconstructing Strongly Reflecting Fiber Bragg Gratings"*, IEEE J of Quantum Electron., vol. 39, no. 8, pp. 1018–1026, 2003.

[27] J. Skaar and O. H. Waagaard, *"Design and Characterization of Finite-Length Fiber Gratings"*, IEEE J. of Quantum Electron., vol. 39, no. 10, pp. 1238–1245, 2003.

[28] R. Feced, M. N. Zervas, and M. A. Muriel, *"An Efficient Inverse Scattering Algorithm for the Design of Nonuniform Fiber Bragg Gratings"*, IEEE J. Quantum Electron., vol. 35, no. 8, pp. 1105–1115, 1999.

[29] P. L. Mason, A. Wonfor, D. D. Marcenac, D. G. Moodie, M. C. Brierley, R. V. Penty, I. H. White, and S. Bouchoule, *"The Effects of Pedestal Suppression on Gain Switched Laser Sources for 40 Gbit/s OTDM Tranmission"*, 10th Annual Meeting of IEEE LEOS, vol. 1, pp. 289–290, May 1997.

[30] R. A. Gabel and R. A. Roberts, *"Signals and linear systems"*, John Wiley and Sons, 1987.

5. Conclusion

The increasing demand for bandwidth, driven by the massive increase in internet usage and other broadband applications such as high definition TV and video conferencing, has created the need for communication networks to handle much higher data rates. As current commercially available electronic devices struggle to move beyond the established single channel rates, which is currently about 10 Gb/s, optical multiplexing techniques are seen as the best choice to overcome the electronic bottle necks encountered. By using techniques such as WDM, OTDM and hybrid WDM/OTDM it is possible to make better use of the available bandwidth of optical fibers and achieve data rates of > 1 Tb/s. However, to move to data rates of 40 Gb/s and above, it is likely that RZ coding will be used for data transmission as it is easier to compensate for dispersion and non-linear effects in the fiber.

As a result, the development of an optical pulse source which produces transform limited, ultra short optical pulses which are both temporally and spectrally pure is vital for future high-speed optical communication systems. This work focuses on the technique of gain switching a laser diode as a source of such transform limited optical pulses due to its simplicity, compactness and ability to produce pulses at a high repetition rate

An initial experimental investigation into the gain switching of a DFB laser diode yielded 12 ps pulses with an associated spectral width of 0.5 nm resulting in a TBP of 0.75. However the pulse SMSR was 9 dB as opposed to 35 dB when running in CW mode and the temporal jitter of the pulses was about 3 ps. For a gain switched pulse source to be used in a high-speed optical communication system, the complications of a poor SMSR and large temporal jitter must be dealt with. Two methods that maybe used to over come these difficulties are self seeding and external injection both of which we investigated. Both techniques resulted in an improvement in the SMSR, reduced jitter and, to a small degree, they also compensated for the chirp across the pulse. Self seeding a DFB laser resulted in the generation of 14 ps pulses with an improved SMSR of about 34 dB and a reduced jitter of 1.6 ps. A reduction in the linewidth to 0.34 nm and therefore an enhanced TBP of 0.6 was also noted. Results from external injection produced an 11 ps pulse train with an improved SMSR of 28 dB, a reduced jitter of 1.3 ps and a spectral width of 1.2 nm. In order to achieve a wider wavelength tunable range, in a cost effective manner, we extended the technique of gain switching to an FP laser diode. Gain switching the FP laser generated a 32 ps pulse train with a multi-mode spectrum and a timing jitter of about 2 ps. To switch the output spectrum of the gain switched pulses from multimode to single mode emission, a small portion of light was fed back into the laser. This self seeding of a gain switched laser diode is one of the most reliable methods available

to generate wavelength tunable optical pulses. The SSGS pulses from the FP laser exhibited a pulse width of about 30 ps and had a spectral width of 0.3 nm. These pulses displayed a very small timing jitter of 1.3 ps, and an improved SMSR of about 30 dB. While the TBP was 1.13, the results did not yield a transform limited pulse. Pulse shaping using an external modulator was also investigated at two different operating wavelengths. At an operating wavelength of 1544 nm, the pulse width was about 29 ps and the 3 dB spectral width was 0.13 nm resulting in a TBP of 0.47. At 1549 nm the pulse width was about 28 ps and the spectral width 0.14 nm resulting in a TBP of 0.51. Neither temporal jitter, about 1 ps at either wavelength, or the SMSR, measured to be greater than 32 dB, are issues with this method of pulses generation. Table 5.1 below summarises these results.

	Spectral Width (nm)	Pulse Width (ps)	TBP	SMSR (dB)	Jitter (ps)	Peak Power (mW)	Average Power (mW)
GS DFB @ 2.5GHz	0.5	12	0.75	9.66	3	6.02	0.18
GS DFB @ 2.5GHz	0.5	12.3	0.75	9.66	3	6.18	0.19
SSGS DFB @ 2.5GHz	0.34	14	0.6	33.9	1.6	5.4	0.18
GS DFB @10 GHz	1.4	9.5	1.66	11	3.3		
EIGS DFB @10 GHz	1.2	11	1.63	28	1.4	4.7	0.47
GS FP @ 2.5 GHz	0.7	29.6	2.6	9.66	2		
SSGS FP @ 2.5 GHz	0.3	30	1.13	30.35	1.3	4.5	0.32
EAM @ 10 GHz 1554nm	0.13	29.7	0.47	32	1.8	1.92	0.55
EAM @ 10 GHz 1549nm	0.14	28.8	0.51	32	1.9	4.36	1.29

Table 5.1: Pulse parameters from gain-switching, self-seeding, external injection and pulse shaping using an external modulator

We next carried out an investigation into the addition of noise on filtered SSGS pulses which exhibited degrading levels of inherent SMSR. It was found that, regardless of the output SMSR being maintained at a high level of ~ 35 dB, if the inherent SMSR is less than 25 dB then the interaction of MPN with spectral filtration would create a large amount of amplitude noise on the output pulses. This noise can leave such pulses unsuitable for data transmission in optical communication systems. Table 5.2 below shows that when the inherent SMSR was changed in steps of 5 dB there was a larger increase in the noise floor for weaker inherent SMSR's.

Change in Input SMSR	Change in Noise Floor
30 – 25 dB	4.52 dB
25 – 20 dB	5.33 dB
20 – 15 dB	13.16 dB
30 – 15 dB	23.02 dB

Table 5.2: Change in noise floor with decreasing inherent SMSR (offset from carrier = 1 GHz)

This large fluctuation is due to a larger increase in the percentage of power in the side modes, Table 5.3 below, which leads to larger fluctuations in the lasing mode and additional amplitude noise on the transmitted signal.

Change in Input SMSR	Increase in percentage power in side modes
30 – 25 dB	0.3 %
20 – 15 dB	2.3 %

Table 5.3 Increase of power in side modes with decreasing inherent SMSR

We conclude that a SSGS pulse source must have a large inherent SMSR, of 30 dB or greater, particularly before experiencing optical filtering, in order to prevent the degradation of the signal-to-noise ratio brought about by MPN. Additionally it is important to include in the characterisation of these pulses, the SMSR and amplitude noise measurements.

Having observed the addition of amplitude noise on filtered SSGS pulses as a result of a reduced SMSR, we then investigated the effect of chirp on the temporal purity of gain switched pulses. By developing a novel technology based on an externally injected gain switched laser and a NC FBG, the induced chirp across a gain switched pulse is completely compensated for, eliminating any side pedestals that are typically created when known compression techniques such as DCF or LC FBG are used. The measurement system called FROG was used to characterise the chirp across a gain switched pulse and a NC FBG which had a non-linear group delay profile opposite to that of the pulse was designed. The grating also incorporated a non-linear reflection profile to ensure the output pulse exhibited a more Gaussian shaped spectrum. This produced near transform limited 3.5 ps pulses with a TPSR greater than 35 dB, making them ideal for use in an 80 Gb/s OTDM communication system.

Appendix: Publications Resulting From This Thesis

Referred Journals

Optimized Pulse Source Employing an Externally Injected Gain switched Laser Diode in Conjunction with a Non-linearly Chirped Grating.
P. M. Anandarajah, C. Cuignard, A. Clarke, M. Rensing, D. Reid, L. P. Barry, G. Edvell, & J. D. Harvey. Accepted for publication in IEEE Journal of Selected Topic in Quantum Electronics, 2006.

Signal Degradation due to Output Filtering of Self-Seeded Gain switched Pulses Exhibiting Weak Inherent SMSR. P. Anandarajah, M. Rensing, and L.P. Barry. Optical Society of America, Journal of Applied Optics, Vol. 44, pp 7867-7871, 2005.

Reviewed Conferences

Effects of Weak Input Side Mode Suppression Ratio and Output Filtration on the Intensity Noise of a Self-Seeded Gain Switched Optical Pulses at 2.5GHz.
M. Rensing, P. M. Anandarajah and L. P. Barry.
Proceeding of International Conference on Transparent Optical Networks (ICTON), Paper Tu.C2.6, Barcelona, Spain, 3-7 July 2005.

80 Gb/s Optimised Pulse Source using a Gain switched Laser Diode in Conjunction with a Non-linearly Chirped Grating.
A. Clarke, M. Rensing, P. M. Anandarajah, L. P. Barry and J. D. Harvey.
Proceeding of International Conference on Transparent Optical Networks (ICTON), Paper Tu.P.11, Barcelona, Spain, 3-7 July 2005.

80 Gb/s Pulse Source using a gain switched laser diode and a non-linearly chirped grating. A. M. Clarke, M. Rensing,, D. Reid, P. M Anandarajah, G. D. Edvell, L. P Barry, and J. D. Harvey.
European Conference on Optical Communications (ECOC), Paper Th1.3.5, Glasgow, UK, 25-29 September 2005.

Optimized Pulse Source Employing an Externally Injected Gain-Switched Laser Diode in Conjunction With a Nonlinearly Chirped Grating

P. M. Anandarajah, *Member, IEEE*, C. Guignard, A. Clarke, *Student Member, IEEE*, D. Reid, M. Rensing, L. P. Barry, *Member, IEEE*, G. Edvell, and J. D. Harvey, *Member, IEEE*

***Abstract*—In this paper, we demonstrate the generation of transform-limited short optical pulses, which display excellent spectral and temporal qualities by employing a novel technology, based on an externally injected gain-switched laser in conjunction with a nonlinearly chirped grating. Using this technique, 3.5-ps optical pulses exhibiting a time-bandwidth product (TBP) of 0.45 are generated, which are suitable for use in high-speed 80 Gb/s optical time-division multiplexing (OTDM) communications systems. The numerical integration of a set of rate equations using suitable parameters for the devices used in the experiments were carried out to further confirm the feasibility of the proposed method for developing an optimized pulse source for high-speed photonic systems.**

***Index Terms*—Fiber Bragg gratings (FBGs), optical fiber communication, optical pulse compression, optical pulse generation, semiconductor lasers.**

I. Introduction

THE increasing demand for media-rich content delivery and the escalation of IP traffic has been fueling the massive growth in demand for bandwidth. This extensive increase in bandwidth usage, which shows no sign of abating in the coming decade, is pushing carriers and service providers to deploy increasing optical backbone transmission capacity. The goal of developing future terabit all-optical communication systems may be achieved by a reduction in channel spacing of wavelength-division multiplexed (WDM) systems [1] or an increase in the per-channel data rate. The latter one could be achieved by exploiting electrical time division multiplexing (ETDM) as in WDM/ETDM [2] systems or optical time-division multiplexing (OTDM) [3] as in hybrid WDM/OTDM systems [4].

The ceiling for base data rates in high-speed optical networks for the past few years has been 10 Gb/s (OC-192/STM- 64). An attractive alternative to deploying higher wave counts at 10 Gb/s, taking into account the amount of successful research efforts, is the deployment of higher capacities per wavelength. For example, the 40 Gb/s (OC-768/STM-256) solution provides better spectral efficiency and results in lower overall cost for capacity, relative to existing 10-Gb/s systems. The higher line rate also provides better terminal density, which results in smaller terminals for a given capacity [5], [6]. One of the remarkable factors, with the move to higher line rates, is the coding used at the transmitter. Most of the current systems, 2.5–10 Gb/s, have tended to employ Non-return-to-zero (NRZ) coding. However, to achieve line rates of 40 Gb/s and higher, it may become necessary to use return-to-zero (RZ) coding. RZ (pulse) modulation formats offer a number of advantages over NRZ modulation schemes, especially in long-haul transmission, which result in higher signal-to-noise ratio and lower system bit error rate translating into better overall system performance [7]–[10].

The rigorous requirements placed on the transmitter performance by the reduced channel spacing and increased line rate act as an immense challenge to manufacturers. Hence, the design of an optical transmitter, capable of generating pulses with adequate temporal and spectral purity for acceptable operation in high-speed optical communication systems, is crucial. There are numerous methods available to generate picosecond optical pulses [4]. Some of the most common and commercially available optical pulse sources are mode-locked semiconductor and fibre ring lasers [11], [12]. However, it has widely been accepted that the gain-switching technique is one of the simplest and most reliable in comparison to the rest [13], [14]. While the advantages in employing this method are numerous, one of its major drawbacks is the spectral purity of the generated pulses. The direct modulation of the laser diode causes a time-varying carrier density in the active region of the device, which in turn causes a variation in the output wavelength from the laser during the emission of the optical pulse. This results in a frequency chirp across the pulse, which degrades the performance of these pulses when used in practical optical communication systems [15]. It has been reported how this chirp can be used to compress the pulses using dispersion-compensating fibre [16] or linearly chirped gratings [17], to obtain near transform-limited pulses. However, because of the chirp being nonlinear across the pulse, this compression typically results in pedestals on either side of the pulses that make them unsuitable for use in practical systems. By using more complex arrangements involving nonlinear loop mirrors or external modulators, after the linearly compressed pulse, it is possible to greatly reduce the pedestal [18]. Degradation of the side-mode suppression ratio (SMSR) and a relatively large temporal jitter are other inherent problems associated with

Manuscript received October 4, 2005; revised January 27, 2006. This work was supported in part by Science Foundation Ireland (Investigator Program) and Enterprise Ireland (Proof of Concept).

P. M. Anandarajah, C. Guignard, A. Clarke, M. Rensing, and L. P. Barry are with the Research Institute for Networks and Communications Engineering (RINCE), School of Electronic Engineering, Dublin City University, Dublin 9, Ireland (e-mail: anandara@eeng.dcu.ie; guignard@eeng.dcu.ie; clarkea@eeng.dcu.ie; marc.rensing@eeng.dcu.ie; barry1@eeng.dcu.ie).

D. Reid and J. D. Harvey are with the Physics Department, University of Auckland, Auckland 1020, New Zealand (e-mail: d.reid@southernphotonics.com; j.harvey@auckland.ac.nz).

G. Edvell is with Redfern Optical Components, Eveleigh NSW 1430, Australia (e-mail: G.Edvell@redfernoptics.com).

Digital Object Identifier 10.1109/JSTQE.2006.872057

the technique of gain switching. However, by externally injecting into a gain-switched laser, the above-mentioned shortcomings could be overcome [18], [19].

The work described in this paper concerns the generation of temporally and spectrally pure short optical pulses (temporal pedestal, and spectral SMRSs greater than 30 dB). The pulse source comprises a nonlinearly chirped fiber Bragg grating (NC FBG) in conjunction with an externally injected gain-switched laser [20]. The design of the NC FBG is determined by the complete characterization of the gain-switched pulse using the technique of frequency resolved optical gating (FROG) [21]. This characterization yields the parameters that are required for the design of an NC FBG with a group-delay profile that is opposite to that measured across the pulse. By employing the tailor-made NC FBG after the gain-switched laser, we can achieve direct compression of the gain-switched pulses to obtain near transform-limited pulses. We show experimental results, obtained by employing this novel technique, where 3.5-ps pulses (FWHM) at a repetition rate of 10 GHz and an associated spectral width of 130 GHz are generated. The resulting pulse and spectral widths show that this technique yields near transform-limited pulses with a time–bandwidth product (TBP) of 0.45. These pulses also portray an extinction of the temporal pedestals up to about 35 dB below the peak of the pulse. This excellent temporal pedestal suppression ratio (TPSR) is achieved not only by the grating filter having a nonlinear group-delay profile that is the inverse of that across the gain-switched pulse directly from the laser, but also by ensuring that the grating filter has a specially adapted filter-transfer characteristic. The NC FBG has a custom-designed nonlinear reflective profile that optimizes the output pulse spectrum thereby further enhancing the temporal quality of the pulses. The spectral and temporal characteristics of such a pulse source would make it suitable for use as a transmitter in 80 Gb/s OTDM or hybrid WDM/OTDM systems.

This paper is divided into four main sections as follows. Section II focuses on the layout of the externally injected gain-switched laser and the complete characterization of the generated pulses. Section III then concentrates on the fabrication of two types of gratings that could be used to compress the externally injected gain-switched pulses. The employment of the two types of gratings to achieve pulse compression is explained in Section IV. Finally, Section V presents the numerical modeling carried out to validate our experimental results.

II. Externally Injected Gain-Switched Laser

The experimental setup employed in this work is shown in Fig. 1. A 10-GHz sine wave is amplified with the aid of a high-power RF amplifier. A bias tee is then used to combine the electrical RF signal with a dc bias (2.5 $I_{\rm th}$) to enable gain switching of a commercially available NEL DFB laser contained within a hermetically sealed high-speed package. The laser used has a 3-dB bandwidth of 20 GHz, and an output power of 4.7 dBm, both measured at a bias current of 3 $I_{\rm th}$. The resulting pulses generated were at a wavelength of 1549.35 nm. Wavelength tunability of the laser mode over a range of 2 nm could be achieved by temperature controlling the diode.

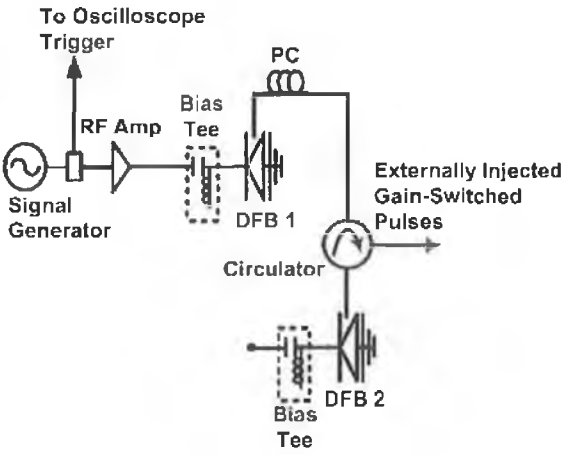

Fig. 1. Experimental setup for pulse generation using an externally injected gain-switched laser.

To overcome the poor SMSR (~5 dB) and timing jitter (~2 ps) of the gain-switched pulses, we use external injection (via an optical circulator) from a second DFB (2) laser biased at 23.5 mA ($\sim 1.2 I_{\rm th}$). A polarization controller was also used to ensure that the light being injected was aligned with the optical axis of the modulated laser. The injected power, incident on the modulated laser diode, was measured to be about −20 dBm after considering the losses incurred in the optical injection path. External light injection improves the SMSR to around 30 dB and reduces the timing jitter to <1 ps (as measured using an Agilent Digital Communications Analyzer). The actual jitter on the externally injected gain-switched output is expected to be in the order of 200 fs or less as demonstrated in previous work [22]. The generated pulses can then be characterized using an optical spectrum analyzer (OSA), a high-speed oscilloscope in conjunction with a 50-GHz pin detector, and also a FROG measurement system.

Fig. 2(a) and (b) displays the optical spectra of the gain-switched laser both without and with external injection, respectively, and it can be seen that the case without injection results in a degraded SMSR of about 5 dB. The overlapping of the broadened modes prevents the side mode being distinguished from the main mode. However, with external injection, a vast improvement in the SMSR (>30 dB) is evident. Moreover, from the same figure, the spectral width of the externally injected gain-switched laser is determined to be about 140 GHz. Fig. 3 shows the nonaveraged oscilloscope trace of the detected pulse from which the low temporal jitter can be noted. The ringing in this pulse is due to its duration being shorter than the response time of the detector. To accurately characterize this pulse, it is thus necessary to use the FROG technique.

In these experiments, a standard second harmonic generation (SHG) FROG based on the spectral resolution of the output from a noncollinear autocorrelator, as described in [21], was used. SHG was performed in a beta barium borate (BBO) crystal with an interaction length of 250 μm. With this interaction length, the expected variation in the SHG response [23] was

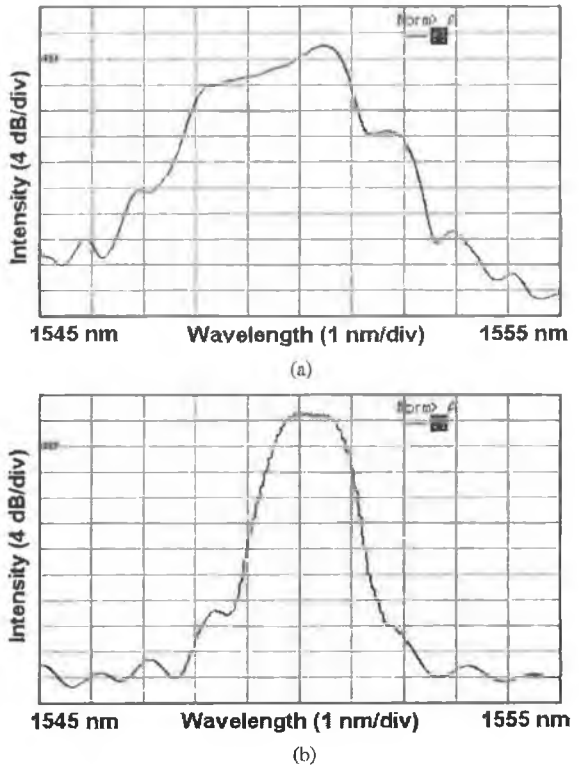

Fig. 2. Spectra of gain-switched laser (a) without and (b) with injection.

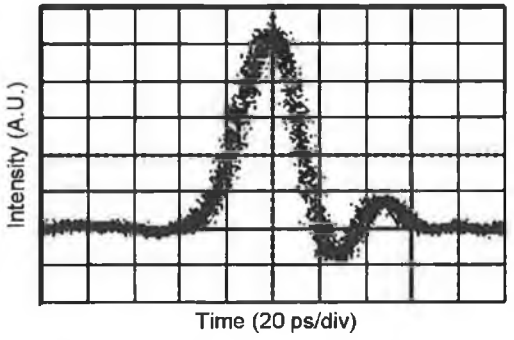

Fig. 3. Oscilloscope trace of the externally injected gain-switched pulse.

negligible over a 100-nm bandwidth around 1550 nm. The SHG output was spectrally resolved using a grating spectrometer with a 1024-element cooled photodiode array mounted on the output. The spectral resolution was $\Delta\lambda = 0.04$ nm at an SHG wavelength of 775 nm. The autocorrelator delay was controlled by a stepping motor with temporal resolution of $\Delta\tau = 6.7$ fs. The complete electric field of the input optical pulse can be determined from the measured spectrogram by using standard retrieval techniques [21]. A short-pulse erbium-doped fibre amplifier (EDFA), specifically designed for the amplification of pulses with a duration in the order of 2 ps (FWHM), is used before the FROG measurement setup to improve the signal-to-noise ratio of the measurement. From the FROG measurement, we can accurately characterize the intensity and chirp profile across the optical pulses from the gain-switched laser with external injection. Fig. 4 indicates that the pulses had a duration

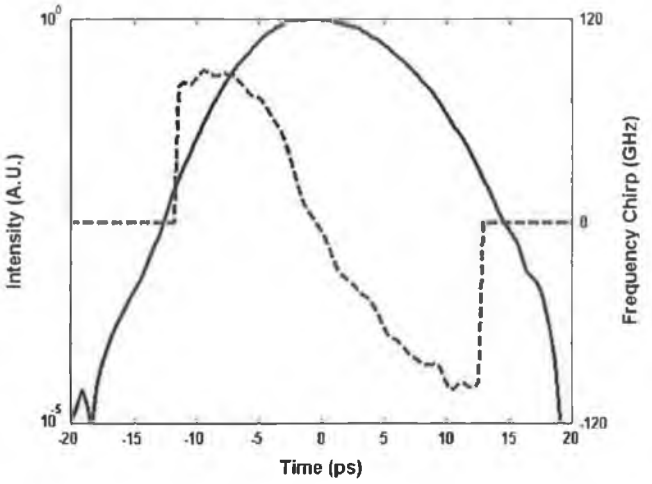

Fig. 4. Intensity (solid line) and chirp (dashed line) of optical pulses from the externally injected gain-switched laser.

(FWHM) of about 10.5 ps and that the frequency chirp (dashed line) becomes nonlinear in the wings of the pulse generated due to the gain-switching mechanism. The resulting TBP of the pulse is 1.5.

III. Grating Fabrication

We subsequently use the measured nonlinear chirp across the pulse to design and fabricate an NC FBG. This process involves the initial creation of the group-delay response for the FBG based on the group-delay data derived from the FROG measurements of the externally injected gain-switched pulse. The FBG target group-delay response is simply selected as the inverse of the pulse group-delay response, which should result in the pulse having a constant group-delay profile over the pulse bandwidth after it has reflected from the FBG. In addition to a constant group-delay profile across the pulse bandwidth, for an optimized pulse source, we also require the pulse to exhibit a Gaussian spectrum. Generally, gain-switched spectra tend to be more rectangular than Gaussian spectra. The reflection profile of the NC FBG is constructed as the difference between the spectral amplitude of the gain-switched output and a Gaussian profile, which should result in the compressed pulse portraying a Gaussian spectrum. Once the FBG target spectrum and group-delay profile are obtained, it is relatively straightforward to calculate an FBG design that can be implemented into the optical fibre by using an inverse scattering algorithm [24]–[26]. The FBGs are fabricated by using a holographic writing method [27], where a computer electronically controls the FBG phase and amplitude and does not require a custom-made phase mask. Hence, it is even possible to fabricate NC FBGs for each individual DFB laser in larger volumes at a low cost (as there is no need for a custom-made phase mask), if the nonlinear chirp is different from laser to laser.

The reflective and group-delay profiles of the fabricated NC FBG are shown in Fig. 5. We also fabricated a linearly chirped fibre grating that had a chirp profile opposite to a linear approximation of the chirp across the gain-switched pulse. In both

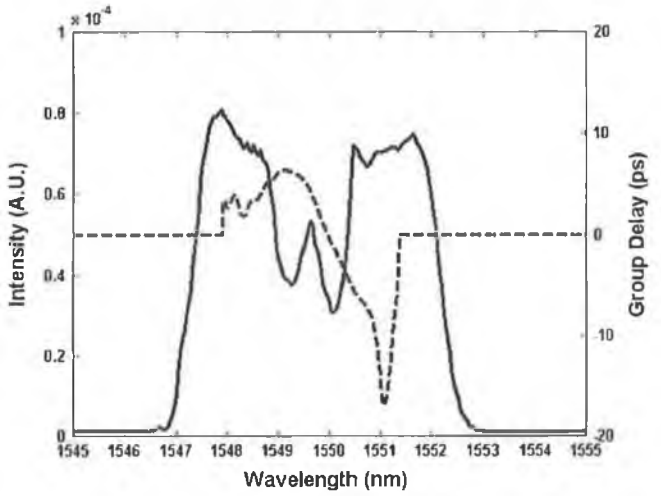

Fig. 5. Reflection (solid line) and group delay (dashed line) profiles of the nonlinearly chirped fiber grating.

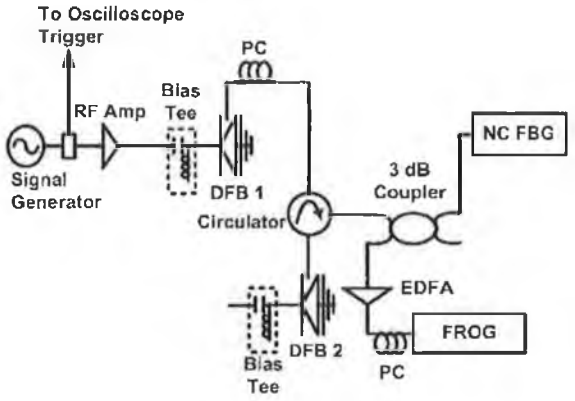

Fig. 6. Experimental setup for optimized pulse generation.

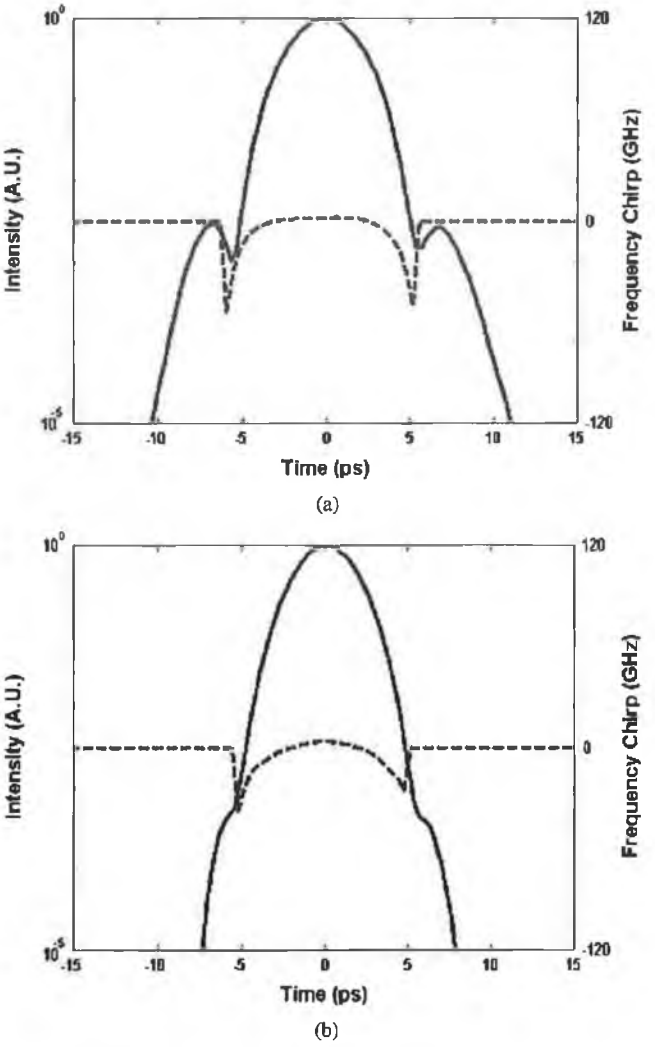

Fig. 7. Intensity (solid line) and chirp (dashed line) profiles of externally injected gain-switched pulses after (a) linearly chirped and (b) nonlinearly chirped gratings.

the cases, the agreement between the measured and the target group-delay profile was very good, with a standard deviation of the measured error <1.5 ps, which is quite close to the estimated noise level of $+/-1$ ps for the group-delay measurements.

IV. Pulse Compression

By placing the nonlinear and linear fibre gratings after the externally injected gain-switched laser, as shown schematically in Fig. 6, we subsequently characterize the pulse compression in the fibre gratings using the FROG technique. In the experimental work presented here, the pulse recovery routinely gave retrieval errors of $G < 0.005$ on a 128×128 grid [21], which indicated the accuracy of our retrievals.

Fig. 7(a) and (b) shows the measured intensity and chirp profile of the gain-switched optical pulses after compression with the linearly and nonlinearly chirped fibre gratings, respectively. In both cases, the gratings have eliminated any frequency chirp across the center of the pulses. However, when the linearly chirped grating is used, we can see how the nonlinearity of the chirp directly from the gain-switched laser results in significant pedestals on the leading and trailing edges of the pulse [Fig. 7(a)]. Such pedestals, which are around 23 dB down from the peak of the pulse, would clearly pose significant problems (through intersymbol interference) for the use of these pulses in high-speed OTDM systems [28].

The compression in the nonlinear fibre grating results in a 3.5-ps FWHM pulse [pulse and corresponding chirp profile shown in Fig. 7(b)]. It can clearly be seen that the resultant chirp is flat and has a very small order of magnitude across the pulse. Also, as can be seen in the figure, the pedestals have almost been eliminated (TPSR > 35 dB). The latter one is due to not only the elimination of the chirp across the pulse but also the output pulse spectrum being Gaussian due to the nonlinear reflection profile of the grating, as explained earlier. It is important to note that, for a non-Gaussian spectrum, even if the group delay is entirely compensated, temporal pedestals could exist. The Fourier transform of a rectangular spectrum, which results in a Sinc temporal pulse [29], could be used to justify the presence of such pedestals. It is also important to note that a large group delay ripple (GDR) in the compressing FBG could cause

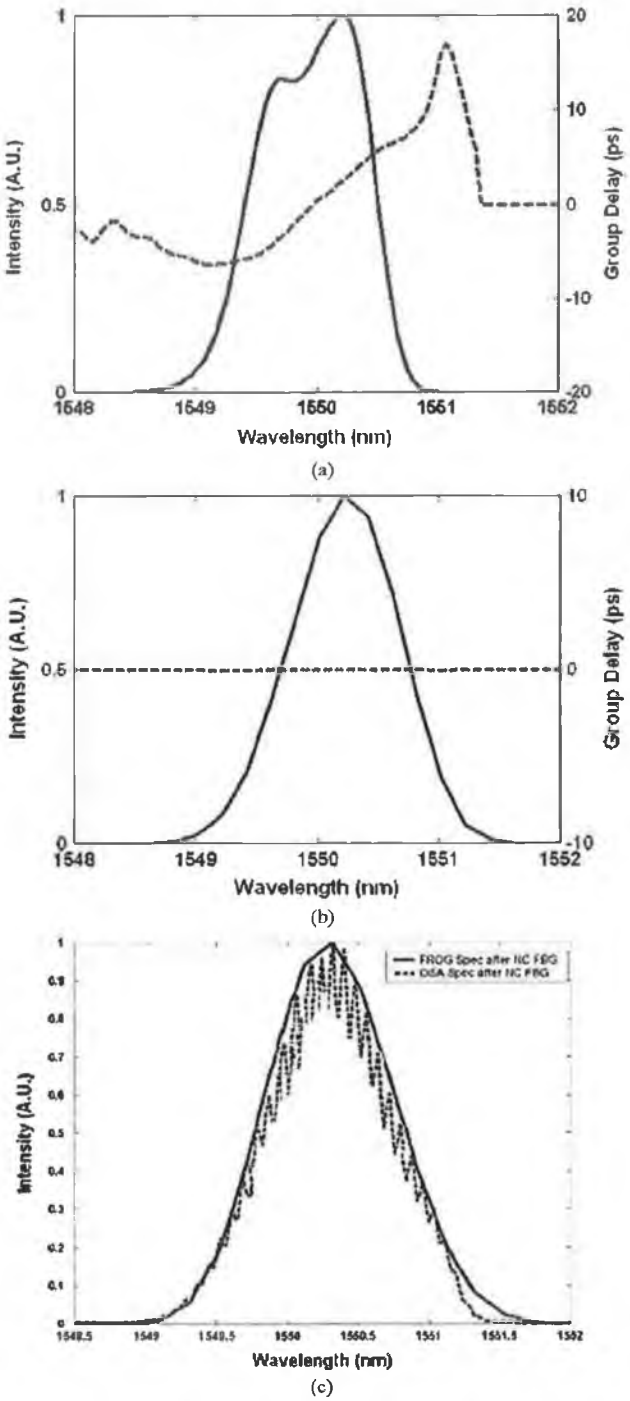

Fig. 8. (a) The input to and (b) output spectrum (solid line) from the NC FBG and their corresponding group delays (dashed lines) and (c) a comparison of the spectrum obtained by the FROG (solid line) and the OSA (dashed line) after the NCFBG.

low-intensity temporal pedestals. However, in this experiment, no such pedestals were observed mainly due to the low level of GDR, as mentioned earlier, with a standard deviation of less then half the compressed pulsewidth.

The spectra and the group delay of the input and output pulses to and from the NC FBG are shown in Fig. 8(a) and (b), respectively. It is clear that the group delay has been compensated for entirely by the tailor-made NC FBG. The output spectrum is more Gaussian shaped and symmetric in comparison to the input, which is due to the compensation by the nonlinear reflection profile of the NC FBG. The OSA spectrum, which is in excellent agreement with the pulse spectrum obtained from the FROG measurement, shows that the spectral width is around 130 GHz as shown in Fig. 8(c). The quoted pulsewidth and associated spectral width result in a TBP of 0.45.

This pulse generation/compression technique portrays excellent repeatability. Furthermore, within laboratory conditions, the scheme exhibited stable operation over about a 24 hour period. This could be mainly attributed to the bias current and temperature of the two DFB (modulated and seeding) lasers being controlled with the aid of Profile current/temperature controllers. Hence, drifts in wavelength of the lasers, due to current or temperature variations were negligible. Furthermore, the wavelength variation with temperature of the fabricated FBGs being relatively small ($\sim$0.009 nm/°C) also leads to the stable generation of optimized pulses over very long periods of time.

V. Simulations

A. Theoretical Model

To further confirm the effect of both the group-delay and the reflectivity profiles of the FBG on the pulse compression and to validate the experimental results, numerical simulations were carried out. The laser is described by the following single-mode rate equations [30], [31], which are given for the carrier density $N(t)$ and the complex electric field $E(t) = \sqrt{S(t)}e^{i(\omega t+\varphi(t))}$, where $S(t)$ is the photon density and $\varphi(t)$ is the phase

$$\dot{E}(t) = \frac{1}{2}\left[\Gamma_c g(N,S) - \frac{1}{\tau_p}\right]E(t) + i\frac{\alpha_H}{2}\left[\Gamma_C G_N(N(t)-N_t) - \frac{1}{\tau_p}\right]E(t) \quad (1)$$

$$\dot{N}(t) = J - \frac{N(t)}{\tau_e} - g(N,S)S(t). \quad (2)$$

These equations call for the physical constants described below. N_t and N_{th} are, respectively, the carrier density at transparency and at threshold with $N_{th} = N_t + (1/\Gamma_C G_N \tau_p)$. Γ_C is the field confinement factor, G_N is the differential gain, and α_H is the linewidth enhancement factor. ω_0 is the angular frequency of the solitary laser at threshold. The nonlinear gain is expressed as $g(N,S) = G_N(N(t)-N_t)(1-\varepsilon_{nl}S(t))$, where ε_{nl} is the gain compression factor. The carrier lifetime τ_e is determined at threshold by $1/\tau_e = A + BN_{th} + CN_{th}^2$ with A the rate of nonradiative recombinations, B the rate of spontaneous radiative recombinations, and C the rate of Auger recombination processes. The photon lifetime τ_p is determined by the full losses of the solitary laser: $1/\tau_p = v_g\alpha_{in} - 1/\tau_c \ln(R_1R_2)$. Here, α_{in} corresponds to the scattering losses in the active volume, $v_g = c/n_g$ is the group velocity with c the speed of light in vacuum and n_g the group index of the active medium. The parameters R_1 and R_2 are the power reflectivity of the left and

TABLE I
SOME PARAMETER VALUES FOR THE LASER DIODE USED IN THE NUMERICAL SIMULATIONS

Physical constant	Value
Length of the active medium (L_D)	3×10^{-4}m
Width of the active medium (l)	9×10^{-7}m
Thickness of the active medium (e)	8.5×10^{-8}m
Group index of the active medium (n_g)	3.57
Scattering losses (α_{in})	4020 m^{-1}
Confinement factor (Γ_C)	0.51
Differential gain (G_N)	$5.2\times10^{-20}m^{-2}$
Gain compression factor (ε_{nl})	$5.2\times10^{-20}sm^3$
Carrier density at transparency (N_t)	$1.0\times10^{-24}m^{-3}$
Rate of non-radiative recombinations (A)	2.7×10^{6} s^{-1}
Rate of spontaneous radiative recombinations (B)	$9\times10^{-17}s^{-1}m^{-3}$
Rate of Auger recombination processes (C)	1.8×10^{-39} s^{-1} m^{-6}
Carrier lifetime at threshold (τ_e)	0.31 ns
Round trip time in laser cavity (τ_c)	7.14 ps
Linewidth enhancement factor (α_H)	2
Amplitude reflectivity (R_1)	0.3
Amplitude reflectivity (R_2)	0.3

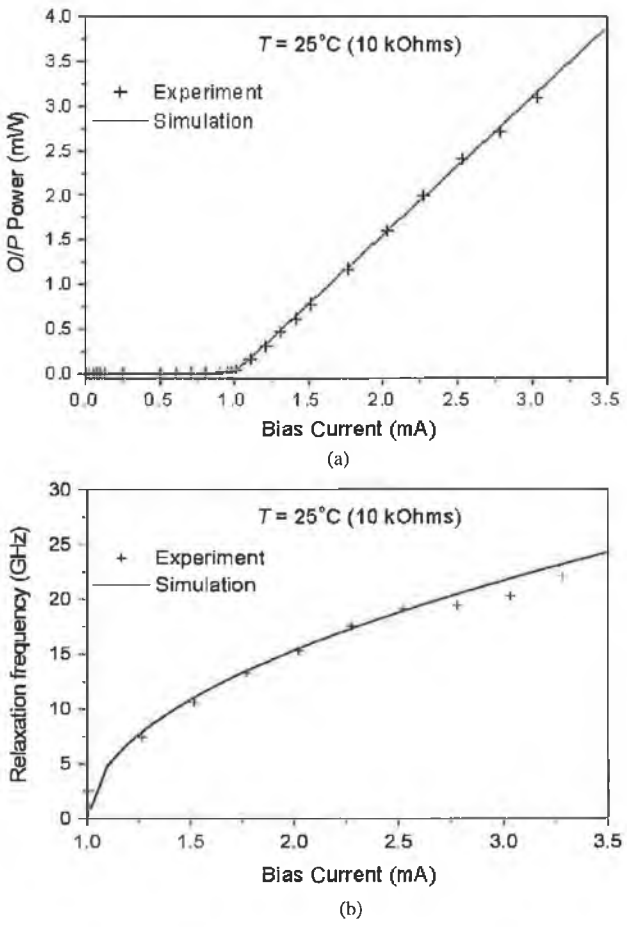

Fig. 9. (a) Experimental and numerical curves for PI and (b) the evolution of the relaxation frequency against the bias current.

right facets of the laser: $R_{1,2} = r_{1,2}^2$. $\tau_c = 2L_D/v_g$ corresponds to the cavity lifetime and L_D is the laser diode length. Finally, $J = (I/qV)$ is the injection current density with V the volume of the active medium. When the laser is gain switched, its current consists of the bias I_b and the modulation current $\Delta I(t)$. $I(t) = I_b + \Delta I(t) = I_b + m\sin(2\pi f_m t)$, where m corresponds to the modulation depth and f_m to the modulation frequency.

Table I gives the values of the parameters we used in our simulations. Most of them were provided by the constructor, while a few such as the nonradiative recombination and the Auger recombination process were estimated from experimental results. Fig. 9 displays both the experimental and theoretical graphs for the *PI* curve and the evolution of the relaxation frequency against the bias current. The good agreement between the experimental and theoretical results (both static and dynamic characteristics) demonstrates that our model is reasonably accurate.

To simplify the study, we have not considered external optical injection in these simulations. In fact, the low level of injection, used experimentally, should not have great influence on the chirp. The sole reason for injection is to improve the SMSR and jitter. As a consequence, the simulation results presented can be easily compared and contrasted to the experimental results.

B. Results

Setting the bias current I_b at $2I_{th}$ and the modulation frequency at 10 GHz, we examined the effect of filtering the gain-switched pulse with both linearly and nonlinearly chirped FBG, when the reflection profile of the grating was either square topped, or had a nonlinear profile to achieve a Gaussian spectral output. In the simulations, (1) and (2) were solved directly using a fourth-order Runge–Kutta algorithm. The initial conditions are

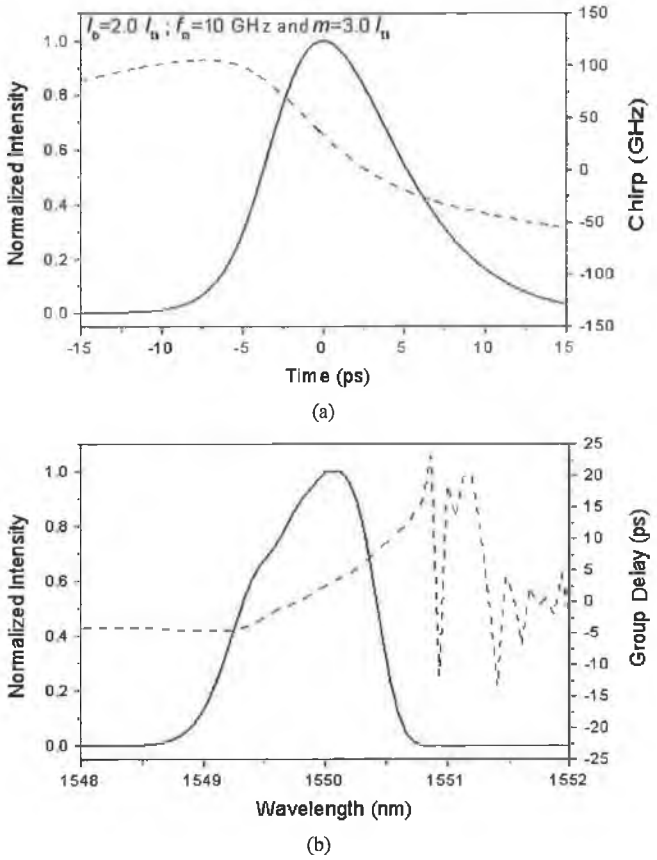

Fig. 10. Characteristics of the optical pulses from the gain-switched laser. (a) The intensity (solid line) and the chirp (dashed line) of the pulse. (b) Pulse spectrum (solid line) and its corresponding group delay (dashed line).

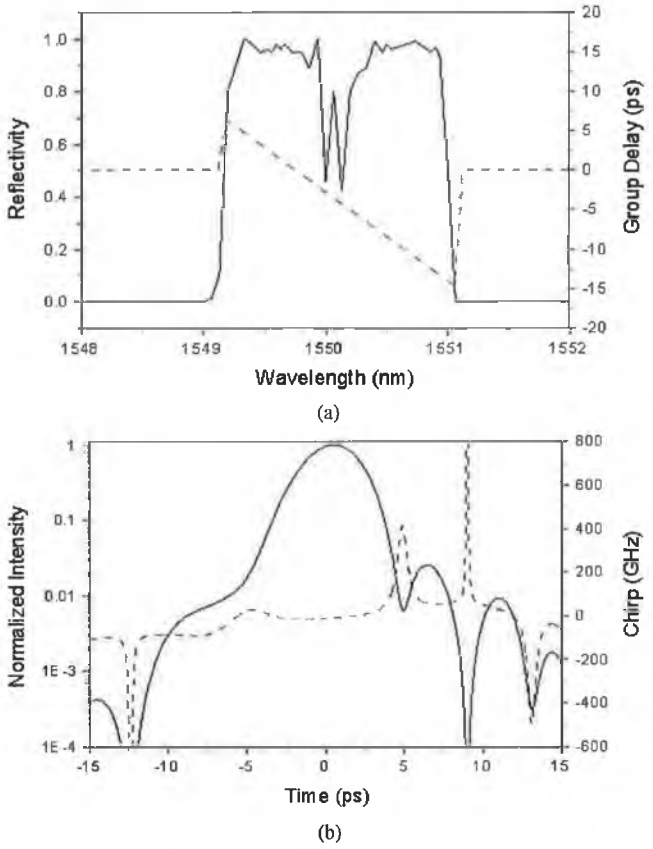

Fig. 11. (a) Reflection (solid line) and group delay (dashed line) profiles of the linearly chirped FBG with a filter response altered to achieve Gaussian output. (b) Intensity (solid line) and chirp (dashed line) of gain-switched pulses after reflection on this FBG.

taken from (1) and (2) by setting the left-hand side of the equations to zero. A trajectory of at least 50 ns was discarded to allow for transients to die out.

Fig. 10(a) presents the intensity and the chirp of the gain-switched optical pulses when the modulation amplitude is set to $3I_{\text{th}}$, which corresponds to experimental RF modulation level. The spectrum and group-delay profile of the gain-switched pulse is also shown in Fig. 10(b). The instantaneous frequency chirp $\delta\upsilon(t)$ (in gigahertz) across the pulse is directly obtained from the phase $\phi(t)$ by $\delta\upsilon(t) = (1/2\pi)(d\varphi/dt)$. It is noted that that the 9.5-ps pulse generated exhibits a TBP of 1.3, which gives evidence of a large frequency chirp across the pulse. Moreover, as presented experimentally, the profile of the frequency chirp is similar and becomes nonlinear in the wings of the pulse. As explained previously, two types of dispersion compensation are compared in this article: one that compensates only the linear part of the pulse's group delay, whereas the other compensates the entire pulse's group delay. Figs. 11(a) and 12(a) show group-delay and reflection profiles of the two filters used. The intensity and chirp profiles of the gain-switched pulses after reflection on the linearly and the nonlinearly chirped FBG are shown in Figs. 11(b) and 12(b), respectively.

In both cases, the reflection profile of the grating is set to have a nonlinear response to obtain a Gaussian spectral output. The use of an FBG with a group delay opposite to that of the gain-switched laser allows us to achieve transform-limited pulses. In the example used in the simulations, a 3.4-ps pulse is achieved, and there are no pedestals on the wings of the pulse. However, if the group delay of the FBG is opposite to the linear fit of the pulse's group delay, the frequency chirp across the center of the pulse is eliminated but the nonlinear chirp remains visible in the wings of the pulse. As a consequence, the 4-ps pulse is characterized by a TBP of 0.54 and contains pedestals around 16 dB down from the peak of the pulse as shown in Fig. 11(b). These numerical results reproduce the experimental features: compensation of only the linear portion of the chirp results in significant pedestals in the leading and trailing edges of the pulse due to the remaining nonlinear chirp.

Using our simulation model, we subsequently went on to examine the effect of using a nonlinearly chirped fibre grating with a reflection profile that is square topped and does not affect the shape of the spectrum. The grating profile and resulting output pulses are displayed in Fig. 13. As can be seen, the output pulse is characterized by a TBP of 0.57 and the pedestals are reduced around 21 dB down from the peak of the pulse [see Fig. 13(b)]. This result clearly shows that to obtain optimum pulses having pedestal suppression greater than 30 dB [28], it is

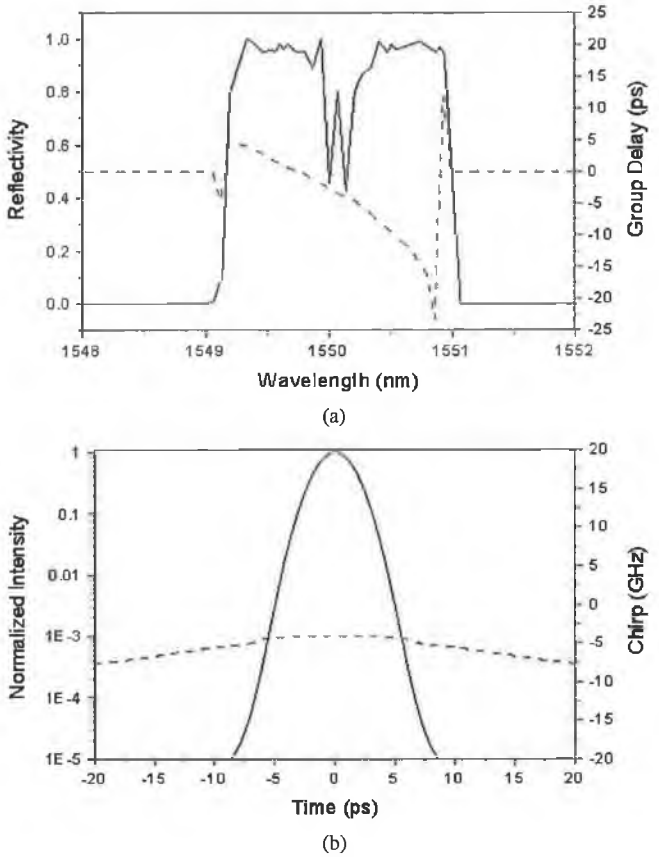

Fig. 12. (a) Reflection (solid line) and group delay (dashed line) profiles of the nonlinearly chirped fiber Bragg grating with a filter response altered to achieve Gaussian output. (b) Intensity (solid line) and chirp (dashed line) of gain-switched pulses after reflection on this FBG.

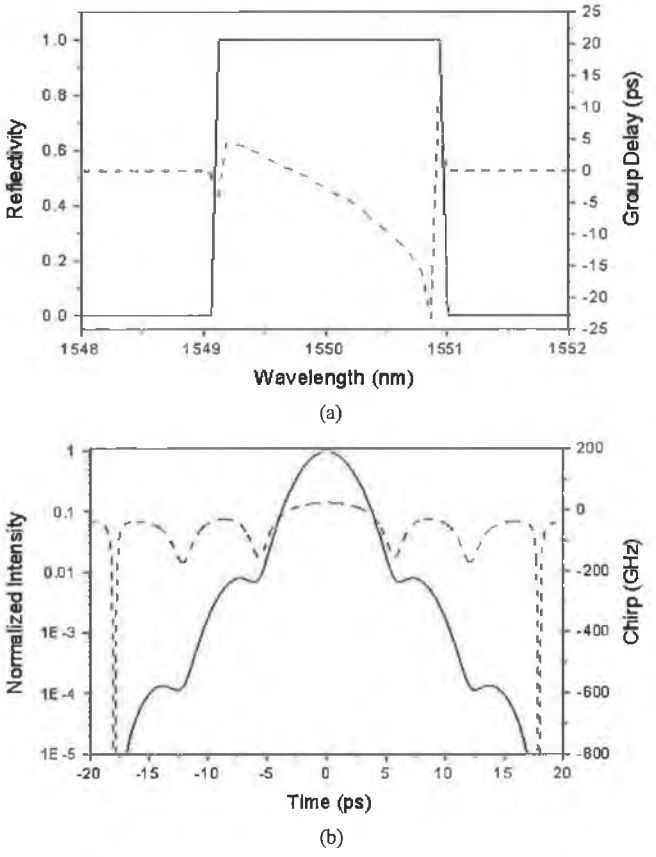

Fig. 13. (a) Reflection (solid line) and group delay (dashed line) profiles of the nonlinearly chirped fiber Bragg grating with a square filter response. (b) Intensity (solid line) and chirp (dashed line) of gain-switched pulses after reflection on this FBG.

necessary to compensate for both the nonlinear chirp of the gain-switched laser and the non-Gaussian spectral output. Another possible method that we investigated through simulation, to reduce the height of the pulse pedestals obtained when a linearly chirped fibre grating is used, is to reduce the bandwidth of the FBG filter. By altering the filter bandwidth, it should be possible to filter out and eliminate the edges of the spectrum where the group delay becomes nonlinear. For this simulation, we used an FBG having a group delay that was the inverse of the linear group delay across the center of the gain-switched pulse, and a reflection profile that was set to obtain a Gaussian spectral output. We then proceeded to reduce the bandwidth of the FBG.

Fig. 14 displays the evolution of both the pedestal and the TBP of the pulse when the FBG's bandwidth is varied (as a percentage of the bandwidth of the spectrum from the gain-switched laser). When the FBG is characterized by a bandwidth that corresponds to half the pulse's bandwidth, the pedestals are reduced 28.5 dB down from the peak of the pulse. The resulting TBP is around 0.47 but the pulsewidth has been broadened to 7 ps. Thus, although this technique does greatly reduce the level of the pedestals, this is achieved at the expense of pulse duration, which is significantly increased.

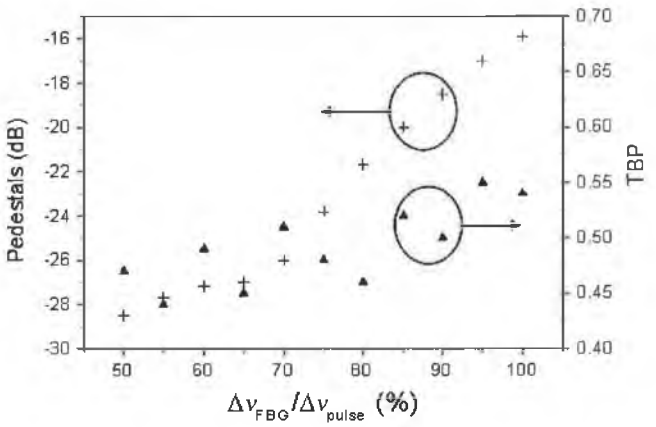

Fig. 14. Evolution of the pedestals and the time–bandwidth product of the pulses when the bandwidth of the linearly chirped fiber Bragg grating is varied.

VI. Conclusion

We have demonstrated the generation of near transform-limited 3.5-ps gain-switched pulses that exhibit an excellent TPSR by using an NC FBG. The initial gain-switched pulses display a large nonlinear chirp across the wings of the pulse, and by using the measurement technique of FROG, the chirp across the pulses has been completely characterized. From this

complete characterization, we subsequently design and fabricate a nonlinearly chirped fiber Bragg grating that has a nonlinear group-delay profile opposite to the group delay of the input pulse. The fabricated grating also has a nonlinear reflection profile to optimize the output spectrum of the generated pulses. The resultant output pulses display excellent temporal and spectral purity, which would make this pulse source ideal for use in 80 Gb/s OTDM systems. Moreover, the experimental results were compared to a numerical analysis of the rate equations, which were found to validate the experimental results, including the reduction of the pedestals when both a specific reflective profile (to compensate for the asymmetry of the pulse spectrum) and a nonlinear group delay (to compensate for the group delay of the gain-switched laser) are used. The rate-equation analysis was utilized to investigate a possible improvement of the results obtained with a linearly chirped FBG by decreasing the FBG's bandwidth, but the reduction of the pedestals resulted in a broadening of the pulse.

REFERENCES

[1] H. Kogelnik, "High-capacity optical communications: Personal recollections," *IEEE J. Sel. Topics Quantum Electron.*, vol. 6, no. 6, pp. 1279–1286, Nov./Dec. 2000.

[2] W. S. Lee, V. Filsinger, L. Klapproth, H. G. Bach, and A. Beling, "Implementation of an 80 GBit/s Full ETDM multi-format ASK optical transmitter," in *Proc. Eur. Conf. Optical Communications*, Glasgow, U.K., Sep. 2005, vol. 3, pp. 383–384.

[3] J. P. Turkiewicz, E. Tangdiongga, G. Lehmann, H. Rohde, W. Schairer, Y. R. Zhou, E. S. R. Sikora, A. Lord, D. B. Payne, G.-D. Khoe, and H. de Waardt, "160 Gb/s OTDM networking using deployed fiber," *IEEE J. Lightw. Technol.*, vol. 23, no. 1, pp. 225–235, Jan. 2005.

[4] M. Saruwatari, "All-optical signal processing for terabit/second optical transmission," *IEEE J. Sel. Topics Quantum Electron.*, vol. 6, no. 6, pp. 1363–1374, Nov./Dec. 2000.

[5] B. Mikkelsen, C. Ramussen, P. Mamyshev, F. Liu, S. Dey, and F. Rosca, "Deployment of 40 Gb/s systems: Technical and cost issues," in *Proc. Optical Fiber Communications Conf.*, Los Angeles, CA, Oct. 2004, vol. 2, p. 3.

[6] A. Belahlou, S. Bickham, D. Chowdhury, P. Diep, A. Evans, J. M. Grochocinski, P. Han, A. Kobyakov, S. Kumar, G. Luther, J. C. Mauro, M. Yihong, M. Mlejnek, M. S. K. Muktoyuk, M. T. Murtagh, S. Raghavan, V. Ricci, A. Sevian, N. Taylor, S. Tsuda, M. Vasilyev, and L. Wang, "Fibre design considerations for 40 Gb/s systems," *IEEE J. Lightw. Technol.*, vol. 20, no. 12, pp. 2290–2305, Dec. 2002.

[7] R. Ludwig, U. Feiste, E. Dietrich, H. G. Weber, D. Breuer, M. Martin, and F. Küppers, "Experimental comparison of 40 Gbit/s RZ and NRZ transmission over standard single mode fibre," *Electron. Lett.*, vol. 35, no. 25, pp. 2216–2218, Dec. 1999.

[8] M. I. Hayee and A. E. Willner, "NRZ versus RZ in 10–40 Gb/s dispersion-managed WDM transmission systems," *IEEE Photon. Technol. Lett.*, vol. 11, no. 8, pp. 991–993, Aug. 1999.

[9] C. R. S. Fludger, Y. Zhu, V. Handerek, and R. J. Mears, "Impact of MPI and modulation format on transmission systems employing distributed Raman amplification," *Electron. Lett.*, vol. 37, no. 15, pp. 970–972, Jul. 2001.

[10] P. J. Winzer, M. Pfennigbauer, M. M. Strasser, and W. R. Leeb, "Optimum filter bandwidths for optically preamplified NRZ receivers," *IEEE J. Lightw. Technol.*, vol. 19, no. 9, pp. 1263–1273, Sep. 2001.

[11] R. G. M. P. Koumans and R. Van Roijen, "Theory for passive mode-locking in semiconductor laser structures including the effects of self-phase modulation, dispersion, and pulse collisions," *IEEE J. Quantum Electron.*, vol. 32, no. 3, pp. 478–492, Mar. 1996.

[12] J. M. Roth, T. G. Ulmer, N. W. Spellmeyer, S. Constantine, and M. E. Grein, "Wavelength-tunable 40-GHz picosecond harmonically mode-locked fiber laser source," *IEEE Photon. Technol. Lett.*, vol. 16, no. 9, pp. 2009–2011, Sep. 2004.

[13] K. Y. Lau, "Gain switching of semiconductor injection lasers," *Appl. Phys. Lett.*, vol. 52, no. 4, pp. 257–259, Jan. 1988.

[14] L. P. Barry, R. F. O'Dowd, J. Debeau, and R. Boittin, "Tunable transform limited pulse generation using self-injection locking of an FP laser," *IEEE Photon. Technol. Lett.*, vol. 5, no. 10, pp. 1132–1134, Oct. 1993.

[15] J. M. Dudley, L. P. Barry, J. D. Harvey, M. D. Thomson, B. C. Thomsen, P. G. Bollond, and R. Leonhardt, "Complete characterization of ultrashort pulse sources at 1550 nm," *IEEE J. Quantum Electron.*, vol. 35, no. 4, pp. 441–450, Apr. 1999.

[16] K. A. Ahmed, H. F. Liu, N. Onodera, P. Lee, R. S. Tucker, and Y. Ogawa, "Nearly transform limited pulse (3.6 ps) generation from gain-switched 1.55 μm distributed feedback laser by using fibre compression technique," *Electron. Lett.*, vol. 29, no. 1, pp. 54–56, Jan. 1993.

[17] B. J. Eggleton, P. A. Krug, L. Poladian, K. A. Ahmed, and H. F. Liu, "Experimental demonstration of compression of dispersed optical pulses by reflection from self-chirped optical fibre Bragg gratings," *Opt. Lett.*, vol. 19, no. 12, pp. 877–879, Jun. 1994.

[18] P. Gunning, J. K. Lucek, D. G. Moodie, K. Smith, R. P. Davey, S. V. Chernikov, M. J. Guy, J. R. Taylor, and A. S. Siddiqui, "Gain-switched DFB laser diode pulse source using continuous wave light injection for jitter suppression and an electroabsorption modulator for pedestal suppression," *Electron. Lett.*, vol. 32, no. 11, pp. 1010–1011, May 1996.

[19] D.-S. Seo, D. Y. Kim, and H.-F. Liu, "Timing jitter reduction of gain-switched DFB laser by external injection seeding," *Electron. Lett.*, vol. 32, no. 1, pp. 44–45, Jan. 1996.

[20] A. Clarke, P. Anandarajah, D. Reid, G. Edvell, L. P. Barry, and J. Harvey, "Optimized pulse source for 40 Gbit/s systems based on a gain-switched laser diode in conjunction with a non-linearly chirped grating," *IEEE Photon. Technol. Lett.*, vol. 17, no. 1, pp. 196–198, Jan. 2005.

[21] R. Trebino, K. W. DeLong, D. N. Fittinghoff, J. N. Sweetser, M. A. Krumbugel, and B. A. Richman, "Measuring ultrashort laser pulses in the time-frequency domain using frequency-resolved optical gating," *Rev. Sci. Instrum.*, vol. 68, pp. 3277–3295, May 1997.

[22] S. Nogiwa, Y. Kawaguchi, H. Ohta, and Y. Endo, "Generation of gain-switched optical pulses with very low timing jitter by using external CW-light injection seeding," *Electron. Lett.*, vol. 36, no. 3, pp. 235–236, Feb. 2000.

[23] A. Weiner, "Effect of group velocity mismatch on the measurement of ultrashort optical pulses via second harmonic generation," *IEEE J. Quantum Electron.*, vol. 19, no. 8, pp. 1276–1283, Aug. 1983.

[24] A. Rosenthal and M. Horowitz, "Inverse scattering algorithm for reconstructing strongly reflecting fiber Bragg gratings," *IEEE J. Quantum Electron.*, vol. 39, no. 8, pp. 1018–1026, Aug. 2003.

[25] J. Skaar and O. H. Waagaard, "Design and characterization of finite-length fiber gratings," *IEEE J. Quantum Electron.*, vol. 39, no. 10, pp. 1238–1245, Oct. 2003.

[26] R. Feced, M. N. Zervas, and M. A. Muriel, "An efficient inverse scattering algorithm for the design of non-uniform fibre Bragg gratings," *IEEE J. Quantum Electron.*, vol. 35, no. 8, pp. 1105–1115, Aug. 1999.

[27] C. Knothe and E. Brinkmeyer, "Reset-free phase shifter in a Sagnac-type interferometer for control of chirp and apodization of Bragg gratings," presented at the BGPP, Monterey, CA, 2003, Paper TuB3.

[28] P. L. Mason, A. Wonfor, D. D. Marcenac, D. G. Moodie, M. C. Brierley, R. V. Penty, I. H. White, and S. Bouchoule, "The effects of pedestal suppression on gain switched laser sources for 40 Gbit/s OTDM transmission," in *Proc. 10th Annu. Meeting IEEE LEOS*, Nov. 10–13, 1997, vol. 1, pp. 289–290.

[29] R. A. Gabel and R. A. Roberts, *Signals and Linear Systems*. New York: Wiley, 1987.

[30] H. Statz and G. A. deMars, *Quantum Electronics*. New York: Columbia Univ. Press, 1960.

[31] G. P. Agrawal and N. K. Dutta, *Long Wavelength Semiconductor Lasers*. New York: Van Nostrand and Reinhold, 1986.

P. M. Anandarajah (S'00–M'04) received the B.Eng. degree in electronic engineering from the University of Nigeria, Nsukka, Nigeria, in 1992, and the M.Eng. and Ph.D. degrees from Dublin City University, Dublin, Ireland, in 1998 and 2003, respectively.

From 1993 to 1997, he was an Instructor/Maintenance Engineer in the Aeronautical Telecommunications Department, Nigerian College of Aviation Technology (NCAT), Zaria, Nigeria. Since September 2003, he has been a Postdoctoral Researcher with the Radio and Optical Communications Laboratory at the Research Institute for Networks and Communications Engineering (RINCE), Dublin City University.

C. Guignard received the Eng. degree in optronics in 2001, the Masters degree in Sciences and Techniques of Communications (D.E.A.) in optics communications, also in 2001, and the Ph.D. degree in optronics in 2005 from the University of Rennes, Rennes, France.

Since April 2005, she has been a Postdoctoral Researcher in the Radio and Optical Communications Laboratory, Research Institute for Networks and Communications Engineering (RINCE), Dublin City University, Dublin, Ireland. Her research work includes optical pulse generation using actively mode-locked semiconductor laser diode submitted to nonlinear and filtered feedback and the effect of optical injection on these pulses.

A. Clarke (S'03) received the B.Eng. degree in electronic engineering in 2002 from Dublin City University, Dublin, Ireland, where she is currently pursuing the Ph.D. degree in optical communications. The main topic of her research is high-speed all-optical processing using semiconductor optical amplifiers (SOAs).

D. Reid received the B.Tech. degree in optoelectronics and the M.Sc. degree in physics in 2000 and 2002, respectively, from the University of Auckland, Auckland, New Zealand, where he is currently working toward the Ph.D. degree in physics (specializing in optical communications).

His research interests include the development of techniques for the characterization of ultrashort optical pulses, in particular, the use of FROG and other linear spectrographic techniques for real-time measurement of optical communication pulses. Other areas of interest include the design of optimized pulse sources and compressors, the latter being made possible by accurate pulse characterization.

M. Rensing received the B.Sc. (honors) degree in physics from the University of Hull, Hull, U.K., in 2001, and the H.Dip. degree in applied physics from University College Cork (UCC), Cork, Ireland, in 2004. He is currently working toward the M.Eng. degree in optical communications at Dublin City University, Dublin, Ireland.

L. P. Barry (M'98) received the B.E. degree in electronic engineering and the M.Eng.Sc. degree in optical communications from University College Dublin, Dublin, Ireland, in 1991 and 1993, respectively, and the Ph.D. degree from the University of Rennes, Rennes, France.

From February 1993 to January 1996, he was a Research Engineer in the Optical Systems Department of France Telecom's Research Laboratories (CNET), Lannion, France. In February 1996, he joined the Applied Optics Centre, University of Auckland, Auckland, New Zealand, as a Research Fellow. In March 1998, he took up a lecturing position in the School of Electronic Engineering, Dublin City University, Dublin, Ireland, where he has since developed the Radio and Optical Communications Laboratory.

G. Edvell is a Senior Research and Development Engineer with Redfern Optical Components, Eveleigh, Australia.

J. D. Harvey (M'76) received the B.Sc. and M.Sc. degrees from the University of Auckland, Auckland, New Zealand, in 1965 and 1967, respectively, and the Ph.D. degree from the University of Surrey, Surrey, U.K.

In 1970, he joined the University of Auckland, where he now holds a Chair in the Physics Department. His research interests include nonlinear fiber optics, ultrafast processes, and mode-locked lasers.

Prof. Harvey is a Fellow of the New Zealand Institute of Physics and a member of the Optical Society of America and the Australian Optical Society.

Signal degradation due to output filtering of self-seeded gain-switched pulses exhibiting weak inherent side-mode-suppression ratios

Prince Anandarajah, Marc Rensing, and L. P. Barry

We show the importance of achieving an acceptable level of output side-mode-suppression ratio when generating pulses by using the self-seeded gain-switched technique. Experiments carried out on such pulses exhibiting poor side-mode-suppression ratios that are subsequently filtered to improve the latter demonstrate that they possess an associated level of noise. This buildup of noise with a decreasing inherent side-mode-suppression ratio is noted regardless of the improved output-filtered side-mode-suppression ratio of 35 dB that is maintained. The degradation of the signal is due to the mode partition effect and may render these pulses unsuitable for use in high-speed optical communications systems. © 2005 Optical Society of America

OCIS codes: 320.0320, 320.5390.

1. Introduction

The development of a source of short optical pulses is extremely important for use in future optical time-division-multiplexed (OTDM) and hybrid WDM/OTDM optical communications systems.[1] Picosecond pulse generation can be accomplished with many different techniques such as gating continuous-wave light with an external modulator, mode locking and gain-switching lasers, or by use of fiber lasers.[2] Mode locking is one of the most common techniques that is used to generate short optical pulses at fixed repetition rates. However, it requires specially designed laser structures that result in higher cavity complexity. On the other hand, the technique of gain switching, when compared with the above-mentioned alternatives, offers smaller footprint, efficient wavelength-stable performance, and the ability to produce high-repetition-rate pulses.[3]

One of the simplest, reliable, and most attractive options to generate wavelength-tunable picosecond optical pulses involves the self-seeding of a gain-switched Fabry–Perot (FP) laser. Essentially this method involves gain switching a FP laser and then feeding back one of the laser modes into the FP diode by use of a wavelength-selective external cavity. Provided that the optical signal reinjected into the laser arrives during the buildup of an optical pulse in the FP laser, then a single-mode, low-jitter output pulse can be obtained.[4] Recent experiments using the self-seeded gain-switched (SSGS) technique have also demonstrated the generation of multiwavelength pulses suitable for use in WDM networks.[5]

One difficulty associated with the use of SSGS pulses in high-speed optical communication systems may be mode partition noise (MPN). MPN in digital transmission systems has been known for a long time and can severely affect the performance of an optical communication system, even when distributed-feedback lasers with a nonideal side-mode-suppression ratio (SMSR) are used. It is mainly caused by the total optical power in a multilongitudinal-mode laser diode, remaining relatively constant, but the distribution of this power is a stochastic process[6]. The spectral fluctuation in the laser modes may thus manifest itself as an intensity fluctuation (noise) on the transmitted optical signal, and this manifestation of noise in optical communication systems that is due to MPN can occur in two ways. First, the effects of fiber dispersion in long-haul links result in temporal fluctuations of received power because the fluctuating modes become separated in time because of the fiber dispersion. Second, output optical filtering of the SSGS signal may result in fluctuations in the output power of the signal after the filter, which results in a degradation of the

The authors are with the Radio and Optical Communications Laboratory, Research Institute for Network and Communications Engineering, School of Electronic Engineering, Dublin City University, Glasnevin, Dublin 9, Ireland.

Received 23 May 2005; accepted 29 July 2005.
0003-6935/05/367867-05$15.00/0

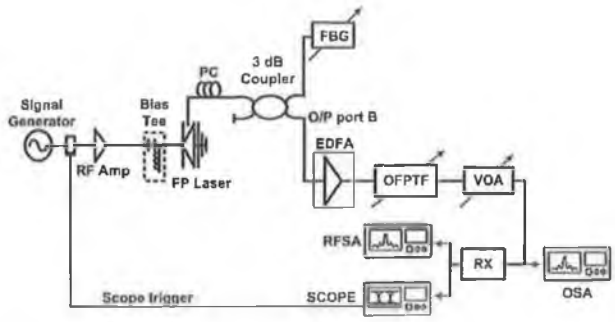

Fig. 1. Experimental set-up for the SSGS pulse degradation characterization: PC, polarization controller; FBG, fiber Bragg grating; OFPTF, optical FP tunable filter; VOA, variable optical attenuator; RFSA, RF spectrum analyzer; RX, receiver; OSA, optical spectrum analyzer.

signal quality. An important parameter that could be used to characterize the level of MPN is the SMSR.

In this work, a detailed experimental investigation on the increase in the noise of filtered SSGS pulses[7] with degrading inherent SMSR is presented. The inherent SMSR, in this work, could be defined as the SMSR directly at the output of the SSGS laser or, alternatively, as the SMSR of the SSGS laser before filtering. Generally, filtering of SSGS pulses is used to either select a particular wavelength in multiwavelength SSGS pulses, to improve the inherent SMSR of the SSGS pulses, or to remove amplified spontaneous emission power from an erbium-doped fiber amplifier (EDFA) placed after the SSGS setup. Our results show that, although many of the previously reported wavelength-tunable SSGS pulse sources use output filtering on pulses that exhibit low inherent SMSRs of ~15–20 dB to achieve a final SMSR of >30 dB,[8–10] in practice, such pulses may be unsuitable for use in either WDM or OTDM systems. The reason for this lies in the buildup of noise on the filtered optical pulses that is due to the mode partition effect. Hence it is vital that any pulse source based on the SSGS technique possesses a large-enough inherent SMSR, especially before filtering to prevent the degradation of the signal-to-noise ratio that is due to MPN. It is thus important when characterizing such pulses for use in optical systems that both the SMSR and the amplitude noise of these pulses should be accurately described, as there maybe a direct relationship between them.

2. Experimental Setup

Figure 1 shows the experimental setup used. The FP laser used was a commercial 1.5 μm InGaAsP device, with a threshold current of ~25 mA and longitudinal mode spacing of 1.1 nm. Gain switching of the laser was carried out by application of a dc bias current of ~17 mA and a sinusoidal modulation signal amplified to a power of ~29 dBm at a frequency of approximately 2.5 GHz. Self-seeding of the gain-switched laser diode was achieved with an external cavity containing a polarization controller (PC), a 3-dB coupler, and a tunable fiber Bragg grating (FBG) with a bandwidth of 0.4 nm. The fundamental frequency of the external cavity used was ~42.89 MHz. The level of feedback, taking into account the losses incurred in the external cavity and coupling, was measured to be approximately −15 dBm. To achieve optimum SSGS pulse generation, the central wavelength of the FBG was initially tuned to one of the longitudinal modes of the gain-switched laser. The frequency of the sinusoidal modulation was then varied to ensure that the signal reinjected into the laser from the external cavity arrives as an optical pulse is building up in the laser. The same could be achieved with an optical delay line to vary the round-trip time in the cavity. An operating frequency of 2.488 GHz (58th harmonic of fundamental frequency) was found to be suitable.

Typically the amount of light reinjected and hence the SMSR of the optical pulses could be varied by tuning the FBG and the modulation frequency. However, by varying the PC, the power coupled into the lasing mode could be changed, which effectively changes the SMSR of the optical pulses. The pulses at the lower arm of the 3 dB coupler (labeled output port B in Fig. 1) are then amplified with the aid of an EDFA, after which they are filtered by an optical FP tunable filter (OFPTF). The OFPTF had a FWHM passband of ~0.7 nm (84 GHz) and an extinction ratio of about 20 dB. Hence, we could improve the

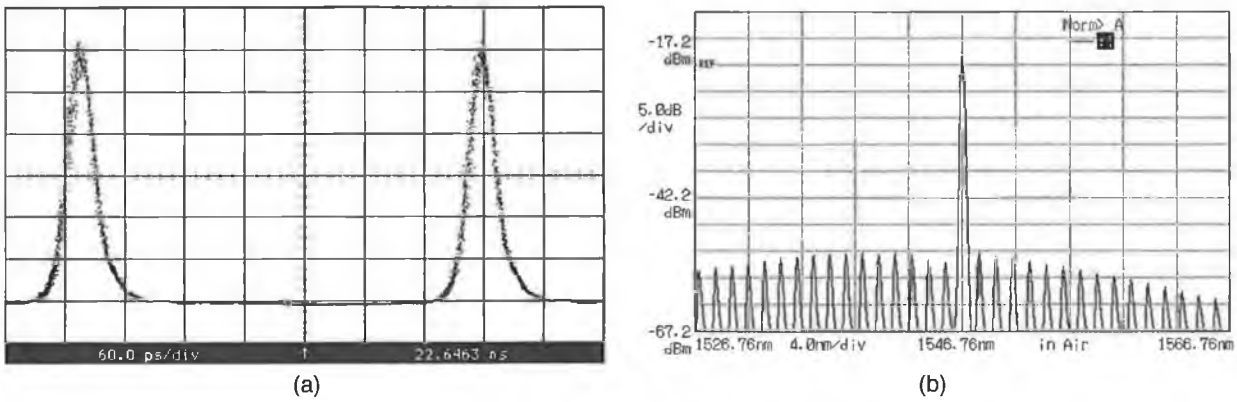

(a) (b)

Fig. 2. (a) Optical pulse with inherent SMSR of 37 dB, (b) optical spectrum with inherent SMSR of 37 dB.

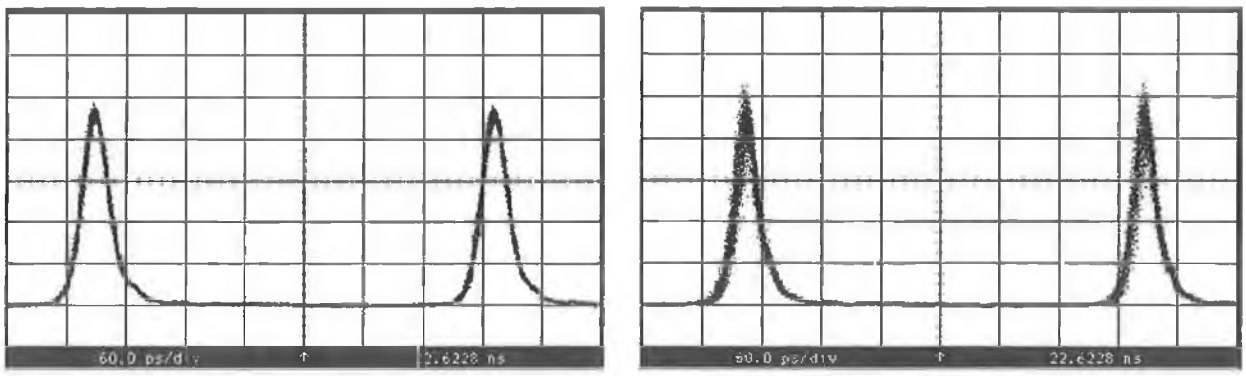

Fig. 3. (a) Optical pulse with inherent SMSR of 30 dB, (b) optical pulse with inherent SMSR of 15 dB.

inherent SMSR of the pulses by ~20 dB by passing the signal through the center of filter passband. To characterize the noise on the filtered SSGS pulses as a function of the input SMSR, the output SMSR had to be kept constant. When the inherent SMSR of the SSGS signal was high (30 dB), we maintained the output SMSR at 35 dB by tuning the filter away from the central wavelength of the SSGS signal. On the other hand, when the inherent SMSR of the SSGS signal was low (15 dB), we maintained the output SMSR at 35 dB by tuning the filter to the central wavelength of the SSGS signal. The lower and the upper SMSR limits were set by the extinction ratio of the filter, which meant that the inherent SMSR could be varied within a range of 15–30 dB while still maintaining an output SMSR of 35 dB. However, the tuning of the filter toward and away from the central wavelength meant that the output power of the filtered SSGS signal would vary since it would experience various levels of attenuation at the different portions of the filter's transfer characteristic. To overcome this problem and ensure that the power falling on the detector was always kept constant, a variable optical attenuator (VOA) with an incorporated in-line power meter was added after the filter.

The output pulses were then characterized in the temporal domain by use of a 50 GHz photodiode in conjunction with a 50 GHz sampling oscilloscope. Pulse characterization in the spectral domain was carried out with the aid of an optical spectrum analyzer. The high-speed detector was alternated between the oscilloscope and an RF spectrum analyzer, which was used to measure the RF noise spectrum.

3. Results and Discussion

With the PC adjusted to maximize the feedback into the FP device, the resulting pulses from the SSGS setup, without output filtration, are shown in Fig. 2(a). Assuming a total response time of ~9 ps for the combination of the photodiode and the oscilloscope, we can deconvolve the output pulse duration to be ~26 ps. Figure 2(b) shows that the spectral output, from which we can determine that the FP mode selected by using the FBG, was at a wavelength of 1547.08 nm. In addition, the inherent SMSR of the signal was 37 dB, and the 3 dB spectral width was ~0.3 nm.

To vary the SMSR of the generated optical pulses from 30 down to 15 dB, we simply had to adjust the PC in order to reduce the amount of light fed back into the laser diode. The reduction in feedback and SMSR also resulted in a slight decrease in the pulse duration and a slight increase in the spectral width, as expected from previous work.[11] Figures 3(a) and 3(b) show the SSGS pulses at the output of the filter when the inherent SMSR was set at 30 and 15 dB,

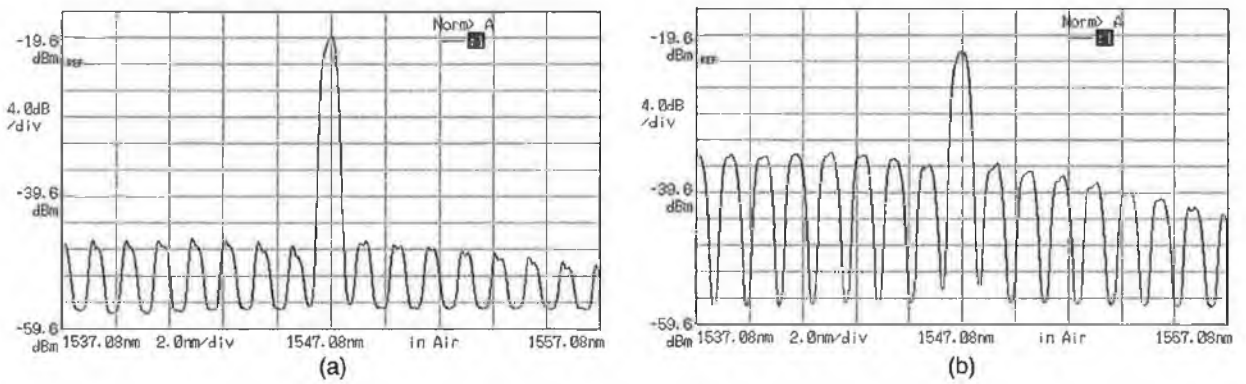

Fig. 4. Optical spectra with inherent SMSR of (a) 30 dB and (b) 15 dB.

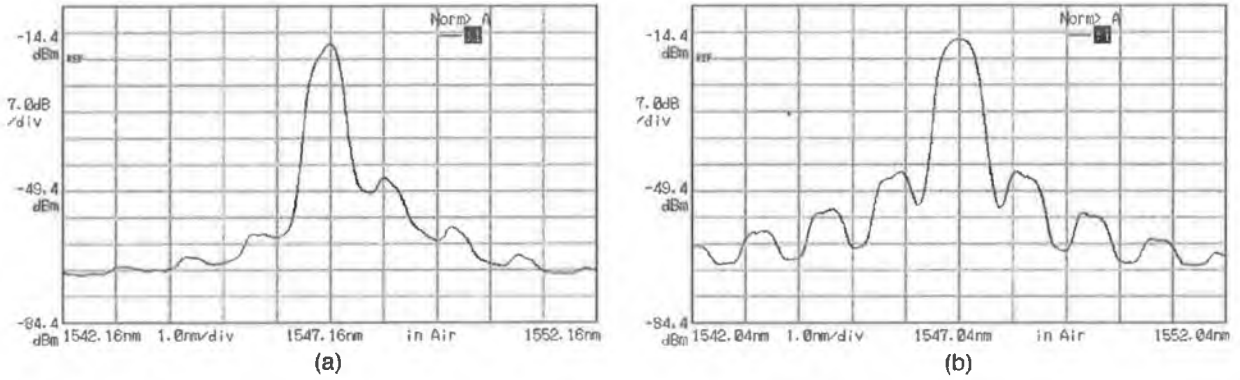

Fig. 5. Optical spectra with output SMSR of 35 dB and inherent SMSR of (a) 30 dB and (b) 15 dB.

respectively, and the output SMSR maintained at a constant value of 35 dB. It can be seen clearly that the noise level on the output pulse that corresponds to an inherent SMSR of 30 dB [Fig. 3(a)] is lower than that of the output pulse corresponding to an inherent SMSR of 15 dB [Fig. 3(b)].

The corresponding inherent SMSRs (high and low) are shown in Figs. 4(a) and 4(b), and the output spectra are shown in Figs. 5(a) and 5(b), respectively. The output spectra show that, even though the inherent SMSR is varied (15–30 dB), when the filter was tuned the output SMSR could still be maintained at a constant 35 dB.

The increase in noise as the inherent SMSR is reduced is associated with the mode partition effect of the FP laser that, as mentioned earlier, essentially involves the energy of each laser mode fluctuating with time because of a constant transfer of energy between the laser modes.[6] Because only the main mode is transmitted through the optical filter, any temporal fluctuations in the energy level of this mode will result in amplitude noise on the transmitted pulse. Clearly, as the SMSR is reduced, the energy in the side mode increases and the fluctuation of the energy in the main mode increases, resulting in additional amplitude noise on the transmitted pulse. To eliminate this noise it is necessary to ensure that the inherent SMSR of SSGS pulses that undergo output filtration must exhibit a high SMSR (total power in the side modes should be negligible).

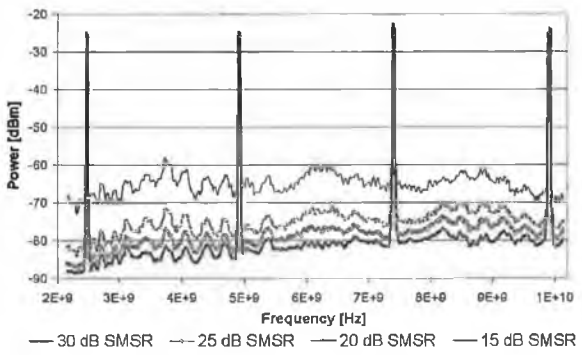

Fig. 6. RF spectrum of SSGS pulses exhibiting various inherent SMSRs.

We made a more detailed investigation into the noise introduced on the filtered SSGS pulses as the SMSR is degraded by performing RF spectral measurements on the detected pulses. The latter was carried out, with the aid of a RF spectrum analyzer, within a span of 8 GHz over a range of 2–10 GHz at a resolution band-width of 1 MHz. The measurement carried out over this range included the fundamental and the first three harmonics of the pulse train and is shown in Fig. 6. It can be seen that the power levels of each of the plots, corresponding to the various inherent SMSRs (30, 25, 20, and 15 dB) and a constant output SMSR of 35 dB, have been equalized with the aid of the VOA. Also from the graph, we can see an increase in the noise floor for decreasing values of the inherent SMSR. A degrading sweep (30 to 15 dB) of the inherent SMSR with a step width of 5 dB and the corresponding changes in the noise floor are outlined in Table 1 (measured at an offset of ~1 GHz). The table clearly shows that, for a 5 dB change in the inherent SMSR, the increase in the noise level is more at lower inherent SMSRs. This is because there is a bigger increase in the percentages of power in the side modes, which in turn leads to larger fluctuations in the main lasing mode. The larger fluctuations result in additional amplitude noise on the detected pulse.

On the whole, going from an input SMSR of 30 to 15 dB results in the level of the noise floor increasing by ~23 dB even though the output SMSR is maintained at an impressive 35 dB. This result clearly quantifies the difference in the noise floor of an

Table 1. Change in Noise Floor with Decreasing Inherent SMSR (Offset from Carrier = 1 GHz)

Change in input SMSR (dB)	Change in noise floor (dB)
30–25	4.52
25–20	5.33
20–15	13.16
30–15	23.02

output-filtered SSGS pulse that exhibits a weak inherent SMSR (15 dB) and a strong inherent SMSR (30 dB).

4. Conclusion

This paper has examined the effect of output filtration on SSGS pulses that exhibit varying levels of inherent SMSR. The results obtained categorically show that a reduction in the inherent SMSR of an SSGS pulse train would result in an increase in the level of the noise floor of the detected pulse after filtering. Hence we could conclude that, regardless of a high-output SMSR, if the inherent SMSR of SSGS pulses are weak then the interaction of MPN with spectral filtering would result in a large amount of amplitude noise on the output pulses. This noise or degradation of the signal-to-noise ratio will render such pulses totally unsuitable for data transmission in optical communication systems. It is thus imperative when characterizing optical pulses generated by the SSGS technique to simultaneously describe the SMSR and amplitude noise of the generated optical pulse train.

This research work has been partially supported by Enterprise Ireland (Proof of Concept) and Science Foundation Ireland (Investigator Program).

References

1. T. Morioka, H. Takara, S. Kawanishi, O. Kamatani, K. Takiguchi, K. Uchiyama, M. Saruwatari, H. Takahashi, M. Yamada, T. Kanamori, and H. Ono, "1Tbit/s (100Gbit/s times 10 channel) OTDM/WDM transmission using a single supercontinuum WDM source," Electron. Lett. **32,** 906–907 (1996).
2. S. Kawanishi, "Ultrahigh-speed optical time-division-multiplexed transmission technology based on optical signal processing," IEEE J. Quantum Electron. **34,** 2064–2079 (1998).
3. Y. J. Chai, K. A. Williams, R. V. Penty, and I. H. White, "High quality femtosecond pulse generation from a gain switched DFB laser using a novel self-seeding scheme," presented at LEOS/CLEO Europe, Munich, Germany, 22–27 June 2003.
4. M. Schell, W. Utz, D. Huhse, J. Kassner, and D. Bimberg, "Low jitter single mode pulse generation by a self-seeded, gain-switched Fabry–Perot semiconductor laser," Appl. Phys. Lett. **65,** 3045–3047 (1994).
5. C. Shu and S. P Yam, "Effective generation of tunable single- and multiwavelength optical pulses from a Fabry Perot laser diode," IEEE Photonics Technol. Lett. **9,** 1214–1216 (1997).
6. N. H. Jensen, H. Olesen, and K. E. Stubkjaer, "Partition noise in semiconductor lasers under CW and pulsed operation," IEEE J. Quantum Electron. **QE-23,** 71–79 (1987).
7. D. Curter, P. Pepeljugoski, and K. Y. Lau, "Noise properties of electrically gain-switched 1.5 μm DFB lasers after spectral filtering," Electron. Lett. **30,** 1418–1419 (1994).
8. K. Lee, C. Shu, and H. F. Liu, "Subharmonic pulse gating in self-seeded laser diodes for time- and wavelength interleaved picosecond pulse generation," IEEE J. Quantum Electron. **40,** 205–213 (2004).
9. D. N. Wang and M. F. Lim, "Tunable dual-wavelength optical short pulse generation by use of a fiber Bragg grating and a tunable optical filter in a self seeding scheme," Appl. Opt. **43,** 4106–4109 (2004).
10. S. Li, K. S. Chiang, W. A. Gambling, Y. Liu, L. Zhang, and I. Bennion, "Self-seeding of Fabry–Perot laser diode for generating wavelength-tunable chirp compensated single-mode pulses with high-sidemode suppression ratio" IEEE Photonics Technol. Lett. **12,** 1441–1443 (2000).
11. L. P. Barry, B. C. Thomsen, J. M. Dudley, and J. D. Harvey, "Characterization of 1.55 μm pulses from a self-seeded gain-switched Fabry–Perot laser diode using frequency-resolved optical gating," IEEE Photonics Technol. Lett. **10,** 935–937 (1998).